

I. STOKES FLOW PAST A THIN SCREEN
II. VISCOUS FLOWS PAST POROUS BODIES OF FINITE SIZE

Thesis by
Cheng-chung Shen

In Partial Fulfillment of the Requirements

For the Degree of
Doctor of Philosophy

California Institute of Technology

Pasadena, California

1968

(Submitted May 21, 1968)

To My Parents

ACKNOWLEDGMENTS

The author wishes to express his sincere gratitude to Professor Theodore Y. T. Wu for the constant guidance and supervision given him during the course of his graduate studies and the writing of this thesis. Both his professional competence and friendship have been great sources of encouragement and inspiration.

Thanks are due to Professors A. J. Acosta, N. H. Brooks and R. F. Scott, Dr. C. Y. Wang, Messrs. Arthur Whitney and Michael Wilson for many helpful discussions, particularly to Mr. Wilson for review of the manuscript. Thanks are also due to Mrs. Barbara Hawk for many helps. Miss Cecilia Lin for making the fine drawings and Mrs. Alrae Tingley for typing the final manuscript.

The author must give the deepest appreciation to his wife, Mrs. Helena Shen, for her patience and perseverance in producing the manuscript and performing the computer programming. After all, without her understanding and sacrifices throughout the difficult years, this work would have been impossible.

The author is grateful to the California Institute of Technology for the award of tuition fellowships, teaching assistantships, research assistantships and Woodrow Wilson Foundation Fellowships. Part of this investigation has been conducted under Contract Nonr 220(35) with the Office of Naval Research, Department of the Navy.

ABSTRACT

Part I

The slow, viscous flow past a thin screen is analyzed based on Stokes equations. The problem is reduced to an associated electric potential problem as introduced by Roscoe. Alternatively, the problem is formulated in terms of a Stokeslet distribution, which turns out to be equivalent to the first approach.

Special interest is directed towards the solution of the Stokes flow past a circular annulus. A "Stokeslet" formulation is used in this analysis. The problem is finally reduced to solving a Fredholm integral equation of the second kind. Numerical data for the drag coefficient and the mean velocity through the hole of the annulus are obtained.

Stokes flow past a circular screen with numerous holes is also attempted by assuming a set of approximate boundary conditions. An "electric potential" formulation is used, and the problem is also reduced to solving a Fredholm integral equation of the second kind. Drag coefficient and mean velocity through the screen are computed.

Part II

The purpose of this investigation is to formulate correctly a set of boundary conditions to be prescribed at the interface between a viscous flow region and a porous medium so that the problem of a viscous flow past a porous body can be solved.

General macroscopic equations of motion for flow through

porous media are first derived by averaging Stokes equations over a volume element of the medium. These equations, including viscous stresses for the description, are more general than Darcy's law. They reduce to Darcy's law when the Darcy number becomes extremely small.

The interface boundary conditions of the first kind are then formulated with respect to the general macroscopic equations applied within the porous region. An application of such equations and boundary conditions to a Poiseuille shear flow problem demonstrates that there usually exists a thin interface layer immediately inside the porous medium in which the tangential velocity varies exponentially and Darcy's law does not apply.

With Darcy's law assumed within the porous region, interface boundary conditions of the second kind are established which relate the flow variables across the interface layer. The primary feature is a jump condition on the tangential velocity, which is found to be directly proportional to the normal gradient of the tangential velocity immediately outside the porous medium. This is in agreement with the experimental results of Beavers, et al.

The derived boundary conditions are applied in the solutions of two other problems: (1) Viscous flow between a rotating solid cylinder and a stationary porous cylinder, and (2) Stokes flow past a porous sphere.

TABLE OF CONTENTS

<u>Chapter</u>	<u>Title</u>	<u>Page</u>
	<u>PART ONE</u>	
	STOKES FLOW PAST A THIN SCREEN	1
I	INTRODUCTION	2
II	GENERAL MATHEMATICAL FORMULATION FOR STOKES FLOW PAST A THIN SCREEN OF FINITE SIZE	7
III	STOKES FLOW PAST A CIRCULAR ANNULUS	16
IV	STOKES FLOW PAST A THIN CIRCULAR SCREEN	32
	REFERENCES	43
	<u>PART TWO</u>	
	VISCOUS FLOWS PAST POROUS BODIES OF FINITE SIZE	46
I	INTRODUCTION	47
II	EQUATIONS OF MOTION FOR FLOW THROUGH POROUS MEDIA	53
	2.1. Empirical Darcy's Law	53
	2.2. Microscopic and Macroscopic Descriptions	57
	2.3. Idealized Models of Porous Media	62
	2.4. Derivation of General Macroscopic Equations of Motion	74
	2.5. Energy Consideration	81
III	INTERFACE BOUNDARY CONDITIONS	87
	3.1. Interface Boundary Conditions of the First Kind--For General Macroscopic Equations of Motion	89
	3.2. An Illustrative Example	97

<u>Chapter</u>	<u>Title</u>	<u>Page</u>
	3.3. Interface Boundary Conditions of the Second Kind--For Darcy's Law	105
IV	VISCOUS FLOWS PAST POROUS BODIES OF FINITE SIZE	116
	4.1. Viscous Flow Between a Rotating Solid Cylinder and a Stationary Porous Cylinder	116
	4.2. Stokes Flow Past a Porous Sphere	125
V	CONCLUSIONS AND DISCUSSION	138
	REFERENCES	143

PART ONE
STOKES FLOW PAST A THIN SCREEN

I. INTRODUCTION

The viscous flow past a group of obstacles or a porous body has recently attracted extensive investigations.[†] As in the case of a single, isolated, solid body, there appears at present to be no exact solution of this many-body problem based on the Navier-Stokes equations. The theoretical studies of this class of problems have been largely based on either Stokes' or Oseen's equations,[‡] which are linear. Even for such approximate equations, exact solutions are scarce.

In the category of a group of obstacles, Tamada and Fujikawa [3] investigated the Oseen flow past an infinite row of equally-spaced circular cylinders, whereas Miyagi [4] studied the same problem using Stokes' equations. Kuwabara [5] dealt with the Oseen flow past a lattice of elliptic cylinders. All these solutions are based on an expansion method in terms of a small obstacle size to distance ratio. By applying the Fourier transform method, Kuwabara [6] also obtained a solution of the Stokes flow past a lattice of parallel flat plates in the limit of both small and large distances between two consecutive plates. Keller [7] applied the lubrication theory to obtain an approximate solution for the flow past a row or several rows of closely packed circular cylinders. Furthermore, Hasimoto [8] found approximate solutions of the Stokes flows past cubic arrays of small spheres. Most

[†] See references [3] through [14].

[‡] For a comprehensive treatment of Stokes' and Oseen's equations, see references [1] and [2]. Stokes and Oseen flow are also defined there.

interesting of all, Hasimoto [9] , in another investigation of the Stokes flow past a thin screen, was able to obtain an exact solution for the case of a series of equal and equidistant flat plates (or slits) held normal to the flow. In this solution the method originally developed by Roscoe [10] was followed, by which the problem of the Stokes flow past plane obstacles is related to an analogous problem of the electrostatic potential due to a set of earthed conducting plates of the same shape.

In the category of porous bodies, Joseph and Tao [11] treated the problem of the Stokes flow past a porous sphere. They obtained an analytic solution satisfying Stokes' equations in the external flow field, an empirical Darcy's law in the porous sphere, and a set of boundary conditions prescribed at the interface. The interface boundary conditions they used state that the pressure and the normal velocity are continuous across the interface, and that the tangential velocity vanishes on the fluid side of the interface. Their result shows that the drag of a porous sphere is always less than that of a solid one for the entire range of porosity regarded as valid for Darcy's law. Additional treatments of the same nature by Joseph and Tao are given in [12] , [13] and [14]. These problems are all concerned with viscous flows past porous bodies. In a few cases, however, the porous bodies are not finite in size as in the first case of a porous sphere.

Some of the boundary conditions proposed by Joseph and Tao [11] are, however, questionable. It can be argued that a slip velocity condition, rather than an adherence condition, should hold at the interface. Since in their boundary conditions the fluid is allowed to move on the porous side along the interface, it is hardly conceivable that

the tangential velocity of the fluid on the fluid side must be zero. Because of these doubtful boundary conditions, the theory of Joseph and Tao, and the other analytic results obtained previously, cannot be considered as established at all. It is therefore clear that for the problems of flow past a porous obstacle it is important to determine the boundary conditions which can describe correctly the physical situation.

We are interested in investigating analytically the viscous flow past a porous body. In particular, we shall determine the change of the flow quantities, such as the drag, caused by the porous body as it replaces a solid one of the same exterior geometrical configuration. In the case when the porous body consists of numerous interconnected holes such that it may be approximated by a porous medium to which Darcy's law is applicable, correct interface boundary conditions, as stressed previously, are required to ensure correct solutions. The nature of these boundary conditions will be discussed in detail in Part Two of this thesis. In Part One, we are mainly concerned with the case in which the porous body has a very simple geometry. In this case, exact solutions can be obtained to satisfy the non-slip boundary condition on all walls. Due to the inherent difficulty associated with the Navier-Stokes equations, our analysis is restricted to Stokes flow. As a specific example, the exact solution is derived for the Stokes flow past a circular annulus. Based on the results obtained for this case we can predict, at least qualitatively, the same kind of porosity effects for more general porous bodies. In addition to this problem, a solution which satisfies a set of approximate boundary conditions is also

obtained for the Stokes flow past a circular screen with numerous holes.

A general mathematical formulation is given in Chapter II for the Stokes flow past a thin screen of finite size. The problem is transformed to the one of electrostatic potential satisfying the Laplace equation and the boundary conditions which state that the screen is perfectly conducting and is charged to a constant potential. This idea is much the same as that introduced by Roscoe [10] for the Stokes flow past plane obstacles. It was also used by Hasimoto [9] in solving the Stokes flow past two-dimensional infinite screens. An alternative formulation using a Stokeslet distribution is also attempted. It turns out to be equivalent to the first formulation.

In Chapter III an exact solution for the case of a simple screen, namely, a circular annulus, is obtained. In fact, this solution is a particular case of Roscoe's work. The annulus is geometrically simple enough to admit an exact solution, but it offers good indication of the porosity-effect as the hole size varies. With regard to the corresponding potential problem of a charged conducting annulus, it is only recently that great attention has been given to it. It was solved either by triple integral equations as given by Cooke [15], or by a simpler method developed by Williams [16]. Their results may be appropriated directly to obtain our solution for flow past an annulus, but their published information is very limited. To obtain flow properties other than just drag, the problem is worthwhile to be re-examined. For providing an alternative way of approach, the method of Stokeslet distribution will be used in the derivation.

In Chapter IV, the solution for a circular screen possessing a great number of holes is attempted. The exact non-slip boundary condition is replaced by an approximate one, that is, a pressure jump proportional to the local average fluid velocity through the screen is prescribed at the screen. The corresponding potential problem, using an approach parallel to Williams' [16], is eventually reduced to a Fredholm integral equation of the second kind and a solution is, thus, obtained.

II. GENERAL MATHEMATICAL FORMULATION FOR STOKES FLOW PAST A THIN SCREEN OF FINITE SIZE

For incompressible, viscous flows in which the inertial effect is negligible, Stokes' equations are

$$-\nabla p + \mu \nabla^2 \vec{u} = 0, \quad (2.1)$$

$$\nabla \cdot \vec{u} = 0, \quad (2.2)$$

where μ is the coefficient of viscosity, p is the pressure and \vec{u} is the velocity vector (its components in Cartesian coordinates will be denoted by u, v, w , in the x, y, z directions, respectively). These equations together with the non-slip boundary condition on solid walls are sufficient to determine the solution of the flow past a three-dimensional finite obstacle, or in the case of two-dimensional flows, an obstacle in a bounded region.

The stress tensor σ is given by

$$\sigma = -pI + \mu[\nabla \vec{u} + (\nabla \vec{u})^*], \quad (2.3)$$

where I is an identity tensor and the superscript "*" designates the transpose of a tensor.

Taking the divergence of (2.1), and making use of (2.2), we see that p is a harmonic function, that is

$$\nabla^2 p = 0. \quad (2.4)$$

Similarly, by taking the curl of (2.1), the vorticity $\vec{\omega}$ as defined by

$$\vec{\omega} = \nabla \times \vec{u} \quad (2.5)$$

is seen to satisfy

$$\nabla^2 \vec{\omega} = 0 . \quad (2.6)$$

Thus, each component of the vorticity in Cartesian coordinates is also a harmonic function, and the vorticity transport in Stokes flow is governed by steady-state diffusion only.

Our problem of the Stokes flow past a thin screen of finite size is to solve (2.1) - (2.2) under the boundary conditions

$$\vec{u} = 0 \quad \text{on walls of screen,} \quad (2.7)$$

$$\vec{u} \rightarrow U\vec{e}_1, \quad p \rightarrow p_\infty \quad \text{as} \quad |\vec{x}| \rightarrow \infty, \quad (2.8)$$

where \vec{e}_1 is a unit vector in the direction of the uniform flow at infinity.

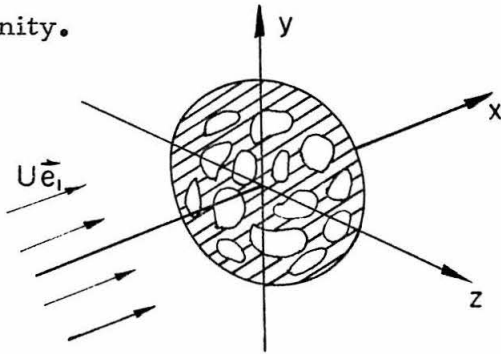


Fig. 1. Stokes flow past a thin screen of finite size.

In Cartesian coordinates (x,y,z) with the x-axis lying in the direction of \vec{e}_1 , the screen is chosen to lie in the plane $x = 0$ (see Fig. 1). On account of the symmetry of the obstacle with respect to the plane $x = 0$, Stokes' equations (2.1) - (2.2) admit a solution of the following symmetry:

$$\left. \begin{aligned}
 u(x,y,z) &= u(-x,y,z) , \\
 v(x,y,z) &= -v(-x,y,z) , \\
 w(x,y,z) &= -w(-x,y,z) , \\
 (p(x,y,z) - p_{\infty}) &= -(p(-x,y,z) - p_{\infty}) ,
 \end{aligned} \right\} \quad (2.9)$$

Since $v,w,(p-p_{\infty})$ are odd in x , it is required that

$$v,w,(p-p_{\infty}) = 0 \quad , \quad \text{on the part of } x = 0 \text{ plane complementary to the screen walls.} \quad (2.10)$$

Since p is a harmonic function and is odd in x , we may write

$$p = p_{\infty} + 2\mu \frac{\partial \Phi}{\partial x} , \quad (2.11)$$

where Φ itself is a harmonic function but is even with respect to x , that is

$$\nabla^2 \Phi = 0 \quad , \quad (2.12)$$

and

$$\Phi(x,y,z) = \Phi(-x,y,z) . \quad (2.13)$$

Substituting (2.11) into (2.1), we obtain

$$\nabla_{\vec{u}}^2 = 2 \frac{\partial}{\partial x} \nabla \Phi . \quad (2.14)$$

A particular solution of \vec{u} satisfying (2.14) is $x\nabla\Phi$, as can be easily verified by direct substitution. However, $\vec{u} = x\nabla\Phi$ alone does not satisfy the continuity equation (2.2). We shall also require a homogeneous solution to be added to the particular solution so that the

continuity equation (2.2) is satisfied. The correct homogeneous solution is seen to be $(U - \Phi)\vec{e}_1$ as can be readily verified. Therefore, a solution of (2.1) - (2.2) is

$$\vec{u} = (U - \Phi)\vec{e}_1 + x\nabla\Phi . \quad (2.15)$$

This representation (2.15) automatically makes v and w vanish at $x = 0$, as required by (2.7) and (2.10). The rest of the boundary conditions in (2.7), (2.8) and (2.10) are also satisfied provided that

$$\Phi = U \quad , \quad \text{on walls at } x = 0 , \quad (2.16)$$

$$\frac{\partial\Phi}{\partial x} = 0 \quad , \quad \text{outside the wall at } x = 0 \quad , \quad (2.17)$$

$$\Phi \rightarrow 0 \quad , \quad \text{as } |\vec{x}| \rightarrow \infty . \quad (2.18)$$

Condition (2.17) follows from the requirement that Φ is a function even in x .

Now the problem of Stokes flow specified by (2.1), (2.2), (2.7), (2.8) and (2.10) has been reduced to an associated problem of electric potential Φ satisfying the Laplace equation (2.12) and the boundary conditions (2.16) - (2.18). This potential problem can be regarded as

1. a Dirichlet problem in an infinite space, with an equipotential U prescribed on the screen walls at $x = 0$; or
2. a mixed type boundary value problem in the half space $x > 0$, with potential U and its normal derivative equal 0 prescribed respectively on the wall's part and the non-wall's part of the plane

$x = 0$.

Both of these problems have been thoroughly treated. The uniqueness and existence properties of their solutions are well-known. In turn, these properties may be appropriated for the original Stokes problem.

The Dirichlet problem above actually can give more physical insight than the other. The problem can be interpreted in terms of a source distribution at the screen wall. The sources should be so distributed that the potential Φ on the screen wall is a constant U . This is exactly the electrostatic problem of the potential Φ due to a charged conducting screen maintained at an equipotential U .

In electrostatics[†], the potential $\Phi(\vec{x})$ due to a surface-charge (source) distribution $\gamma(\vec{\zeta}')$ is given by

$$\Phi(\vec{x}) = \int_W \frac{\gamma(\vec{\zeta}')}{|\vec{x} - \vec{\zeta}'|} dS_{\vec{\zeta}'} \quad (2.19)$$

For the present problem, the integral in (2.19) is carried over the wall part of the screen, W .

By applying the boundary condition (2.16) to (2.19), we obtain an integral equation for the surface-charge density $\gamma(\vec{\zeta}')$,

$$U = \int_W \frac{\gamma(\vec{\zeta}')}{|\vec{\zeta} - \vec{\zeta}'|} dS_{\vec{\zeta}'} \quad (\vec{\zeta} \text{ on } W), \quad (2.20)$$

where both $\vec{\zeta}$ and $\vec{\zeta}'$ lie on the screen wall. This integral equation is generally not easy to solve, even for screens of relatively simple

[†]For a general treatment of electrostatics, see, for example, Jackson [17].

geometry. However, once $\gamma(\vec{\zeta}')$ is obtained, the potential Φ is simply given by (2.19) and the original Stokes flow problem is determined by (2.15).

It is also known in electrostatics that there is a jump $4\pi\gamma$ in the normal component of the electric field $(-\nabla\Phi)$ across a surface distributed with a surface-charge of density γ ; in other words, across the screen wall we have

$$\left(\frac{\partial\Phi}{\partial x}\right)_{-} - \left(\frac{\partial\Phi}{\partial x}\right)_{+} = 4\pi\gamma, \quad (2.21)$$

where "-" and "+" designate the negative and positive sides of $x = 0$, respectively.

By virtue of the symmetry (2.13) of Φ with respect to x ,

$$\left(\frac{\partial\Phi}{\partial x}\right)_{+} = - \left(\frac{\partial\Phi}{\partial x}\right)_{-};$$

and therefore,

$$\left(\frac{\partial\Phi}{\partial x}\right)_{\pm} = \mp 2\pi\gamma \quad (\text{for } y, z \text{ on } W). \quad (2.22)$$

For the purpose of calculating the drag on the screen, the stress tensor (2.3) is first written in terms of Φ , so that

$$\sigma = - (p_{\infty} + 2\mu \frac{\partial\Phi}{\partial x})\mathbf{I} + 2\mu x \nabla(\nabla\Phi). \quad (2.23)$$

The viscous stresses, represented by the last term of (2.23), are identically zero at $x = 0$. This leaves the pressure as the only stress acting on the screen. The wall pressures on the positive and the negative sides of $x = 0$, by virtue of equation (2.22), are seen to

be related directly to γ as follows :

$$p_{\pm} = p_{\infty} + 2\mu \left(\frac{\partial \Phi}{\partial x} \right)_{\pm} = p_{\infty} \mp 4\pi\mu\gamma . \quad (2.24)$$

The drag D on the screen is contributed by the pressure alone, giving

$$D = \int_W (p_- - p_+) dS = 8\pi\mu \int_W \gamma dS = 8\pi\mu Q , \quad (2.25)$$

in which use has been made of (2.24), and Q stands for the total charge on the screen.

Furthermore, if the electrostatic capacity C of the screen is defined as the charge per unit potential on the screen (namely, $C = Q/U$), then (2.25) becomes

$$D = 8\pi\mu UC . \quad (2.26)$$

This simple result is remarkable; it is noted that the drag is directly proportional to the electrostatic capacity of the screen of the associated problem.

The foregoing formulation is along the reasoning of Roscoe [10]. We shall see that an alternative approach using "Stokeslet" distribution is also possible. A Stokeslet of strength $\vec{\alpha}$ is a singularity in Stokes flow such that it experiences a force of magnitude $-8\pi\mu\vec{\alpha}$. In other words, the Stokeslet is equivalent to a point force $8\pi\mu\vec{\alpha}$ applied to the fluid. The corresponding pressure and velocity field of a Stokeslet can be obtained from the following equations :

$$-\nabla p + \mu \nabla^2 \vec{u} + 8\pi\mu\vec{\alpha} \delta(\vec{x} - \vec{\zeta}) = 0 , \quad (2.27)$$

$$\nabla \cdot \vec{u} = 0 , \quad (2.2)$$

and the solutions are

$$p(\vec{x}) = 2\mu \frac{\vec{\alpha} \cdot (\vec{x} - \vec{\zeta})}{|\vec{x} - \vec{\zeta}|^3} , \quad (2.28)$$

$$\vec{u}(\vec{x}) = \frac{\vec{\alpha}}{|\vec{x} - \vec{\zeta}|} + \frac{[\vec{\alpha} \cdot (\vec{x} - \vec{\zeta})](\vec{x} - \vec{\zeta})}{|\vec{x} - \vec{\zeta}|^3} , \quad (2.29)$$

for a Stokeslet situated at $\vec{x} = \vec{\zeta}$.

Since Stokes' equations are linear, more complicated solutions can be constructed by superimposing Stokeslets together with other elementary solutions of Stokes' equations. In particular, we shall consider Stokeslet distribution at a surface. Let a surface Stokeslet of density $\alpha \vec{e}_1$ be distributed over the wall part of the screen (denoted by W), all the Stokeslets being in the x -direction, then such a distribution plus a uniform flow gives the pressure and the velocity field as follows,

$$p(\vec{x}) = p_\infty + 2\mu \int_W \frac{x\alpha(\vec{\zeta}')}{|\vec{x} - \vec{\zeta}'|^3} dS_{\vec{\zeta}'} , \quad (2.30)$$

$$\vec{u}(\vec{x}) = \left[U + \int_W \frac{\alpha(\vec{\zeta}')}{|\vec{x} - \vec{\zeta}'|} dS_{\vec{\zeta}'} \right] \vec{e}_1 + x \int_W \frac{\alpha(\vec{\zeta}')(\vec{x} - \vec{\zeta}')}{|\vec{x} - \vec{\zeta}'|^3} dS_{\vec{\zeta}'} . \quad (2.31)$$

This formulation thus yields a successful solution for flow past a screen when the density function $\alpha(\vec{\zeta}')$ can be found such that both

boundary conditions (2.7) and (2.8) are satisfied. We can prove that it is indeed the case.

Condition (2.8) is obviously satisfied by (2.30) and (2.31), whereas the other boundary condition (2.7) can be satisfied if

$$U = \int_W \frac{-\alpha(\vec{\zeta}')}{|\vec{\zeta} - \vec{\zeta}'|} dS_{\vec{\zeta}'} . \quad (2.32)$$

But this is precisely the integral equation for $\alpha(\vec{\zeta}')$, and we observe that (2.32) is identical to the integral equation (2.19) provided $\alpha(\vec{\zeta}') = -\gamma(\vec{\zeta}')$, namely, the surface Stokeslet density is equal to the negative of the surface charge density considered in the associated electric potential problem. As a matter of fact, if we write

$$\Phi(\vec{x}) = \int_W \frac{-\alpha(\vec{\zeta}')}{|\vec{x} - \vec{\zeta}'|} dS_{\vec{\zeta}'} , \quad (2.33)$$

equations (2.30), (2.31) and (2.32) are also reduced exactly to (2.11), (2.15) and (2.16) as already derived in the previous formulation. Thus, the two formulations, one by relating to an associated electric potential and the other by using Stokeslets, are seen to lead to the same result.

III. STOKES FLOW PAST A CIRCULAR ANNULUS

Consider a Stokes flow past a circular annulus with a uniform free stream velocity U perpendicular to the annulus, as shown schematically in Fig. 2. By virtue of the axial symmetry of the annulus, cylindrical polar coordinates (r, θ, x) will be used throughout the following analysis. The annulus lies in the plane $x = 0$, with its center at the origin. Its inner and outer radii are a and b respectively.

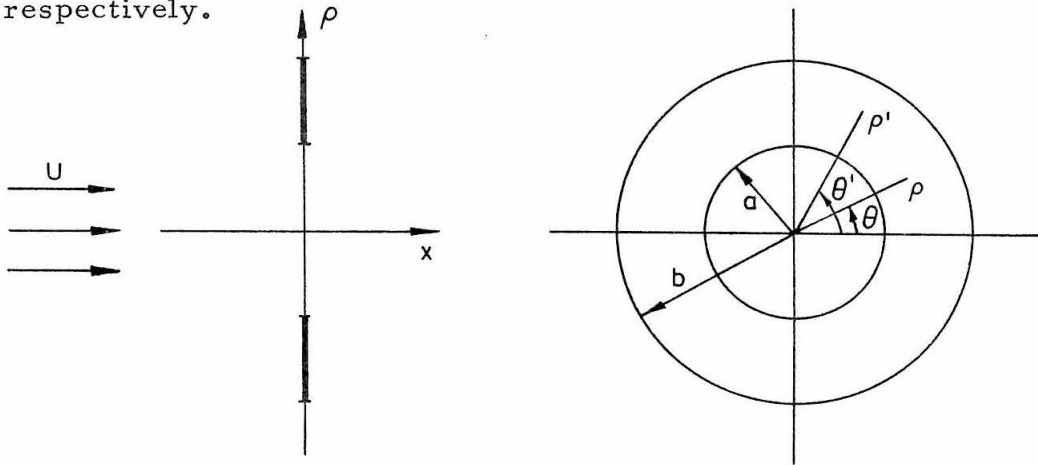


Fig. 2. Stokes flow past a circular annulus.

Such an annulus is probably the simplest screen which can illustrate the general analytic method outlined in the preceding chapter, and at the same time demonstrate the effect of porosity in an obstacle to the flow.

The equations governing Stokes flow past a circular annulus are Stokes' equations (2.1) and (2.2),

$$-\nabla p + \mu \nabla^2 \vec{u} = 0 \quad , \quad (3.1)$$

$$\nabla \cdot \vec{u} = 0 \quad , \quad (3.2)$$

where for convenience the equations have been re-numbered for this chapter. The non-slip boundary condition and the conditions at infinity for this particular case are

$$\vec{u} = 0 \quad , \quad \text{at } x = 0 \quad , \quad a < \rho < b \quad , \quad (3.3)$$

and

$$\vec{u} \rightarrow U \vec{e}_1 \quad , \quad p \rightarrow p_\infty \quad , \quad \text{as } |\vec{x}| \rightarrow \infty \quad . \quad (3.4)$$

This Stokes problem, according to the general formulation of the preceding chapter, can be reduced to an associated electric potential problem described by (2.11), (2.12), (2.15)-(2.18), namely,

$$p = p_\infty + 2\mu \frac{\partial \Phi}{\partial x} \quad , \quad (3.5)$$

$$\vec{u} = (U - \Phi) \vec{e}_1 + x \nabla \Phi \quad , \quad (3.6)$$

where

$$\nabla^2 \Phi = 0 \quad , \quad (3.7)$$

and the electric potential Φ satisfies the boundary conditions:

$$\Phi = U \quad , \quad \text{at } x = 0 \quad , \quad a < \rho < b \quad , \quad (3.8)$$

$$\frac{\partial \Phi}{\partial x} = 0 \quad , \quad \text{at } x = 0 \quad , \quad \rho < a \quad \text{and} \quad \rho > b \quad , \quad (3.9)$$

$$\Phi \rightarrow 0 \quad , \quad \text{as } |\vec{x}| \rightarrow \infty \quad . \quad (3.10)$$

The problem (3.7) - (3.10) may be interpreted as that of finding the electric potential Φ due to a conducting circular annulus charged

to a constant potential U . It can be solved either by using triple integral equations employed by Cooke [15], or by a simpler method developed by Williams [16]. Our formulation in terms of the integral equation (2.20) is in accordance with the method of Williams. Both Cook and Williams eventually reduced the electrostatic annulus problem to that of the solution of a Fredholm integral equation of the second kind. Cooke obtained a solution numerically and determined the electric capacity of the conducting annulus. Since the drag on the screen has been found in (2.26) to be directly proportional to the electric capacity, the Stokes annulus problem is considered solved insofar as the drag is concerned. Nevertheless, we are also interested in other flow properties, such as the discharge through the hole of the annulus, etc. Such information is not derivable from Cooke's published results. Hence, we shall re-examine the Stokes problem. Moreover, since an alternative but equivalent formulation in terms of Stokeslet distribution has been introduced in Chapter II, it might be fruitful to follow this approach at this time so as to avoid using the terminology of electrostatics.

Stokeslets are assumed to be distributed symmetrically on the annulus about its axis, the surface density $\alpha(\rho)$ has a radial dependence only. The "Stokeslet" formulation, as given in (2.30), (2.31) and (2.32), may be written down specifically for the annulus problem:

$$p(\rho, \theta, x) = p_{\infty} + 2\mu \int_a^b \int_0^{2\pi} \frac{x\alpha(\rho')\rho' d\theta' d\rho'}{R^3}, \quad (3.11)$$

$$\begin{aligned} \vec{u}(\rho, \theta, x) = & \left[U + \int_a^b \int_0^{2\pi} \frac{\alpha(\rho') \rho' d\theta' d\rho'}{R} \right] \vec{e}_1 \\ & + x \int_a^b \int_0^{2\pi} \frac{\alpha(\rho') (\vec{x} - \vec{\zeta}') \rho' d\theta' d\rho'}{R^3}, \end{aligned} \quad (3.12)$$

where $\alpha(\rho')$ is to be determined from the integral equation,

$$U = \int_a^b \int_0^{2\pi} \frac{-\alpha(\rho') \rho' d\theta' d\rho'}{R'} \quad (a < \rho < b), \quad (3.13)$$

and where

$$\begin{aligned} R &= |\vec{x} - \vec{\zeta}'| = \sqrt{x^2 + \rho^2 + \rho'^2 - 2\rho\rho' \cos(\theta - \theta')}, \\ R' &= |\vec{\zeta} - \vec{\zeta}'| = \sqrt{\rho^2 + \rho'^2 - 2\rho\rho' \cos(\theta - \theta')}, \\ \vec{x} &= (\rho, \theta, x), \quad \vec{\zeta} = (\rho, \theta, 0), \quad \vec{\zeta}' = (\rho', \theta', 0). \end{aligned}$$

We begin now to solve the integral equation (3.13). After $\alpha(\rho)$ is obtained, the velocity and pressure are simply given by (3.11) and (3.12). Before starting with the solution, we shall first discuss some mathematical preliminaries which will have frequent use in later calculations.

Lemma 1. If ρ and ρ' are positive, then

$$\int_0^{2\pi} \frac{d\theta'}{\sqrt{\rho^2 + \rho'^2 - 2\rho\rho' \cos(\theta - \theta')}} = 4 \int_0^{\min(\rho, \rho')} \frac{dt}{\sqrt{\rho^2 - t^2} \sqrt{\rho'^2 - t^2}}. \quad (3.14)$$

The proof is given by Copson [18] in his treatment of the electrified disc.

Lemma 2. If $f(\rho)$ is once continuously differentiable on (a, b) , then the integral equation

$$f(\rho) = \int_a^\rho \frac{G(t) dt}{(\rho^2 - t^2)^c} \quad (a < \rho < b, \quad 0 < c < 1), \quad (3.15)$$

has the solution

$$G(t) = \frac{2 \sin \pi c}{\pi} \frac{d}{dt} \int_a^t \frac{\rho f(\rho) d\rho}{(t^2 - \rho^2)^{1-c}} \quad (a < t < b) . \quad (3.16)$$

Lemma 3. If $f(\rho)$ is once continuously differentiable on (a, b) , then the integral equation

$$f(\rho) = \int_\rho^b \frac{G(t) dt}{(t^2 - \rho^2)^c} \quad (a < \rho < b, \quad 0 < c < 1) , \quad (3.17)$$

has the solution

$$G(t) = - \frac{2 \sin \pi c}{c} \frac{d}{dt} \int_t^b \frac{\rho f(\rho) d\rho}{(\rho^2 - t^2)^{1-c}} \quad (a < t < b) . \quad (3.18)$$

Both Lemma 2 and Lemma 3 are generalizations of Abel's integral equations. The proofs are given, for example, by Sneddon [19].

In making use of Lemma 1, or equation (3.14), equation (3.13) is reduced to

$$-4 \int_a^b \rho' \alpha(\rho') d\rho' \int_0^{\min(\rho, \rho')} \frac{dt}{\sqrt{\rho^2 - t^2} \sqrt{\rho'^2 - t^2}} = U \quad (a < \rho < b). \quad (3.19)$$

This equation can be re-written as

$$\left[\int_a^\rho \int_0^{\rho'} + \int_b^\rho \int_0^\rho \right] \frac{\rho' \alpha(\rho') dt d\rho'}{\sqrt{\rho^2 - t^2} \sqrt{\rho'^2 - t^2}} = -\frac{U}{4},$$

or

$$\left[\int_a^\rho \int_0^a + \int_a^\rho \int_a^{\rho'} + \int_\rho^b \int_0^a + \int_\rho^b \int_a^\rho \right] \frac{\rho' \alpha(\rho') dt d\rho'}{\sqrt{\rho^2 - t^2} \sqrt{\rho'^2 - t^2}} = -\frac{U}{4}.$$

Upon interchanging the order of integration,

$$\left[\int_0^a \int_a^\rho + \int_a^\rho \int_t^\rho + \int_0^a \int_\rho^b + \int_a^\rho \int_\rho^b \right] \frac{\rho' \alpha(\rho') d\rho' dt}{\sqrt{\rho^2 - t^2} \sqrt{\rho'^2 - t^2}} = -\frac{U}{4},$$

and then combining terms to give

$$\left[\int_0^a \int_a^b + \int_a^\rho \int_t^b \right] \frac{\rho' \alpha(\rho') d\rho' dt}{\sqrt{\rho^2 - t^2} \sqrt{\rho'^2 - t^2}} = -\frac{U}{4}.$$

Finally, the above equation takes the form

$$\int_a^\rho \frac{dt}{\sqrt{\rho^2 - t^2}} \int_t^b \frac{\rho' \alpha(\rho') d\rho'}{\sqrt{\rho'^2 - t^2}} = -\frac{U}{4} - \int_a^b \rho' \alpha(\rho') d\rho' \int_0^a \frac{dt}{\sqrt{\rho^2 - t^2} \sqrt{\rho'^2 - t^2}}. \quad (3.20)$$

We write

$$G(t) = \int_t^b \frac{\rho' \alpha(\rho') d\rho'}{\sqrt{\rho'^2 - t^2}} \quad (a < t < b) \quad (3.21)$$

The inversion of (3.21) is a special case ($c = 1/2$) of Lemma 3, or equations (3.17) and (3.18). Accordingly,

$$\rho' \alpha(\rho') = -\frac{2}{\pi} \frac{d}{d\rho'} \int_{\rho'}^b \frac{tG(t) dt}{\sqrt{t^2 - \rho'^2}} \quad (a < \rho' < b) \quad (3.22)$$

Also for simplicity, we write

$$B(\rho) = -\frac{U}{4} - \int_a^b \rho' \alpha(\rho') d\rho' \int_0^a \frac{dt}{\sqrt{\rho^2 - t^2} \sqrt{\rho'^2 - t^2}} \quad (3.23)$$

Equation (3.20) then becomes

$$\int_a^\rho \frac{G(t) dt}{\sqrt{\rho^2 - t^2}} = B(\rho) \quad (3.24)$$

Consider $B(\rho)$ as a known function; the above equation may be inverted according to Lemma 2, or equations (3.15) and (3.16), for the special case $c = 1/2$. The result is as follows:

$$\begin{aligned} G(t) &= \frac{2}{\pi} \frac{d}{dt} \int_a^t \frac{\rho B(\rho) d\rho}{\sqrt{t^2 - \rho^2}} \\ &= \frac{2}{\pi} \frac{d}{dt} \left[-\frac{U}{4} \int_a^t \frac{\rho d\rho}{\sqrt{t^2 - \rho^2}} - \int_a^t \int_a^b \int_0^a \frac{\rho \rho' \alpha(\rho') du d\rho' d\rho}{\sqrt{t^2 - \rho^2} \sqrt{\rho^2 - u^2} \sqrt{\rho'^2 - u^2}} \right] \\ &= -\frac{2}{\pi} \left\{ \frac{U}{4} \frac{t}{\sqrt{t^2 - a^2}} + \int_0^a du \int_a^b \left[\frac{\rho' \alpha(\rho') d\rho'}{\sqrt{\rho'^2 - u^2}} \right. \right. \\ &\quad \left. \left. \times \left(\frac{d}{dt} \int_a^t \frac{\rho d\rho}{\sqrt{t^2 - \rho^2} \sqrt{\rho^2 - u^2}} \right) \right] \right\}. \end{aligned} \quad (3.25)$$

We shall now substitute (3.22) for $\rho' \alpha(\rho')$ into the above equation.

First, observe that

$$\begin{aligned} \int_a^b \frac{\rho' \alpha(\rho') d\rho'}{\sqrt{\rho'^2 - u^2}} &= -\frac{2}{\pi} \int_a^b \frac{1}{\sqrt{\rho'^2 - u^2}} \left(\frac{d}{d\rho'} \int_{\rho'}^b \frac{sG(s) ds}{\sqrt{s^2 - \rho'^2}} \right) d\rho' \\ &= \frac{2}{\pi} \sqrt{a^2 - u^2} \int_a^b \frac{sG(s) ds}{(s^2 - u^2) \sqrt{s^2 - a^2}}, \end{aligned} \quad (3.26)$$

and also

$$\frac{d}{dt} \int_a^t \frac{\rho d\rho}{\sqrt{t^2 - \rho^2} \sqrt{\rho^2 - u^2}} = \frac{t \sqrt{a^2 - u^2}}{(t^2 - u^2) \sqrt{t^2 - a^2}}. \quad (3.27)$$

Thus, equation (3.25) reduces to

$$\begin{aligned} G(t) &= -\frac{2}{\pi} \frac{t}{\sqrt{t^2 - a^2}} \left[\frac{U}{4} + \frac{2}{\pi} \int_0^a \frac{a^2 - u^2}{t^2 - u^2} du \int_a^b \frac{sG(s) ds}{(s^2 - u^2) \sqrt{s^2 - a^2}} \right] \\ &= -\frac{2}{\pi} \frac{t}{\sqrt{t^2 - a^2}} \left[\frac{U}{4} + \frac{2}{\pi} \int_a^b \frac{sG(s) ds}{\sqrt{s^2 - a^2}} \int_0^a \frac{(a^2 - u^2) du}{(t^2 - u^2)(s^2 - u^2)} \right]. \end{aligned} \quad (3.28)$$

The last integral in (3.28) is evaluated to be

$$\begin{aligned} \int_0^a \frac{(a^2 - u^2) du}{(t^2 - u^2)(s^2 - u^2)} &= \frac{1}{2(t^2 - s^2)} \left(\frac{t^2 - a^2}{t} \log \frac{t+a}{t-a} - \frac{s^2 - a^2}{s} \log \frac{s+a}{s-a} \right) \\ &\quad (a < \frac{t}{s} < b). \end{aligned} \quad (3.29)$$

Therefore, (3.28) is finally reduced to a Fredholm integral equation of the second kind,

$$G(t) = -\frac{U}{2\pi} \frac{t}{\sqrt{t^2 - a^2}} - \frac{4}{\pi} \int_a^b K(t, s) G(s) ds \quad (a < \frac{t}{s} < b), \quad (3.30)$$

where the kernel $K(t,s)$ is

$$K(t,s) = \frac{ts}{2\sqrt{t^2-a^2}\sqrt{s^2-a^2}(t^2-s^2)} \left(\frac{t^2-a^2}{t} \log \frac{t+a}{t-a} - \frac{s^2-a^2}{s} \log \frac{s+a}{s-a} \right). \quad (3.31)$$

Fredholm integral equations of the second kind can be evaluated numerically by well established procedures. The problem is thus considered solved. All the flow quantities desired may then be determined from the numerical result of $G(t)$ using equations (3.22), (3.11) and (3.12).

To obtain the pressure distribution on the annulus wall, equation (3.11) is rewritten as

$$p(\vec{x}) = p_\infty + 2\mu \frac{\partial \Phi}{\partial x}, \quad (3.32)$$

where

$$\begin{aligned} \Phi(\vec{x}) &= \int_a^b \int_0^{2\pi} \frac{-\alpha(\rho')\rho' d\theta' d\rho'}{R} \\ &= - \int_W \frac{\alpha(\vec{\zeta}')}{|\vec{x} - \vec{\zeta}'|} dS_{\vec{\zeta}'} \quad , \end{aligned} \quad (3.33)$$

in which W indicates that the integration is over the wall of the annulus. The pressure jump across the annulus wall can then be expressed by

$$p_+ - p_- = 2\mu \left[\left(\frac{\partial \Phi}{\partial x} \right)_+ - \left(\frac{\partial \Phi}{\partial x} \right)_- \right], \quad (3.34)$$

where "+" and "-" denote the positive and negative sides of the plane $x = 0$, respectively. The jump $\left[\left(\frac{\partial \Phi}{\partial x} \right)_+ - \left(\frac{\partial \Phi}{\partial x} \right)_- \right]$, in accordance with (3.33), is known to be $4\pi\alpha$. Hence

$$p_+ - p_- = + 8\pi\mu\alpha . \quad (3.35)$$

Since $(p - p_\infty)$ is odd in x , the pressure distribution on the wall is finally obtained as

$$p_\pm(\rho) = p_\infty \pm 4\pi\mu\alpha(\rho) \quad (a < \rho < b) . \quad (3.36)$$

In terms of the function $G(t)$, the above becomes

$$p_\pm(\rho) = p_\infty \mp \frac{8}{\rho} \frac{d}{d\rho} \int_\rho^b \frac{tG(t) dt}{\sqrt{t^2 - \rho^2}} \quad (a < \rho < b) . \quad (3.37)$$

The drag D experienced by the annulus is seen to be due to the pressure jump alone. It may be evaluated from

$$D = 2\pi \int_a^b (p_- - p_+) \rho d\rho , \quad (3.38)$$

or equivalently, the drag is simply the sum of forces experienced by all Stokeslets, namely

$$D = 2\pi \int_a^b -8\pi\mu\alpha(\rho)\rho d\rho = -16\pi^2\mu \int_a^b \rho\alpha(\rho) d\rho . \quad (3.39)$$

Again, in terms of $G(t)$,

$$D = -32\pi\mu \int_a^b \frac{tG(t) dt}{\sqrt{t^2 - a^2}} . \quad (3.40)$$

Next, we observe that the only non-vanishing component of the velocity through the hole of the annulus is given by

$$u_o(\rho) = U + \int_0^a \int_0^{2\pi} \frac{\rho' \alpha(\rho') d\theta' d\rho'}{\sqrt{\rho^2 + \rho'^2 - 2\rho\rho' \cos(\theta - \theta')}} . \quad (3.41)$$

Substitution of (3.22) for $\rho' \alpha(\rho')$ into the above equation yields

$$u_o(\rho) = U + \frac{8}{\pi} \int_a^b \frac{sG(s) ds}{\sqrt{s^2 - a^2}} \int_0^\rho \frac{\sqrt{a^2 - t^2} dt}{(s^2 - t^2) \sqrt{\rho^2 - t^2}} . \quad (3.42)$$

The rate of discharge through the hole may then be obtained by integrating $u_o(\rho)$ over the hole area, giving

$$\begin{aligned} Q_o = 2\pi \int_0^a \rho u_o d\rho &= \pi a^2 U + 16 a \int_a^b \frac{sG(s) ds}{\sqrt{s^2 - a^2}} \\ &\quad - 8 \int_a^b \sqrt{s^2 - a^2} \log \frac{s+a}{s-a} G(s) ds . \end{aligned} \quad (3.43)$$

The mean velocity \bar{u}_o through the hole is simply given by $Q_o/\pi a^2$, or

$$\begin{aligned} \bar{u}_o = U \left[1 + \frac{16}{\pi a U} \int_a^b \frac{sG(s) ds}{\sqrt{s^2 - a^2}} \right. \\ \left. - \frac{8}{\pi a^2 U} \int_a^b \sqrt{s^2 - a^2} \log \frac{s+a}{s-a} G(s) ds \right] . \end{aligned} \quad (3.44)$$

In the special case of a solid disk, which corresponds to $a = 0$, the Fredholm integral equation (3.30) reduces to a very simple expression,

$$G(t) = - \frac{U}{2\pi} . \quad (3.45)$$

The corresponding Stokeslet distribution is then given by (3.22) as

$$\alpha(\rho) = -\frac{U}{\pi^2} \frac{1}{\sqrt{b^2 - \rho^2}} \quad . \quad (3.46)$$

Accordingly, equation (3.36) gives the pressure on the wall as

$$p_{\pm} = p_{\infty} \mp \frac{4\mu U}{\pi} \frac{1}{\sqrt{b^2 - \rho^2}} \quad , \quad (3.47)$$

and also equation (3.39) gives for the drag

$$D = 16 \mu U b \quad . \quad (3.48)$$

Both of these results for the pressure distribution and the drag are well-known; see for example, Lamb [20].

We now return to a numerical calculation of the integral equation (3.30). To subdue the square root singularity at $s = a$ in the kernel $K(t, s)$, we make the following change of variables

$$\left. \begin{aligned} t &= \frac{a+b}{2} + \frac{a-b}{2} \cos \theta = h(\theta) \quad , \\ s &= \frac{a+b}{2} + \frac{a-b}{2} \cos \phi = h(\phi) \quad . \end{aligned} \right\} \quad (3.49)$$

We also denote

$$\left. \begin{aligned} H(\theta) &= -\frac{2\pi}{U} \sqrt{\beta-1} \frac{h(\theta)}{\sqrt{h(\theta)+1}} \cos \frac{\theta}{2} G(h(\theta)) \quad , \\ H(\phi) &= -\frac{2\pi}{U} \sqrt{\beta-1} \frac{h(\phi)}{\sqrt{h(\phi)+1}} \cos \frac{\phi}{2} G(h(\phi)) \quad , \end{aligned} \right\} \quad (3.50)$$

where $\beta = b/a$.

Then the integral equation (3.30) becomes

$$\chi(\theta)H(\theta) = \cos \frac{\theta}{2} - \frac{2}{\pi} \cos \frac{\theta}{2} \int_0^\pi \Gamma(\theta, \phi)H(\phi) d\phi, \quad (3.51)$$

where

$$\chi(\theta) = \frac{(h(\theta) + 1)\sqrt{h(\theta) - 1}}{\sqrt{\beta - 1} h^2(\theta)}, \quad (3.52)$$

$$\Gamma(\theta, \phi) = \frac{\frac{h^2(\theta) - 1}{h(\theta)} \log \frac{h(\theta) + 1}{h(\theta) - 1} - \frac{h^2(\phi) - 1}{h(\phi)} \log \frac{h(\phi) + 1}{h(\phi) - 1}}{h^2(\theta) - h^2(\phi)}. \quad (3.53)$$

The kernel (3.53) has a removable singularity at $\theta = \phi$, its value at these points may be evaluated by L'Hopital's rule, giving

$$\Gamma(\theta, \theta) = \frac{h^2(\theta) + 1}{2h^3(\theta)} \log \frac{h(\theta) + 1}{h(\theta) - 1} - \frac{1}{h^2(\theta)}, \quad (3.54)$$

which is seen to have a logarithmic singularity at $\theta = 0$ only.

Using the above transformation, the drag and the mean velocity through the hole as given by (3.40) and (3.44) are reduced to

$$D = 16\mu Ua \int_0^\pi H(\theta) d\theta, \quad (3.55)$$

and

$$\bar{u}_0 = U \left\{ 1 - \frac{8}{\pi^2} \int_0^\pi \left[1 - \frac{\sqrt{\beta - 1}}{2} \frac{(h(\theta) + 1)\sqrt{h(\theta) - 1}}{h(\theta)} \log \frac{h(\theta) + 1}{h(\theta) - 1} \sin \frac{\theta}{2} \right] H(\theta) d\theta \right\}. \quad (3.56)$$

The drag coefficient, formed with respect to the solid disk drag given by equation (3.48), is therefore

$$C_D = \frac{1}{\beta} \int_0^\pi H(\theta) d\theta \quad (3.57)$$

The integral equation (3.51) is solved numerically for $H(\theta)$ by a standard method which approximates the equation by a set of algebraic equations. Gaussian quadrature is used to evaluate the integral so as to avoid encountering the corner point $(\theta = 0, \phi = 0)$ which is logarithmically singular as seen in (3.54). Gaussian ordinates of six, eight and ten are used successively in each computation for a given value of β . The values obtained for $H(\theta)$ are seen to be bounded and are converging, having no singularity throughout the interval from 0 to π . The Gaussian quadrature is also used in the computation of the drag coefficient C_D (equation 3.57) and the mean velocity ratio \bar{u}_o/U (equation (3.56)). The results obtained are listed in the following table.

$\beta = \frac{b}{a}$	C_D			\bar{u}_o/U		
	$n^\dagger = 6$	8	10	6	8	10
10.000	0.99968	0.99980	0.99983	0.02748	0.02761	0.02742
5.000	0.99871	0.99883	0.99887	0.05529	0.05495	0.05476
2.000	0.98081	0.98093	0.98098	0.14422	0.14393	0.14381
1.600	0.95955	0.95967	0.95972	0.18825	0.18801	0.18790
1.350	0.92479	0.92491	0.92496	0.23740	0.23721	0.23712
1.250	0.89741	0.89753	0.89757	0.26828	0.26811	0.26805
1.200	0.87744	0.87756	0.87760	0.28853	0.28837	0.28831
1.125	0.83245	0.83256	0.83260	0.32996	0.32984	0.32979
1.070	0.77524	0.77534	0.77538	0.37804	0.37794	0.37789
1.040	0.72190	0.72199	0.72202	0.42068	0.42059	0.42056

$\beta = \frac{b}{a}$	C_D			\bar{u}_o/U		
	$n^\dagger = 6$	8	10	6	8	10
1.020	0.66133	0.66141	0.66144	0.46814	0.46808	0.46805
1.010	0.60793	0.60799	0.60801	0.50992	0.50987	0.50985
1.005	0.56142	0.56147	0.56149	0.54655	0.54650	0.54648
1.001	0.47538	0.47542	0.47543	0.61509	0.61506	0.61505
1.0001	0.38919	0.38922	0.38919	0.68459	0.68456	0.68458
1.0000	(0)			(1)		

$^\dagger n$ is the number of Gaussian ordinates used.

We see from this table that the convergence is good. The values corresponding to ten Gaussian ordinates may be considered accurate to the fourth decimal place. The total time consumed on an IBM 7094 computer for this problem was 33 sec.

The drag coefficient C_D and the mean velocity ratio \bar{u}_o/U are plotted against the porosity η of the annulus in Fig. 3. The porosity η is defined to be the ratio of the hole area πa^2 to the total area πb^2 , namely, $\eta = a^2/b^2 = 1/\beta^2$. The reduction in drag is seen to be very small when the porosity is small or moderate. Even when as much as 50% of area is missing from a solid disk, the drag is only reduced by 6%. When the porosity approaches unity, however, C_D reduces rapidly to zero. It is also apparent from this plot that it is difficult for the flow to go through the hole; the mean velocity \bar{u}_o is only a fraction of the free stream velocity U when η is small. As η approaches unity, of course, \bar{u}_o approaches U . These characteristics are expected in general for a porous body in very viscous flow.

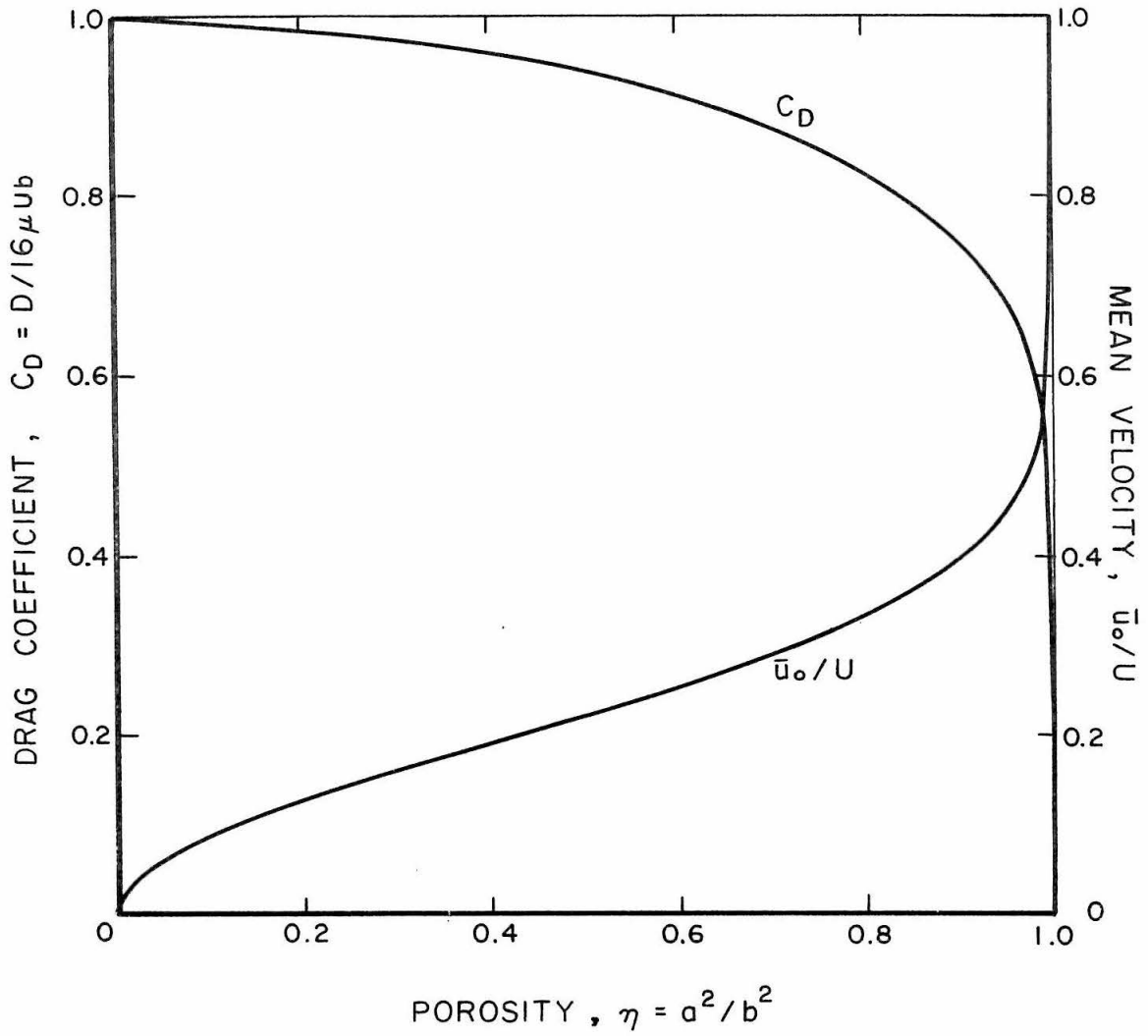


Fig. 3. Drag coefficient and mean velocity through the hole of a circular annulus in Stokes flow.

IV. STOKES FLOW PAST A THIN CIRCULAR SCREEN

Consider a uniform Stokes flow past a thin circular screen possessing numerous holes. The screen has a radius a and its plane coincides with the coordinate plane $x = 0$. Cylindrical polar coordinates (r, θ, x) will be used in this analysis. The velocity components in the corresponding directions will be denoted by v , w and u respectively.

Obtaining a solution for the microscopic flow in this case is, of course, beyond our means, but we may consider a mean flow instead of the microscopic one. In particular, the mean velocity and pressure at the screen are assumed to be the averages over a screen area which is small compared with the total area of the screen and yet still includes a large number of holes. The mean quantities are further assumed to vary smoothly throughout the flow field.

The mean flow should also satisfy Stokes equations (2.1) and (2.2), because these equations are linear. We shall use the same symbols for the mean quantities as for their microscopic counterparts. Therefore,

$$-\nabla p + \mu \nabla^2 \vec{u} = 0 , \quad (4.1)$$

$$\nabla \cdot \vec{u} = 0 . \quad (4.2)$$

The symmetrical nature of the flow expressed by (2.9) should still hold for the mean flow. In particular,

$$v, w = 0 , \quad \text{at } x = 0 , \quad (4.3)$$

for points on the screen as well as those outside the screen.

The mean pressure must have a jump across the screen. The magnitude of the jump is expected to be linked somehow with the local mean normal velocity through the screen. In fact, assuming a local uniform flow through the screen, we may perform a dimensional analysis for the following group of parameters: u , Δp , μ , ℓ where $\Delta p = p_+ - p_-$ denotes the pressure jump and ℓ denotes a characteristic size of the holes. The analysis yields the following linear relation:

$$u = - \frac{k}{\mu} \Delta p \quad (x = 0, \quad \rho < a) , \quad (4.4)$$

where k is a proportionality constant which is termed the permeability. The magnitude of the permeability k measures the ease with which the flow passes through the screen. The relation (4.4) is very much like Darcy's law for flow through porous media, except that k here has a dimension of length while that in Darcy's law has a dimension of length squared. The permeability is expected to be dependent upon the detailed structure of the screen alone, such as the hole size ℓ , the hole shapes, and the porosity of the screen. It should not depend upon the fluid properties, nor upon the overall size and shape of the screen. We shall assume the screen has a homogeneous structure so that k is a constant of the screen material.

The permeability k must be determined by experiment, but for some idealized hole structures, it may also be deduced by a theoretical analysis. For example, an ideal screen may consist of a

series of equal, parallel slits. Hasimoto [9] obtained an exact solution for a uniform Stokes flow past such a screen of infinite size. From his solution, we deduce that

$$k = \frac{1}{4\pi} \frac{|\log \cos \frac{\pi}{2} \eta|}{1 - \eta} d , \quad (4.5)$$

where η is the porosity of the screen defined as the ratio of the hole area to the total area of the screen. For the case of equal parallel slits,

$$\eta = \frac{\ell}{\ell + d} , \quad (4.6)$$

where ℓ is the width of the slit and d is the width of the wall between the successive slits.

The Stokes problem for the above circular screen is described by equations (4.1) and (4.2) under the approximate boundary conditions (4.3) and (4.4) together with the following condition at infinity:

$$\vec{u} \rightarrow U\vec{e}_1 , \quad p \rightarrow p_\infty , \quad \text{as } |x| \rightarrow \infty , \quad (4.7)$$

where \vec{e}_1 is a unit vector in the direction of the x -axis.

The problem may be reduced to an associated electric potential problem similar to that formulated generally in Chapter II.

$$p = p_\infty + 2\mu \frac{\partial \Phi}{\partial x} , \quad (4.8)$$

$$\vec{u} = (U - \Phi)\vec{e}_1 + x\nabla\Phi , \quad (4.9)$$

where

$$\nabla^2 \Phi = 0 \quad , \quad (4.10)$$

with the boundary conditions ,

$$\begin{aligned} U - \Phi &= -2k \left[\left(\frac{\partial \Phi}{\partial x} \right)_+ - \left(\frac{\partial \Phi}{\partial x} \right)_- \right] \\ &= \mp 4k \left(\frac{\partial \Phi}{\partial x} \right)_\pm \quad (x = 0, \rho < a) \quad , \quad (4.11) \end{aligned}$$

$$\frac{\partial \Phi}{\partial x} = 0 \quad (x = 0, \rho > a) \quad , \quad (4.12)$$

$$\Phi \rightarrow 0, \quad \text{as} \quad |\vec{x}| \rightarrow \infty \quad . \quad (4.13)$$

The boundary condition (4.11) is a linear combination of "Dirichlet" and "Neumann" conditions. The potential Φ , satisfying this condition and the others, (4.12) and (4.13), should be unique.

To solve the potential problem (4.10) - (4.13), we shall assume a surface source density $\gamma(\rho)$ distributed axisymmetrically over the screen ($\rho < a$). The potential $\Phi(\vec{x})$ due to such a source distribution is given by

$$\Phi(x) = \int_0^a \int_0^{2\pi} \frac{\rho' \gamma(\rho') d\theta' d\rho'}{\sqrt{x^2 + \rho^2 + \rho'^2 - 2\rho\rho' \cos(\theta - \theta')}} \quad , \quad (4.14)$$

The surface source density $\gamma(\rho)$ is then to be determined by requiring the potential Φ to satisfy the boundary conditions (4.11) to (4.13). The last two conditions are automatically satisfied, while the first one reduces to

$$U - \Phi = 8\pi k \gamma(\rho) \quad , \quad (x = 0, \rho < a) \quad , \quad (4.15)$$

by using the following well-known jump relation as given by (2.21):

$$\left(\frac{\partial\Phi}{\partial x}\right)_+ - \left(\frac{\partial\Phi}{\partial x}\right)_- = -4\pi\gamma(\rho) \quad . \quad (4.16)$$

The boundary condition (4.15), written out explicitly, is an integral equation for $\gamma(\rho)$

$$U - \int_0^a \rho' \gamma(\rho') d\rho' \int_0^{2\pi} \frac{d\theta}{\sqrt{\rho^2 + \rho'^2 - 2\rho\rho' \cos(\theta - \theta')}} = 8\pi k\gamma(\rho) \quad . \quad (4.17)$$

Upon application of Lemma 1 of Chapter III, this becomes

$$U - 4 \left[\int_0^\rho \int_0^{\rho'} - \int_\rho^a \int_0^\rho \right] \frac{\rho' \gamma(\rho') dt d\rho'}{\sqrt{\rho^2 - t^2} \sqrt{\rho'^2 - t^2}} = 8\pi k\gamma(\rho) \quad . \quad (4.18)$$

After interchanging the order of integration, we get

$$U - 4 \int_0^\rho \frac{dt}{\sqrt{\rho^2 - t^2}} \int_t^a \frac{\rho' \gamma(\rho') d\rho'}{\sqrt{\rho'^2 - t^2}} = 8\pi k\gamma(\rho) \quad . \quad (4.19)$$

We write

$$G(t) = \int_t^a \frac{\rho' \gamma(\rho') d\rho'}{\sqrt{\rho'^2 - t^2}} \quad (t < a) \quad . \quad (4.20)$$

The inversion of this integral equation has been given by Lemma 3 of Chapter III to be

$$\rho' \gamma(\rho') = -\frac{2}{\pi} \frac{d}{d\rho'} \int_{\rho'}^a \frac{t G(t) dt}{\sqrt{t^2 - \rho'^2}} \quad (\rho' < a) \quad . \quad (4.21)$$

Substitution of both (4.20) and (4.21) into (4.19) yields the

following equation for $G(t)$:

$$U - 4 \int_0^{\rho} \frac{G(t) dt}{\sqrt{\rho^2 - t^2}} = -16k \frac{1}{\rho} \frac{d}{d\rho} \int_{\rho}^a \frac{tG(t) dt}{\sqrt{t^2 - \rho^2}} . \quad (4.22)$$

Multiplied throughout by ρ , this equation is integrated from ρ to a ,

$$\begin{aligned} U \int_{\rho}^a \rho'^2 d\rho' - 4 \int_{\rho}^a \rho' d\rho' \int_0^{\rho'} \frac{G(t) dt}{\sqrt{\rho'^2 - t^2}} \\ = -16k \int_{\rho}^a \frac{d}{d\rho'} \left[\int_{\rho'}^a \frac{tG(t) dt}{\sqrt{t^2 - \rho'^2}} \right] d\rho' , \end{aligned} \quad (4.23)$$

giving

$$\begin{aligned} 4k \int_{\rho}^a \frac{tG(t) dt}{\sqrt{t^2 - \rho^2}} \\ = \frac{U}{8} (a^2 - \rho^2) - \int_0^a \sqrt{a^2 - t^2} G(t) dt + \int_0^{\rho} \sqrt{\rho^2 - t^2} G(t) dt . \end{aligned} \quad (4.24)$$

Let the right-hand side of (4.24) be denoted by $B(\rho)$. Considering $B(\rho)$ as a known function, (4.24) may be inverted according to Lemma 3 of Chapter III to give

$$4ktG(t) = -\frac{2}{\pi} \frac{d}{dt} \int_t^a \frac{\rho B(\rho) d\rho}{\sqrt{\rho^2 - t^2}} . \quad (4.25)$$

Substituting $B(\rho)$ back into the equation and carrying out the integrations and differentiations successively, we finally obtain a Fredholm integral equation of the second kind for the function $G(t)$, that is,

$$2\pi k G(t) = \frac{U}{4} \sqrt{a^2 - t^2} - \int_0^a K(t, s) G(s) ds, \quad (4.26)$$

where

$$K(t, s) = \log \frac{\sqrt{a^2 - t^2} + \sqrt{a^2 - s^2}}{\sqrt{|t^2 - s^2|}}. \quad (4.27)$$

A Fredholm integral equation of the second kind can be solved by a certain standard numerical method, and so the potential problem is considered solved. The flow quantities of the original Stokes problem may then be deduced from the numerical function $G(t)$, and hence the Stokes problem is also considered solved.

For the pressure distribution on the screen, we have from (4.8) and (4.16), taking into consideration that $\partial\Phi/\partial x$ is odd in x ,

$$p_{\pm} = p_{\infty} \mp 4\pi\mu\gamma(\rho) \quad (x = 0, \rho < a). \quad (4.28)$$

Upon substitution from (4.21), we obtain

$$p_{\pm} = p_{\infty} \pm 8\mu \frac{1}{\rho} \frac{d}{d\rho} \int_0^a \frac{tG(t) dt}{\sqrt{t^2 - \rho^2}} \quad (x = 0, \rho < a). \quad (4.29)$$

The mean viscous stresses at the screen can be shown to be zero, and hence the drag of the screen is due to the pressure jump alone. The drag D is therefore

$$\begin{aligned} D &= 2\pi \int_0^a (p_- - p_+) \rho d\rho \\ &= 32\pi\mu \int_0^a G(t) dt. \end{aligned} \quad (4.30)$$

A drag coefficient C_D may be formed with respect to the solid disk drag, $16\mu Ua$, so that

$$C_D = \frac{2\pi}{Ua} \int_0^a G(t) dt . \quad (4.31)$$

The normal velocity through the screen is given by the boundary condition (4.4), that is

$$u = -\frac{k}{\mu} (p_+ - p_-) \quad (x = 0, \rho < a) . \quad (4.4)$$

Averaging (4.4) over the whole screen, we obtain the following simple relation between the mean velocity \bar{u}_0 through the screen and the drag coefficient C_D

$$\frac{\bar{u}_0}{U} = \frac{16}{\pi} \left(\frac{k}{a}\right) C_D . \quad (4.32)$$

To facilitate the numerical computation of the integral equation (4.26) we shall make the following change of variables:

$$t = a\xi \quad , \quad s = a\eta \quad ; \quad (4.33)$$

and

$$H(\xi) = \frac{2\pi}{U} G(a\xi) \quad , \quad H(\eta) = \frac{2\pi}{U} G(a\eta) . \quad (4.34)$$

Equation (4.26), therefore, becomes

$$2\pi \frac{k}{a} H(\xi) = \frac{\pi}{2} \sqrt{1 - \xi^2} - \int_0^1 \Gamma(\xi, \eta) H(\eta) d\eta , \quad (4.35)$$

where

$$\Gamma(\xi, \eta) = \log \frac{\sqrt{1-\xi^2} + \sqrt{1-\eta^2}}{\sqrt{|\xi^2 - \eta^2|}} \quad . \quad (4.36)$$

The drag coefficient, equation (4.31), is reduced to

$$C_D = \int_0^1 H(\xi) d\xi \quad . \quad (4.37)$$

The integral equation (4.35) is solved approximately by a set of algebraic equations. For a given value of a/k , the function $H(\xi)$ is evaluated successively at ten, twenty and forty equally spaced points within the interval (0,1). The logarithmic singularity at $\eta = \xi$ of the kernel $\Gamma(\xi, \eta)$ has been properly taken care of in the evaluation of the integral. To integrate equation (4.37) for C_D , use has been made of Simpson's rule. The results obtained for the drag coefficient C_D are tabulated in the following:

$\frac{a}{k}$	C_D		
	$n^\dagger = 10$	20	40
1	0.163	0.162	0.162
5	0.481	0.480	0.479
10	0.641	0.639	0.638
20	0.772	0.769	0.768
30	0.831	0.827	0.826
50	0.888	0.884	0.882
100	0.939	0.934	
200	0.969	0.965	
300	0.979	0.976	
1000	0.996	0.993	

$^\dagger n$ is the number of ordinates used in the solution of $H(\xi)$.

From this table, we see that the convergence is very good for increasing number of ordinates used in the numerical solution of the integral equation. The total time used on an IBM 7094 Computer for this problem amounted to 58 sec. only.

The drag coefficient C_D is plotted against a/k in Fig. 4. It is seen that its values are always below unity, that is, the drag of a circular screen is less than that of a circular disk of the same radius a . To obtain certain physical feeling as to the porosity effect of the screen, we approximate it by a parallel slit model. Based on (4.5), if the porosity η is 0.5, the value of a/k is 180 for 10 slits and 1800 for 100 slits in the screen. At these values of a/k , C_D is very close to unity and the screen behaves like a solid one. Only when η becomes unrealistically large, can a screen experience a substantial reduction in its drag. For example, $\eta = 0.95$, the ratio a/k becomes 20 for 10 slits and 200 for 100 slits in the screen. The corresponding C_D is 0.77 and 0.97 respectively. At this porosity, however, the width of the slit must be 19 times greater than that of the wall. The plot also gives \bar{u}_0/U as a function of a/k . The mean velocity \bar{u}_0 through the holes of the screen becomes exceedingly small when $a/k > 200$, and hence it shows the tremendous blockage effect of the screen at low Reynolds numbers.

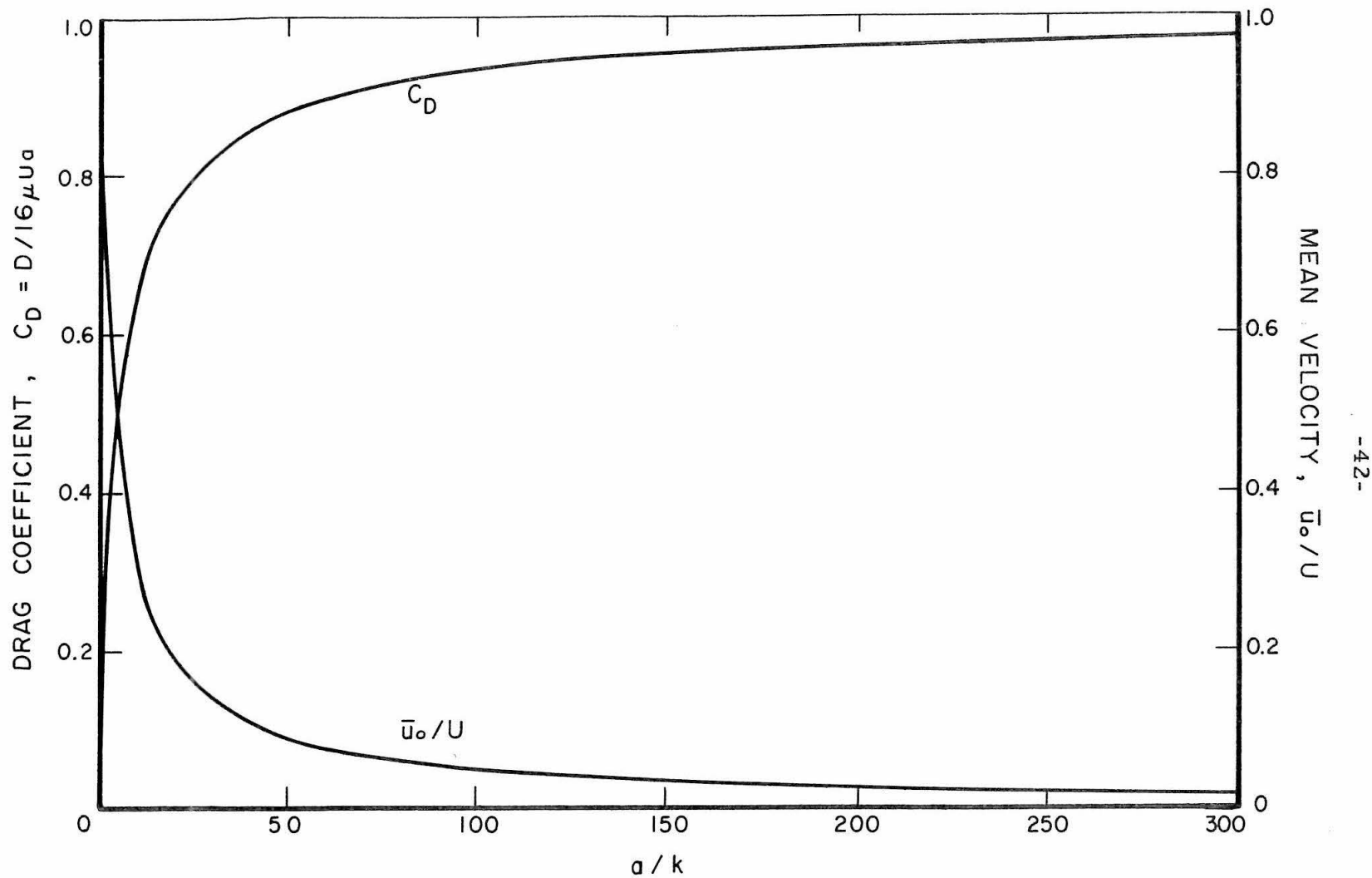


Fig. 4. Drag coefficient and mean velocity through the holes of a circular screen in Stokes flow.

REFERENCES

1. Illingworth, C. R., "Flow at Small Reynolds Number," Chapter IV of Laminar Boundary Layers, ed. by L. Rosenhead, Oxford, (1963).
2. Langlois, W. E., Slow Viscous Flow, Macmillan, N.Y., (1964).
3. Tamada, K. and Fujikawa, H., "The Steady Two-dimensional Flow of Viscous Fluid at Low Reynolds Numbers Passing Through an Infinite Row of Equal Parallel Circular Cylinders," Quart. J. Mech. Appl. Math., Vol. 10, (1967), pp. 425-432.
4. Miyagi, T., "Viscous Flow at Low Reynolds Numbers Past an Infinite Row of Equal Circular Cylinders," J. Phy. Soc. Japan, Vol. 13, (1958), pp. 493-496.
5. Kuwabara, S., "The Forces Experienced by a Lattice of Elliptic Cylinders in a Uniform Flow at Small Reynolds Numbers," J. Phy. Soc. Japan, Vol. 14, (1959), pp. 522-527.
6. Kuwabara, S., "The Forces Experienced by a Lattice of Equal Flat Plates in a Uniform Flow at Small Reynolds Numbers," J. Phy. Soc. Japan, Vol. 13, (1958), pp. 1516-1523.
7. Keller, J. B., "Viscous Flow Through a Grating or Lattice of Cylinders," J. Fluid Mech., Vol. 18 (1964), pp. 94-96.
8. Hasimoto, H., "On the Periodic Fundamental Solutions of the Stokes Equations and Their Application to Viscous Flow Past a Cubic Array of Spheres," J. Fluid Mech., Vol. 5, (1959), pp. 317-328.

9. Hasimoto, H., "On the Flow of a Viscous Fluid Past a Thin Screen at Small Reynolds Numbers," J. Phy. Soc. Japan, Vol. 13, (1958), pp. 633-639.
10. Roscoe, R., "The Flow of Viscous Fluids Round Plane Obstacles," Philosophical Magazine, Vol. 40, (1949), pp. 338-351.
11. Joseph, D. D. and Tao, L. N., "The Effect of Permeability on the Slow Motion of a Porous Sphere in a Viscous Liquid," ZAMM, Vol. 44, (1964), pp. 361-364.
12. Joseph, D. D., "Note on Steady Flow Induced by Rotation of a Naturally Permeable Disk," Quart. J. Mech. Appl. Math., Vol. 18, (1965), pp. 325-331.
13. Joseph, D. D. and Tao, L. N., "Ground Flow Induced by a Moving Cylinder," Phys. of Fluid, Vol. 8, (1965), pp. 1438-1499.
14. Joseph, D. D. and Tao, L. N., "Lubrication of a Porous Bearing -- Stokes' Solution," J. Appl. Mech., Trans. ASME, (1966), pp. 753-760.
15. Cooke, J. C., "Triple Integral Equations," Quart. J. Mech. Appl. Math., Vol. 16, (1963), pp. 193-203.
16. Williams, W. E., "Note on the Electrostatic Problem for a Circular Annulus," Quart. J. Mech. Appl. Math., Vol. 16, (1963), pp. 205-207.
17. Jackson, J. D., Classical Electrodynamics, Chapt. 1-4, John Wiley and Sons, N.Y., (1963).
18. Copson, E. T., "On the Problem of the Electrified Disc," Proc. Edingburgh Math. Soc., Series (2), Vol. 8, (1947), pp. 14-19.

19. Sneddon, I. N. , Mixed Boundary Value Problems in Potential Theory, Chapt. II, North-Holland Publishing Co. , Amsterdam, Distributed in U.S.A. by John Wiley and Sons, N.Y. , (1966).
20. Lamb, H. , Hydrodynamics, sec. 339, Chapt. XI, pp. 604-605, Dover, N.Y. , (1932 ed.).

PART TWO
VISCOUS FLOWS PAST POROUS BODIES OF FINITE SIZE

I. INTRODUCTION

Many physical phenomena and engineering applications involve viscous flow around and through porous bodies. Examples are the lubrication of porous bearings which are often used as machine elements, viscous gravity waves propagating over a permeable bed, viscous flow through porous rollers used in paper mills, etc. There are also flows which have great fundamental interest, such as the viscous flow past a porous sphere and the rotation of a porous cylinder in a viscous fluid.

These flow phenomena have a common feature in that the motions of the fluid can be divided into two distinctive regions. One region is that of the porous material saturated with the fluid, and the other is a pure fluid region where no solid materials are present. The flow in these two regions is governed by two different sets of differential equations, and the flow quantities at the interface joining the two regions must be related by a set of appropriate conditions. These conditions will be called interface boundary conditions. The actual flow in the porous region passes through many interwoven passages. Its complexity necessitates using an averaging method which replaces the detailed flow by an equivalent mean flow. This mean flow is supposed to be distributed homogeneously throughout the space originally occupied by the porous region. The empirical law of Darcy[†] is commonly used to describe such a mean flow

[†]For flow through porous media and Darcy's law, see [1] and [2].

provided certain restrictive conditions are met. For the flow in the fluid region, we shall limit our attention to Newtonian fluids satisfying the full Navier-Stokes equations or satisfying their limiting forms for small Reynolds number flows, i.e. Stokes' and Oseen's equations. The interface boundary conditions, therefore, serve to connect the flow variables of Darcy's law applied on one side of the interface to those of the viscous flow equations applied on the other side. Since the corresponding flow variables in the neighboring regions are actually derived from somewhat different definitions, it is not readily clear how to make associations between them. This is one of the main reasons why the interface boundary conditions have been controversial in recent years. The purpose of this investigation is to clarify the interface boundary conditions and to formulate them correctly.

Recent studies on porous body flows have been made by Tao, Joseph, and Shir [3] - [7]. Their analyses include the slow motion of a porous sphere, the rotation of a porous disc, the ground flow induced by a moving cylinder, as well as the lubrication of a porous bearing. The interface boundary conditions used in these studies were as follows: (1) the normal velocity on the fluid side equals the normal superficial velocity[†] on the porous side; (2) the pressure on the fluid side equals the mean pressure[†] on the porous side; and (3) the tangential velocity on the fluid side vanishes. The third boundary

[†]For definitions of superficial velocity and mean pressure, see Chapter II.

condition on tangential velocity is a debatable one because the interface actually contains many holes and a tangential movement of fluid is possible at least over the hole parts of the interface boundary. The net effect could very well be a slip rather than a non-slip condition for the tangential velocity on the fluid side of the interface.

The authors mentioned above have also assumed that the third condition is approximately valid when the permeability[†] is small compared with some typical gross area of the porous body. However, the slip velocity can still be large and important in some cases even when the above criterion is satisfied. An illustration of this point is seen in an experiment involving Poiseuille channel flow over a naturally permeable block reported by Beavers and Joseph [8]. They found that when the gap of the channel is small, the fluid efflux is greatly increased over the value it would have been if the block were impermeable. This indicates the presence of a large slip velocity immediately adjacent to the permeable surface, and appears to be the case regardless of the value of the permeability. This slip effect was attributed to the existence of a thin layer immediately inside the permeable block, in which Darcy's law is not applicable and across which the tangential velocity changes continuously from its interior mean value to the slip value outside the block. The slip velocity can be considerably greater than the interior mean velocity. Their difference, or the tangential velocity jump across the thin layer, was found to be proportional to the normal gradient of the tangential

[†] For permeability, see [1] and [2], or Chapter II.

velocity outside the block. From these findings, it appears that if Darcy's law is used to model the flow through the porous region, the interface boundary conditions should relate flow variables on the two boundaries of the thin layer instead of at the crudely simplified interface of zero thickness. In particular, the tangential velocity jump condition should replace the non-slip tangential velocity condition mentioned previously.

There have also been studies on the viscous damping of a gravity wave propagating over a porous bed. Hunt [9] in his treatment assumed almost the same set of interface boundary conditions as used by Tao et al. However, instead of relating just the pressures, he included also the normal viscous stresses and required the total normal stresses to be continuous across the interface. Murray [10] repeated the analysis of the same problem but adopted a different set of interface boundary conditions. He related (but did not make equal) both the normal and the tangential velocities across the interface. He established a third condition derived from energy conservation at the interface.

In the literature to date, different sets of interface boundary conditions have been used by different investigators. Unfortunately, none of these sets have been supported by convincing proof. The reason behind the confusion is largely due to the fact that clear cut definitions of the flow variables for the equivalent mean flow in the porous region and an understanding of the true nature of such a flow are still lacking. Therefore, it is necessary that the flow in a porous

medium be studied thoroughly before any interface boundary conditions can be formulated correctly.

The following chapter is devoted to a critical examination of the flow in porous medium. Darcy's law is first reviewed and its limitations concluded. Then, continuing on beyond the usual empirical point of view, we consider the mean flow to be built up from those microscopic flow through the winding narrow passages. Assuming the microscopic flow to be sufficiently random, and that Stokes' equations for slow viscous flow are applicable for their description, general macroscopic equations of motion for the apparent mean flow are derived by a statistical means. This statistical approach also enables us to define unambiguously all the mean flow variables. The resulting macroscopic equations are believed to be more generally valid than Darcy's law, and actually reduce to Darcy's law when the Darcy number is small. The Darcy number, to be defined in the analysis later on, measures the relative importance of the mean viscous force with respect to the mean resistance provided by the solid material in the porous medium. Chapter II concludes with a study of the energy balance in a porous medium.

Establishment of the above mentioned macroscopic equations leads to correct formulations of interface boundary conditions. A correct formulation should be one of the following: (1) Establish correct equations of motion for flow in the whole porous region up to the immediate neighborhood of the interface and then relate corresponding flow variables across the interface of zero thickness.

(2) Continue to use Darcy's law except in a thin but finite porous layer at the interface and then obtain jump conditions on the flow variables across this layer. Both of these formulations will be considered in Chapter III. The macroscopic equations obtained herein are appropriate for the first formulation mentioned above. In addition, when the macroscopic equations are applied, as will be illustrated by an example, the solution clearly shows that there usually exists an interface layer across which the mean tangential velocity varies rapidly and, consequently, the mean viscous stresses are not negligible. This is the layer in which Darcy's law ceases to apply. A nominal thickness of the layer is derived from the analysis and its order of magnitude is comparable to the grain size of porous media arising in general practice. In spite of the thinness of the layer, the contribution to the tangential velocity jump is, however, not small. An analysis of flow within an interface layer of general nature actually leads to the full establishment of the interface boundary conditions of the second kind.

In the last chapter, both types of interface boundary conditions are applied to the analytic solutions of two fundamental problems. One is the Stokes flow past a porous sphere; the other is the viscous flow between two cylinders, the outer one is impermeable and rotating at a constant speed, while the inner one is porous and stationary. Both examples are valuable in demonstrating (1) the existence of a solution of these types of coupled flow problems, and (2) the porosity effect of a porous body on the external flow.

II. EQUATIONS OF MOTION FOR FLOW THROUGH POROUS MEDIA

2.1. Empirical Darcy's Law

We begin with a brief review of the structure of porous media and the empirical law of Darcy.

A porous medium is a solid containing numerous interconnected pores. The pores commonly have two types, one is the intergranular type, like the pores between sand grains; and the other is the interwoven tunnel type, like the pores in material made up by fibers or wires. There are also isolated pores but they do not affect the flow in a porous medium, and are better considered as a part of the solid. The structure of pores, or their complementary solids, can be characterized by many factors, such as surface area, chemical composition, size distributions, etc. In fluid mechanics, two parameters are most important. These are the porosity and the characteristic size. The porosity of a porous medium, η , is defined as the ratio of the volume of all interconnected pores in a gross volume of porous medium to that gross volume. When the distribution of the pores is sufficiently random, both in size and in location, we may consider the porous medium as homogeneous and isotropic. Under such assumptions, if we pass a surface through the medium, the ratio of all surface pores on this surface to the total area of the surface will have the same value as the volume porosity η . Likewise, if we pass a line through such a medium, the line porosity is also the same as the volume porosity. Thus, we have in a homogeneous isotropic porous medium,

$$\begin{aligned}\eta &= \frac{\text{volume of pores}}{\text{total volume}} = \frac{\text{area of surface pores}}{\text{total area}} \\ &= \frac{\text{length of line pores}}{\text{total length}} .\end{aligned}\tag{2.1}$$

All the pores considered are necessarily interconnected. The characteristic size can be defined as the average size either of the solid grains or of the pores of the medium, whichever is more convenient.

The equations governing the flow through the porous medium were established empirically by Darcy in 1856. The equations have since been generalized into the following form:

$$\nabla \cdot \vec{q} = 0,\tag{2.2}$$

$$\vec{q} = - \frac{k}{\mu} \nabla P .\tag{2.3}$$

In the above, \vec{q} is the superficial velocity defined as the rate of volume flow through a cross section of unit area normal to the flow. P is understood to be some sort of mean pressure but without ever being given a clear definition. In an experiment, it is taken to be the pressure measured by a piezometer inserted through the wall of a channel in which fluid flows through a porous medium. Also in the above, μ is the viscosity of the fluid and k is the permeability. The value of permeability measures the ease with which the flow passes through the medium. It is the most important dynamic parameter of flow through a porous medium, because it combines all the influences of the complicated geometrical structure of pores

and solids into a single experimental coefficient. The permeability usually assumes a very small number for ordinary porous media. For example, a sand mixture, of size range 0.139 to 0.211 mm and of porosity 0.37, has a permeability k equal to $0.2 \times 10^{-6} \text{ cm}^2$. Even for wire crimps (each wire crimp is 0.328 mm in diameter and 5.7 mm long) with a porosity 0.76, k is around $1 \times 10^{-4} \text{ cm}^2$.†

Darcy's law has, of course, its intrinsic limitations. According to various investigators, the law is only true under the following conditions:

- i. The macroscopic scale of the porous medium in question is much larger than the characteristic size of the pores.
- ii. The pores in the porous medium are interconnected and saturated with only one fluid.
- iii. The fluid is incompressible, homogeneous and isotropic.
- iv. Both the solids and the fluid are physically and chemically stable and do not react with one another.
- v. The flow through the porous medium is very slow. The slowness is measured by the Reynolds number, $Re = \frac{\rho q d}{\mu}$, where ρ is the fluid density, q is a certain mean velocity in the medium and d is a characteristic size of the pores or of the grains. For example, in a porous medium consisting of uniform spherical particles, Re should be less than 4 if d denotes the diameter of the particle.

Under the conditions outlined above, the permeability k is a

† For some permeability data, see [16].

property of the geometrical structure of the pores or the solids alone. It could in general depend on the position as well as the direction within the medium, but it is independent of the fluid properties. Furthermore, if the porous medium is statistically homogeneous and isotropic, k is a constant of the medium. Then, by dimensional analysis, it can be shown that

$$k = \alpha(\eta, s)d^2, \quad (2.4)$$

where α is a dimensionless coefficient depending on the porosity η and the shape factor s of the pores or the solids.

The Darcy equations (2.2) and (2.3) serve very well in many instances of flow through a bulk of ordinary porous medium, such as flow underneath a dam and underground flow due to pumping of a well.

Mathematically, (2.2) and (2.3) are equivalent to

$$\nabla^2 P = 0, \quad (2.5)$$

$$\vec{q} = -\frac{k}{\mu} \nabla P. \quad (2.3)$$

The harmonic function P can be shown to exist and to be unique when either P or $\frac{\partial P}{\partial n}$ (which is proportional to q_n) or a mixed condition of both of them is prescribed on certain appropriate boundaries.

Further variations of boundary value problems are possible. When P is found, the velocity field is simply given by (2.3).

2.2. Microscopic and Macroscopic Descriptions

Darcy's law, as outlined in the preceding section, is to describe the flow through porous media in a superficial and gross fashion. It is not concerned with the details of the flow throughout the interwoven passages. We call such a gross description a macroscopic description, while one concerned with details of the flows is termed a microscopic description. The microscopic flow is too complicated to analyze, and therefore a macroscopic approach is necessary.

An empirical method, by which Darcy's law was established, is not the only way by which a macroscopic description can be properly deduced or induced. A macroscopic description is most rationally built up from the microscopic flow by statistical means. An adequate statistical formulation does not require a complete knowledge of the microscopic flow.

The same type of concept has been used in kinetic theory which considers random molecular motion as the "microscopic" basis for the "macroscopic" continuous motion of a fluid.

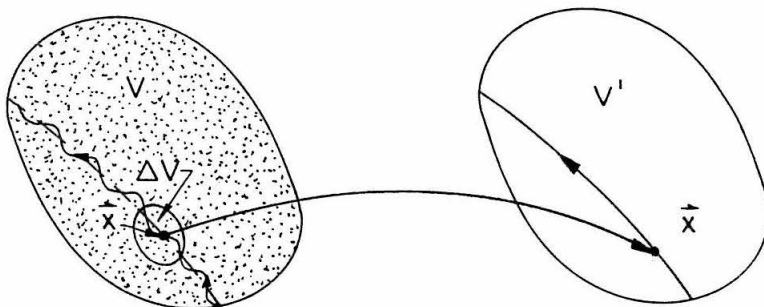


Fig. 1. Microscopic and macroscopic flows.

To begin with the statistical formulation, we consider a porous medium which occupies a region V . Let the microscopic flow inside the region be described by the velocity \vec{u} and the pressure p . A fluid particle usually follows a tortuous path through the medium, as is indicated in Fig. 1. But as viewed from far away the tortuosity of the particle path becomes vague and smoothed. Equivalently, we can consider a smooth mean path, as shown by the dotted line, instead of the original tortuous one. A smoothing effect can be obtained by defining a mean velocity \vec{q}_s and a mean pressure \bar{p} at a point \vec{x} as follows:

$$\vec{q}_s(\vec{x}) = \frac{1}{\Delta V_f} \int_{\Delta V_f(\vec{x})} \vec{u}(\vec{x}') dV , \quad (2.6)$$

$$\bar{p}(\vec{x}) = \frac{1}{\Delta V_f} \int_{\Delta V_f(\vec{x})} p(\vec{x}') dV , \quad (2.7)$$

where the integrations are over ΔV_f , the pore portion of a small region ΔV surrounding \vec{x} . The quantities ΔV_f and ΔV denote the pore volume and the total volume of ΔV , respectively. This averaging process effectively transforms the microscopic flow in the porous medium V to an apparent mean flow, namely, a macroscopic one, in a continuous medium V' . The range of V' is identical to that of V . The transformation is demonstrated graphically in Fig. 1. We shall further assume that the volume ΔV chosen for the averaging is small compared with the overall volume of the region V but is large enough to include sufficiently many pores so that resulting mean values are continuously differentiable to the desired degree throughout the continuous medium V' .

The mean pressure and the mean velocity defined above are seen to be the true average values of their respective microscopic quantities associated with a bulk of fluid. Therefore, \vec{q}_s gives the true velocity of motion of such a bulk of fluid. For this reason, \vec{q}_s will be termed the seepage velocity. In order to compare with the superficial velocity \vec{q} used in Darcy's law, we shall also define a corresponding mean velocity as follows:

$$\vec{q} = \frac{1}{\Delta V} \int_{\Delta V_f(\vec{x})} \vec{u}(\vec{x}') dV . \quad (2.8)$$

The only difference between this and \vec{q}_s is that in the present definition the integral is divided by the total volume ΔV instead of the partial volume ΔV_f . Suppose that the porosity in the neighborhood of \vec{x} is η , the relation between \vec{q} and \vec{q}_s is simply

$$\vec{q} = \eta \vec{q}_s . \quad (2.9)$$

Furthermore, if the porous medium is locally homogeneous and isotropic, it is plausible to assume that the mean value obtained by a volume average will have the same value as obtained by a corresponding surface average, provided both the volume and the surface include the same reference point \vec{x} . The mean velocity \vec{q} of (2.8) may then be calculated alternatively by the surface average. Its physical meaning is precisely the discharge per unit gross area of porous medium normal to the flow. Thus, we have identified \vec{q} of (2.8) with \vec{q} in Darcy's law and we shall call them both superficial velocities. We shall also identify \bar{p} to be the mean pressure P of

Darcy's law when the interface boundary conditions are established in Chapter III.

Having already established a link between the microscopic and the macroscopic points of view, the next task is to establish the equations of motion for macroscopic flow, namely, to find the differential relations between derivatives of the mean velocity and the mean pressure. Before this can be done, it is necessary first to state the law governing the microscopic flow. For the present investigation, we shall limit our attention to a Newtonian fluid satisfying the Navier-Stokes equations:

$$\nabla \cdot \vec{u} = 0 , \quad (2.10)$$

$$\rho \frac{\partial \vec{u}}{\partial t} + \rho (\vec{u} \cdot \nabla) \vec{u} = -\nabla p + \mu \nabla^2 \vec{u} , \quad (2.11)$$

where \vec{u} , p , ρ , μ are respectively the local velocity, pressure, density and viscosity of the fluid defined in the usual sense of continuum mechanics. In principle, the microscopic flow field is completely determined if the non-slip condition is imposed on all the solid surfaces.

By referring to the characteristic velocity in the porous medium, q , the characteristic size of the solid (or the pore), d , and the characteristic frequency, f , the above equations can be made nondimensional by using the following substitutions:

$$\vec{x}' = \frac{\vec{x}}{d} , \quad t' = ft , \quad \vec{u}' = \frac{\vec{u}}{q} , \quad p' = \frac{p}{\mu g} , \quad (2.12)$$

giving

$$\nabla' \cdot \vec{u}' = 0 , \quad (2.13)$$

and

$$f_o \frac{\partial \vec{u}'}{\partial t'} + \text{Re}(\vec{u}' \cdot \nabla') \vec{u}' = -\nabla' p' + \nabla'^2 \vec{u}' , \quad (2.14)$$

where

$$\text{Re} = \frac{qd}{\nu} = \text{Reynolds number} ,$$

$$f_o = \frac{fd^2}{\nu} = \text{reduced frequency} .$$

When both the Reynolds number and the reduced frequency of a microscopic flow are sufficiently small, the inertia terms on the left of (2.14) may be neglected and the result becomes Stokes' equations[†] for slow viscous flow. Recovering the dimensional forms, Stokes' equations become

$$\nabla \cdot \vec{u} = 0 , \quad (2.15)$$

$$-\nabla p + \mu \nabla^2 \vec{u} = 0 . \quad (2.16)$$

In this case, the boundary condition of microscopic flow is again the non-slip one.

For most cases of practical interest, we may limit our studies of viscous flows through a porous medium to the category in which the microscopic flow satisfies Stokes' equations (2.15) - (2.16), and we shall attempt to derive the macroscopic description by applying appropriate statistical means, or an averaging method, to the

[†]For a treatment of Stokes' equations, see [11] and [12].

Stokes' equations. Before doing that, we shall however consider construction of some idealized models of porous media for which the microscopic solutions of Stokes' equations can be obtained.

These simple models are interesting because they can provide valuable insight into the more complicated general case of flow through a randomly distributed porous medium, and thereby enable us to establish the macroscopic equations correctly.

2.3. Idealized Models of Porous Media

Idealized models of porous media are formed by regular arrays of obstacles, for which the solutions of Stokes' equations can be obtained. By applying the averaging processes described by (2.6) and (2.7) of the preceding section to the microscopic solution, a macroscopic equation of motion can be derived for each specific model. Following this approach we shall discuss in the sequel three models: (1) Parallel tubes, (2) an array of circular cylinders, and (3) a lattice of spheres. These models have been described in the literature by various approximations. Here we collect only those solutions obtained analytically.

Model (1). Parallel tubes:-

The parallel tube model consists of a bunch of identical, parallel tubes imbedded in the solid. The flow in each cylindrical tube is assumed to be a Poiseuille flow, maintained by the same constant pressure gradient along the tube. The microscopic velocity distribution over a cross section of the tube generally assumes the following form:[†]

[†]For a treatment of viscous flow through a tube, see [12].

$$u(y, z) = - \frac{1}{\mu} \frac{dp}{dx} f(y, z) , \quad (2.17)$$

where $\nabla^2 f = -1$ within the cross section of the tube, and $f = 0$ on the tube boundary. Here the x -axis coincides with the axis of the tube, and u is the x -component of the velocity. For example, for the flow through a circular tube,

$$u(r) = - \frac{1}{4\mu} \frac{dp}{dx} (R^2 - r^2) , \quad (2.18)$$

in which r is the radial distance, and R is the radius of the circular tube.

For this particular model, the seepage velocity q_s , as defined by (2.6), is the same as the mean velocity through the tube, that is

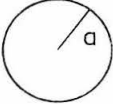
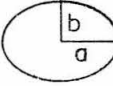
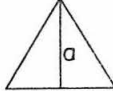
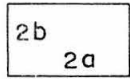
$$q_s = \frac{1}{A} \int_A u(y, z) dS , \quad (2.19)$$

where the integration is over the whole tube cross section and A denotes the cross sectional area of the tube. On the other hand, since the pressure is uniform over the cross section, the mean pressure \bar{p} may be considered to be the same as p . Therefore, upon integration of (2.19), using the velocity distribution (2.17) and substituting \bar{p} for p , the following macroscopic relation is obtained:

$$q_s = -\alpha_1 \frac{\ell^2}{\mu} \frac{d\bar{p}}{dx} , \quad (2.20)$$

where ℓ is the characteristic length of the pores and is now set to be \sqrt{A} . The coefficient α_1 is a constant depending on the shape of the cross section, and may be called a shape factor.

The values of α_1 for various shapes of tube cross sections are tabulated in the following:[†]

	$A = \ell^2$	α_1	
	πa^2	$\frac{1}{8\pi}$	(2.21)
	πab	$\frac{1}{4\pi} \left(\frac{1}{m^2 + 1} \right)$, $m = \frac{b}{a}$	
	$\frac{\sqrt{3}}{3} a^2$	$\frac{\sqrt{3}}{45}$	
	$4ab$	$\frac{1}{12} \left[m - \frac{bm^2}{\pi^2} \sum_{n=0}^{\infty} \frac{\tanh(n + \frac{1}{2}) \frac{\pi}{m}}{(n + \frac{1}{2})^5} \right]$, $m = \frac{b}{a}$	

The wall resistance F provided by a unit length of a single tube is simply

$$F = -A \frac{dp}{dx} = \frac{\mu}{\alpha_1} q_s \quad (2.22)$$

Suppose that this model has a porosity η , then the number of tubes in a unit cross sectional area is η/A , and the total resistance D (drag) per unit volume of the medium is given by

$$D = \frac{\eta}{\alpha_1} \frac{\mu}{\ell^2} q_s \quad (2.23)$$

in which A again has been replaced by ℓ^2 .

If the superficial velocity q instead of the seepage velocity q_s is used, then, by the relation $q = \eta q_s$, (2.20) and (2.23) can be

[†] For solutions of the viscous flow through tubes, see [12].

rewritten as

$$q = -\eta\alpha_1 \frac{\ell^2}{\mu} \frac{d\bar{p}}{dx}, \quad (2.24)$$

and

$$D = \frac{1}{\alpha_1} \frac{\mu}{\ell^2} q. \quad (2.25)$$

In the above the characteristic length ℓ was chosen to be associated with the pore size. Alternatively, a characteristic length may also be chosen appropriate to the solid dimensions. A proper solid length may be defined as:

$$d = \frac{1-\eta}{\eta} \ell. \quad (2.26)$$

In terms of the characteristic length d , (2.24) and (2.25) become

$$q = -\alpha_1 \frac{\eta^3}{(1-\eta)^2} \frac{d^2}{\mu} \frac{d\bar{p}}{dx}, \quad (2.27)$$

and

$$D = \frac{1}{\alpha_1} \frac{(1-\eta)^2}{\eta^2} \frac{\mu}{d^2} q. \quad (2.28)$$

Model (2). An Array of Circular Cylinders:-

In the circular cylinder model, parallel circular cylinders are arranged in a periodic fashion and a uniform mean flow is taken in the direction transverse to the axis of the cylinders. No analytical or numerical solution of Stokes' equations has been found for arbitrary spacing of such an array of cylinders. The existing solutions

are mostly restricted to square arrays in the limit of either small or large gaps between neighboring cylinders. Such a square array is represented in Fig. 2. The cylinders all have the same diameter d , and the distance between centers is h . The number of cylinders per unit length along either the x or the y directions is $1/h$, and the number of cylinders in a unit cross sectional area is $1/h^2$. The porosity η of the medium is therefore

$$\eta = 1 - \frac{\pi}{4} \left(\frac{d}{h} \right)^2 . \quad (2.29)$$

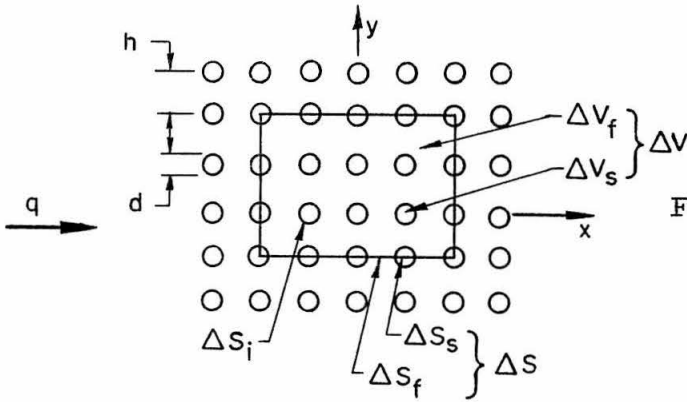


Fig. 2. Uniform flow through a square array of circular cylinders.

The limiting case of very small gaps, with $d/h \sim 1$, was investigated by Keller [13]. He approximated the flow in the narrow gap between the cylinders by the lubrication theory which assumes a locally parallel flow. Based on this theory the drag force acting on a single cylinder in the array has been found as

$$F \approx \frac{9\sqrt{2} \pi \mu}{4 \left(1 - \frac{d}{h}\right)^{5/2}} q \quad \left(\frac{d}{h} \sim 1 \right) . \quad (2.30)$$

In terms of porosity η as given by (2.29), (2.30) becomes

$$F \approx \frac{9\sqrt{2} \pi \mu}{4 \left(1 - \frac{2}{\sqrt{\pi}} \sqrt{1-\eta}\right)^{5/2}} q \quad \left(\eta \sim 1 - \frac{\pi}{4}\right). \quad (2.31)$$

When the gap becomes very large, with $d/h \ll 1$, Hasimoto [14] determined the force on a single cylinder as

$$F \approx \frac{4\pi\mu}{\left(\log \frac{2h}{d} - 1.3105\right)} q \quad \left(\frac{d}{h} \ll 1\right). \quad (2.32)$$

Again in terms of the porosity η , (2.32) becomes

$$F = \frac{8\pi\mu}{-\log(1-\eta) - 1.4764} q \quad (\eta \sim 1). \quad (2.33)$$

The drag per unit volume D is now simply the total force on all the cylinders contained in a unit volume. This may be obtained by multiplying F by the number of cylinders in a unit cross sectional area $1/h^2$. Therefore, for the case $d/h \sim 1$,

$$D \approx \frac{9\sqrt{2} \pi}{4 \left(1 - \frac{2}{\sqrt{\pi}} \sqrt{1-\eta}\right)^{5/2}} \frac{\mu}{d^2} q \quad \left(\eta \sim 1 - \frac{\pi}{4}\right); \quad (2.34)$$

and for the case $d/h \ll 1$,

$$D \approx \frac{32(1-\eta)}{-\log(1-\eta) - 1.4764} \frac{\mu}{d^2} q \quad (\eta \sim 1). \quad (2.35)$$

In order to derive a macroscopic equation for this idealized porous medium, we consider an elementary rectangular parallelepiped ΔV indicated in Fig. 2. The volume ΔV is further divided into two

parts, the pore part ΔV_f and the solid part ΔV_s . The bounding surface ΔS of ΔV is likewise divided into the pore part ΔS_f and the solid part ΔS_s . Let all the internal solid surfaces be denoted by ΔS_i , then the pore volume ΔV_f is bounded externally by ΔS_f and internally by all ΔS_i .

By integrating Stokes' equation (2.16) over ΔV_f , we have

$$\int_{\Delta V_f} (-\nabla p + \nabla \cdot \tau) dV = 0 . \quad (2.36)$$

In the above, $\nabla \cdot \tau$ has replaced $\mu \nabla^2 \vec{u}$ in (2.16), since $\nabla \cdot \tau = \mu \nabla^2 \vec{u}$ by virtue of the continuity equation (2.15) and the expression of the viscous stress tensor

$$\tau = \mu(\nabla \vec{u} + \nabla \vec{u}^*) , \quad (2.37)$$

where the * designates the transpose of a tensor.

Upon using the divergence theorem, (2.36) becomes

$$\int_{\Delta S_f} (-pI + \tau) \vec{n} dS = - \sum \int_{\Delta S_i} (-pI + \tau) \vec{n} dS , \quad (2.38)$$

where \vec{n} is a unit normal pointing outward from the fluid region and I is an identity tensor. The right-hand side of (2.38) is exactly the total drag on all the cylinders in ΔV . It may be written as

$$- \sum_i \int_{\Delta S_i} (-pI + \tau) \vec{n} dS = \int_{\Delta V} \vec{D} dV = D(\Delta V) \vec{e}_x . \quad (2.39)$$

Substituting (2.39) into (2.38) and expressing the left-hand side

explicitly, we have

$$\int_{x+\Delta x} (-p + \tau_{11}) dy - \int_x (-p + \tau_{11}) dy + \int_{y+\Delta y} \tau_{12} dx - \int_y \tau_{12} dx = D(\Delta V) . \quad (2.40)$$

Since the flow velocity is periodic, the viscous stresses must be identical on the two opposite faces of the rectangular parallelepiped chosen. The net effect on the τ -integrations therefore cancels out, leaving only pressure on the surface ΔS_f to balance the drag. Thus (2.40) becomes

$$\frac{1}{\Delta x \Delta y} \left[\int_{x+\Delta x} p dy - \int_x p dy \right] = D . \quad (2.41)$$

In the limit when Δx and Δy are small but still include a large number of cylinders, we may define a mean pressure and a mean pressure gradient consistent with (2.7), by

$$\bar{p} = \frac{1}{\eta \Delta y} \int p dy , \quad (2.42)$$

and

$$\frac{d\bar{p}}{dx} = \lim_{\Delta x \rightarrow 0} \frac{\bar{p}(x + \Delta x) - \bar{p}(x)}{\Delta x} . \quad (2.43)$$

Therefore (2.41) becomes

$$\frac{d\bar{p}}{dx} = \frac{D}{\eta} . \quad (2.44)$$

Substituting (2.34) and (2.35) for D into (2.44), we arrive at the following macroscopic equations for flow through this idealized porous medium:

$$q = -\frac{2\sqrt{2}}{9\pi} \eta \left(1 - \frac{2}{\sqrt{\pi}} \sqrt{1-\eta}\right)^{5/2} \frac{d^2}{\mu} \frac{d\bar{p}}{dx} \quad (\eta \sim 1 - \frac{\pi}{4}) , \quad (2.45)$$

and

$$q = -\frac{[-\log(1-\eta) - 1.4764] \eta}{32(1-\eta)} \frac{d^2}{\mu} \frac{d\bar{p}}{dx} \quad (\eta \sim 1) . \quad (2.46)$$

Model (3). A Lattice of Spheres:-

This model is consisted of a periodic lattice of solid spheres. The mean flow is assumed to be uniform throughout the medium. The exact solution of Stokes' equations for such a configuration is also not available. Hasimoto [14] examined Stokes flow past three types of cubic lattice of spheres, all in the limit of small sphere concentrations. For a simple cubic lattice in which a sphere of diameter d is located at each corner of a cube of length h , he found for the drag on a single sphere,

$$F = \frac{3\pi\mu d}{\gamma} q \quad (\eta \sim 1) , \quad (2.47)$$

where γ is given by

$$\gamma = 1 - 1.7601(1-\eta)^{1/3} + (1-\eta) - 1.5593(1-\eta)^2 + \dots . \quad (2.48)$$

In the above, η again denotes the porosity of the medium and is given by

$$\eta = 1 - \frac{1}{6} \left(\frac{d}{h}\right)^3 \quad (2.49)$$

for the cubic lattice.

This drag on a sphere in the lattice is seen to be greater than that on an isolated sphere, which is $3\pi\mu qd$. For the other two types of lattice investigated by Hasimoto, the drag F was found to differ only slightly from that given by (2.47) so long as the sphere concentration remains small. From these findings it may be inferred that any type of periodic array of spheres would yield a drag close to that of (2.47).

The drag per unit volume, D , is given by the drag F on a single sphere times the number of the spheres in a unit volume, $(1 - \eta)/\frac{1}{6}\pi d^3$, or

$$D = \frac{18(1 - \eta)}{\gamma} \frac{\mu}{d^2} q \quad (\eta \sim 1) . \quad (2.50)$$

This should be approximately valid for any type of sphere lattice.

Again, by integrating Stokes' equation (2.16) over an elementary volume of the porous medium, similar to what was done for the case of circular cylinders, the following macroscopic equation for flow through the present model of porous medium is obtained.

$$q = \frac{-\eta\gamma}{18(1 - \eta)} \frac{d^2}{\mu} \frac{d\bar{p}}{dx} \quad (\eta \sim 1) . \quad (2.51)$$

From the above results of models of porous media, we take note in particular of the following features of uniform flow through porous media.

i. For the above three models, the macroscopic equations of motion, (2.27), (2.45), (2.46) and (2.51) all assume the same form,

$$q = - \frac{k}{\mu} \frac{d\bar{p}}{dx} , \quad (2.52)$$

where k of each model is tabulated as follows:

model	k	range of validity	d
parallel tubes	$\frac{\alpha_1 \eta^3}{(1 - \eta)^2} d^2$ α_1 is given by (2.21)	$0 \leq \eta < 1$	defined by (2.26)
circular cylinders (square arrays)	$\frac{2\sqrt{2}}{9\pi} \eta(1 - \frac{2}{\sqrt{\pi}}\sqrt{1-\eta})^{5/2} d^2$	$\eta \sim 1 - \frac{\pi}{4}$	diameter of the cylinders (2.53)
	$\frac{[-\log(1-\eta) - 1.4764]\eta}{32(1-\eta)} d^2$	$\eta \sim 1$	
spheres (any lattice)	$\frac{\eta\gamma}{18(1-\eta)} d^2$ γ is given by (2.48)	$\eta \sim 1$	diameter of the spheres

(2.52) is seen to be identical to Darcy's law if \bar{p} is identified as P , and k as the permeability of the porous medium. Some of the above tabulated formulas for k are represented graphically in Fig. 3. Equation (2.52) should also hold true for any periodic array of obstacles.

ii. The drag per unit volume given by these three models, (2.28), (2.34), (2.35) and (2.50), are of the same form,

$$D = \frac{\eta\mu}{k} q \quad (2.54)$$

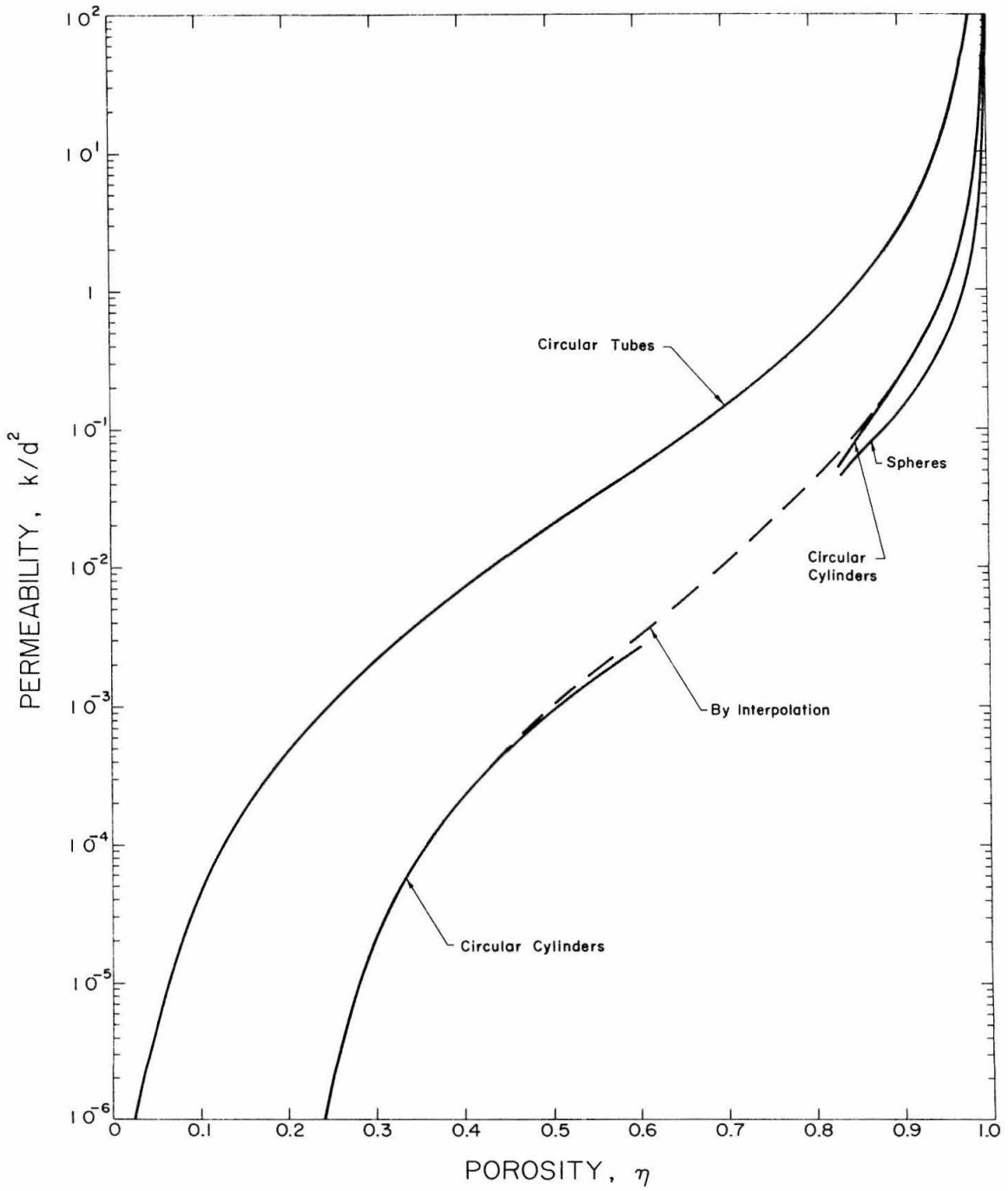


Fig. 3. Permeability for idealized models of porous media.

It is seen that the drag is proportional to the superficial velocity q , and the same should also be true for any periodic array of obstacles.

iii. The physical meaning of the macroscopic equation (2.52), or Darcy's law, states that the mean pressure drop over a distance is balanced by the drag of the solid material within the distance. For a porous medium composed of periodic array of obstacles, the mean viscous stresses are either identically zero, or the stresses on two opposite faces of a well-chosen elementary volume cancel each other. The net effect of viscous stresses on the balance of forces is always zero.

iv. For a uniform, mean flow through a random porous medium which may be considered as statistically homogeneous and isotropic, the same three conclusions above also hold valid. This is so because on all parallel cross sections of such a medium, the viscous stresses are statistically the same, and have no net effect on the balance of forces.

The general case of non-uniform flow through a random porous medium, whether the generalized Darcy's law (2.2) - (2.3) is valid or not, will be investigated in the next section.

2.4. Derivation of General Macroscopic Equations of Motion

We proceed to consider the general case of non-uniform flow in a random porous medium, and derive the macroscopic equations of

motion based on the microscopic Stokes' equations.

The porous medium is assumed to be statistically homogeneous and isotropic, with a prescribed porosity η , and the mean flow in it need not be uniform. The transformation from the microscopic to the macroscopic description is effected by equations (2.6) and (2.7) which define the seepage velocity \vec{q}_s and the mean pressure \bar{p} . In order to obtain the macroscopic equations, it is necessary to determine the relationship between the mean derivatives and the derivatives of the means. For this purpose we consider again a small volume ΔV of the porous medium. The fluid portion of it is denoted by ΔV_f . ΔV is bounded by the surface ΔS of which the fluid portion is ΔS_f ; and ΔV_f is bounded externally by ΔS_f and internally by all ΔS_i 's which designate the surfaces of the solids within ΔV . Such a small volume element is shown schematically in Fig. 4.

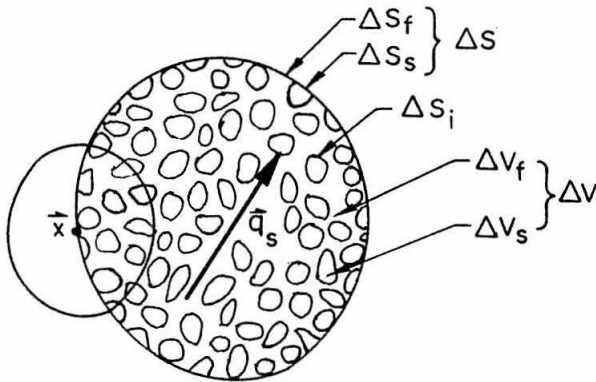


Fig. 4. Non-uniform flow through a random porous medium-- a volume element.

First we consider the mean of the velocity gradient over the volume ΔV_f , that is,

$$\overline{\frac{\partial u_i}{\partial x_j}} = \frac{1}{\Delta V_f} \int_{\Delta V_f} \frac{\partial u_i}{\partial x_j} dV. \quad (2.55)$$

By using the divergence theorem, it transforms into surface integrals

$$\overline{\frac{\partial u_i}{\partial x_j}} = \frac{1}{\Delta V_f} \int_{\Delta S_f} u_i n_j dS + \frac{1}{\Delta V_f} \sum_i \int_{\Delta S_i} u_i n_j dS, \quad (2.56)$$

where n_j is the j th component of the outward unit normal to the bounding surfaces. Since u_i vanishes on solid surfaces, the second integral disappears. In the first integral u_i may be replaced by its local mean value q_{si} , still keeping the identity approximately true. Of course, the criterion is that the volume element chosen for evaluating q_{si} should be considerably smaller than ΔV used in obtaining $\overline{\frac{\partial u_i}{\partial x_j}}$. If this replacement is effected, we have

$$\overline{\frac{\partial u_i}{\partial x_j}} = \frac{1}{\Delta V_f} \int_{\Delta S_f} q_{si} n_j dS. \quad (2.57)$$

Now since q_{si} is defined and assumed to be continuous throughout ΔV as if the solids were not there, it is reasonable to introduce the approximation

$$\int_{\Delta S_f} q_{si} n_j dS = \eta \int_{\Delta S} q_{si} n_j dS, \quad (2.58)$$

where η is the porosity of the medium. Therefore, from (2.57)

$$\overline{\frac{\partial u_i}{\partial x_j}} = \frac{\eta}{\Delta V_f} \int_{\Delta S} q_{si} n_j dS. \quad (2.59)$$

Again on the assumption that q_{si} is continuously differentiable through-

out ΔV , the volume integral may be recovered by applying the divergence theorem, giving

$$\overline{\frac{\partial u_i}{\partial x_j}} = \frac{\eta}{\Delta V_f} \int_{\Delta V} \frac{\partial q_{si}}{\partial x_j} dV . \quad (2.60)$$

We shall further assume that the mean velocity gradient varies only slowly over the small volume ΔV . Consequently, the integrand in (2.60) may be pulled out to give

$$\overline{\frac{\partial u_i}{\partial x_j}} = \frac{\partial q_{si}}{\partial x_j} . \quad (2.61)$$

This states that the mean of the velocity gradient is equal to the gradient of the mean velocity. However, the same conclusion does not hold for the pressure. Following the above steps of analysis, we obtain for the mean pressure gradient

$$\overline{\frac{\partial p}{\partial x_i}} = \frac{\partial \bar{p}}{\partial x_i} + \frac{1}{\Delta V_f} \sum_i \int_{\Delta S_i} p n_i dS . \quad (2.62)$$

The integral term in (2.62) retains in general since p need not vanish on solid boundary.

Similarly, for the viscous stress tensor τ (see Eq. (2.37)),

$$\tau_{ij} = \mu \epsilon_{ij} , \quad (2.63)$$

where

$$\epsilon_{ij} = \frac{\partial u_i}{\partial x_j} + \frac{\partial u_j}{\partial x_i} \quad (2.64)$$

is the rate of strain tensor, we obtain the following expressions for the mean values:

$$\bar{\tau}_{ij} = \mu \left(\frac{\partial q_{si}}{\partial x_j} + \frac{\partial q_{sj}}{\partial x_i} \right) , \quad (2.65)$$

and

$$\frac{\partial \bar{\tau}_{ij}}{\partial x_j} = \frac{\partial \bar{\tau}_{ij}}{\partial x_j} + \frac{1}{\Delta V_f} \sum_i \int_{\Delta S_i} \tau_{ij} n_j dS . \quad (2.66)$$

For future reference, we shall also write the mean vorticity as

$$\bar{\omega}_i = e_{ijk} \frac{\partial \bar{u}_k}{\partial x_j} = e_{ijk} \frac{\partial q_{sk}}{\partial x_j} . \quad (2.67)$$

After all these mean derivatives have been obtained, it is just a straightforward matter to transform the Stokes' equations to the macroscopic equations. Firstly, consider the averaging of the continuity equation (2.15) over the volume ΔV_f ,

$$\overline{\nabla \cdot \vec{u}} = 0 . \quad (2.68)$$

According to (2.61), this is immediately reduced to

$$\nabla \cdot \vec{q}_s = 0 . \quad (2.69)$$

Next consider the averaging of Stokes' equation (2.16). Using the alternative form (2.36), we have

$$-\overline{\nabla p} + \overline{\nabla \cdot \tau} = 0 . \quad (2.70)$$

By substituting (2.62) and (2.66) into (2.70), it follows that

$$-\nabla\bar{p} + \nabla \cdot \bar{\tau} = - \frac{1}{\Delta V_f} \left[\sum_i \int_{\Delta S_i} (-pI + \tau) \bar{n} \, dS \right] , \quad (2.71)$$

where \bar{n} is the unit normal pointing towards the interior of the solids. The sum of the surface integrals on the right-hand side is therefore exactly the total drag in the volume ΔV . Denoting the drag per unit volume of the porous medium by \bar{D} , we have

$$-\nabla\bar{p} + \nabla \cdot \bar{\tau} = \frac{1}{\Delta V_f} \int_{\Delta V} \bar{D} \, dV . \quad (2.72)$$

On the assumption that \bar{D} is a slowly varying function over ΔV , it can be taken out of the integral. After $\bar{\tau}$ is substituted by the relation (2.65) and use is made of the continuity equation (2.69), equation (2.72) finally reduces to

$$-\nabla\bar{p} + \mu \nabla^2 \bar{q}_s = \frac{\bar{D}}{\eta} . \quad (2.73)$$

Furthermore, if the mean velocity \bar{q}_s is also a slowly varying function, we may assume that \bar{D} varies linearly with \bar{q} as shown by (2.54) and \bar{q} in this expression may further be replaced by $\eta \bar{q}_s$. Then (2.73) becomes

$$-\nabla\bar{p} + \mu \nabla^2 \bar{q}_s = \frac{\eta \mu}{k} \bar{q}_s . \quad (2.74)$$

Equations (2.69) and (2.74) are the general macroscopic equations of motion that were to be sought. In order to compare the

above result with Darcy's law, we further express (2.69) and (2.74) in terms of the superficial velocity \vec{q} by using the relation $\vec{q} = \eta \vec{q}_s$, giving

$$\nabla \cdot \vec{q} = 0, \quad (2.75)$$

and

$$-\nabla \bar{p} + \frac{\mu}{\eta} \nabla^2 \vec{q} = \frac{\mu}{k} \vec{q}. \quad (2.76)$$

Here for completeness, we also write the mean stress tensor (2.65) in terms of \vec{q} , that is

$$\bar{\tau} = \frac{\mu}{\eta} (\nabla \vec{q} + (\nabla \vec{q})^*). \quad (2.77)$$

The set of macroscopic equations (2.75) and (2.76) will be adopted in the later analyses of interface boundary conditions. The first one states the conservation of mass, while the second one expresses the balance of the forces. The latter is different from Darcy's law in that the viscous forces in the fluid, in addition to the pressure, are included in balancing the resistance exerted by the solids. However, for an ordinary porous medium, the value of k is always so small that the resistance represented by the right-hand side term of (2.76) always overpowers the viscous forces given by the second term on the left. This means the viscous term is negligible and equation (2.76) tends to Darcy's law unless the mean velocity gradient is also very large.

The whole picture becomes clearer when (2.76) is written in

a dimensionless form. Let the macroscopic characteristic length be L , the characteristic velocity be q , and write the dimensionless variables as follows:

$$\vec{q}_* = \frac{\vec{q}}{q}, \quad \bar{p}_* = \frac{\bar{p}}{\frac{\mu q}{k} L}, \quad \vec{x}_* = \frac{\vec{x}}{L}. \quad (2.78)$$

We have then

$$-\nabla_* \bar{p}_* + \text{Da} \nabla_*^2 \vec{q}_* = \vec{q}_*, \quad (2.79)$$

where Da is the Darcy number defined by

$$\text{Da} = \frac{k}{\eta L^2}. \quad (2.80)$$

Therefore, when the Darcy number is small, the macroscopic equation (2.76) reduces to Darcy's law.

2.5. Energy Consideration

In order to understand more about the mechanism of the flow through porous media, we shall consider the balance of energy.

A macroscopic energy equation may be derived directly from the macroscopic equation of motion, (2.73) or (2.74). Taking the dot product of \vec{q}_s with the equation, we have after certain manipulations

$$\nabla \cdot (-\bar{p} \mathbf{I} + \bar{\tau}) \vec{q}_s = \frac{1}{2} \mu \bar{\epsilon}^2 + \frac{\bar{D}}{\eta} \cdot \vec{q}_s = \frac{1}{2} \mu \bar{\epsilon}^2 + \frac{\eta \mu}{k} \vec{q}_s^2, \quad (2.81)$$

where τ is given by (2.65), or by

$$\bar{\tau} = \mu \bar{\epsilon} , \quad (2.82)$$

where

$$\bar{\epsilon} = \nabla \vec{q}_s + (\nabla \vec{q}_s)^* . \quad (2.83)$$

Integrating the energy equation (2.81) over a volume ΔV bounded by its surface ΔS , we get

$$\begin{aligned} & \int_{\Delta S} (-\bar{p}I + \bar{\tau}) \vec{n} \cdot \vec{q}_s \, dS \\ &= \int_{\Delta V} \frac{1}{2} \mu \bar{\epsilon}^2 \, dV + \int_{\Delta V} \frac{\vec{D}}{\eta} \cdot \vec{q}_s \, dV . \end{aligned} \quad (2.84)$$

In this expression, the left-hand side may be interpreted as the work done on the surface ΔS by all the apparent mean stresses; the first term on the right may be considered as the apparent energy dissipation; and the last term is the work done by the apparent body force distribution. From the macroscopic point of view the equation expresses a sort of energy balance between the various quantities. However, the above interpretation must not be construed to mean that those terms contained in (2.84) are the actual mean work done and the actual mean energy dissipation in the porous medium. It was nevertheless true that those terms in the macroscopic equation of motion (2.73) correspond to the mean stresses or forces in the porous medium.

To clarify this point further, we start alternatively to construct a macroscopic energy equation from the microscopic one. Taking the

inner product of \vec{u} and the Stokes' equation (2.16), we obtain the following microscopic energy equation:

$$\nabla \cdot (-p\mathbf{I} + \tau)\vec{u} = \frac{1}{2}\mu\epsilon^2, \quad (2.85)$$

where τ and ϵ are stress and rate of strain tensor given by (2.63) and (2.64). The term on the right-hand side is commonly known to be the energy dissipation per unit volume of the fluid.

Apply equation (2.85) within a volume ΔV of the porous medium, represented schematically in Fig. 4. Integration over the fluid portion ΔV_f gives

$$\begin{aligned} \int_{\Delta S_f} (-p\mathbf{I} + \tau)\vec{n} \cdot \vec{u} \, dS + \sum_i \int_{\Delta S_i} (-p\mathbf{I} + \tau)\vec{n} \cdot \vec{u} \, dS \\ = \int_{\Delta V_f} \frac{1}{2} \mu \epsilon^2 \, dV. \end{aligned} \quad (2.86)$$

Since \vec{u} vanishes on the solid boundaries, the second term on the left disappears, and so

$$\int_{\Delta S_f} (-p\mathbf{I} + \tau)\vec{n} \cdot \vec{u} \, dS = \int_{\Delta V_f} \frac{1}{2} \mu \epsilon^2 \, dV. \quad (2.87)$$

This is the true balance of energy for a volume of porous medium. Equation (2.87) states that the work done by real stresses on ΔS_f is equal to the total energy dissipation within ΔV_f .

Let each flow variable be written in the sum of its mean component and its fluctuating component, that is

$$\vec{u} = \vec{q}_s + \vec{u}', \quad p = \bar{p} + p', \quad \tau = \bar{\tau} + \tau', \quad \epsilon = \bar{\epsilon} + \epsilon', \quad (2.88)$$

where each mean component has been defined previously in the beginning of the last section. We also recognize that

$$\bar{\tau} = \mu \bar{\epsilon}, \quad \tau' = \mu \epsilon' = \mu (\nabla \vec{u}' + (\nabla \vec{u}')^*) . \quad (2.89)$$

Next we observe that the mean of a product such as $\overline{p\vec{u}}$ may be related to the product of the mean in the following way:

$$\overline{p\vec{u}} = \overline{(\bar{p} + p')(\vec{q}_s + \vec{u}')} = \bar{p}\vec{q}_s + \overline{p'\vec{u}'} , \quad (2.90)$$

where the terms linear in the fluctuating components, such as $\overline{p'\vec{q}_s}$, are zero in view of (2.88). Likewise,

$$\overline{\tau\vec{u}} = \overline{\bar{\tau}\vec{q}_s + \tau'\vec{u}'} = \bar{\tau}\vec{q}_s + \overline{\mu\epsilon'\vec{u}'} , \quad (2.91)$$

and

$$\overline{\epsilon^2} = \bar{\epsilon}^2 + \overline{\epsilon'^2} . \quad (2.92)$$

In the equation (2.87), we may write $(-p\vec{l} + \tau)\vec{n} \cdot \vec{u}$ as $(-p\vec{u} + \tau\vec{u}) \cdot \vec{n}$, and replace each product such as $\overline{p\vec{u}}$ by its local mean value. The result is

$$\int_{\Delta S_f} (-\overline{p\vec{u}} + \overline{\tau\vec{u}}) \cdot \vec{n} \, dS = \int_{\Delta V_f} \frac{1}{2} \mu \overline{\epsilon^2} \, dV . \quad (2.93)$$

Substituting (2.90), (2.91) and (2.92) into (2.93), we have

$$\begin{aligned} \int_{\Delta S_f} [(-\bar{p}\mathbf{I} + \bar{\tau})\vec{n} \cdot \vec{q}_s + (-\overline{p\vec{u}'} + \overline{\mu\epsilon'\vec{u}'}) \cdot \vec{n}] dS \\ = \int_{\Delta V_f} \left(\frac{1}{2} \mu \bar{\epsilon}^2 + \frac{1}{2} \mu \overline{\epsilon'^2} \right) dV . \end{aligned} \quad (2.94)$$

All the mean quantities in (2.94) are actually defined and are continuous over the whole region ΔV bounded by ΔS . Analogous to what was done in (2.58), equation (2.94) may be written as

$$\begin{aligned} \int_{\Delta S} [(-\bar{p}\mathbf{I} + \bar{\tau})\vec{n} \cdot \vec{q}_s + (-\overline{p'\vec{u}'} + \overline{\mu\epsilon'\vec{u}'}) \cdot \vec{n}] dS \\ = \int_{\Delta V} \frac{1}{2} \mu (\bar{\epsilon}^2 + \overline{\epsilon'^2}) dV . \end{aligned} \quad (2.95)$$

So far it is clear that the apparent mean flow does not alone contribute to the total work done on a surface, or to the total energy dissipation within a volume of the porous medium. The fluctuating components have definite contributions. In particular, for a uniform mean flow through the porous medium, the mean velocity gradient vanishes and the energy dissipation is completely contained in the fluctuating components, $\overline{\epsilon'^2}$.

Converting (2.95) to its differential form, we have, after some rearrangement, an alternative macroscopic energy equation in the following form:

$$\nabla \cdot (-\bar{p}\mathbf{I} + \bar{\tau})\vec{q}_s = \frac{1}{2} \mu \bar{\epsilon}^2 + \frac{1}{2} \mu \overline{\epsilon'^2} - \nabla \cdot (-\overline{p'\vec{u}'} + \overline{\mu\epsilon'\vec{u}'}) . \quad (2.96)$$

Comparing (2.96) with (2.81), we identify

$$\frac{\vec{D} \cdot \vec{q}_s}{\eta} = \frac{\eta \mu}{k} q_s^2 = \frac{1}{2} \overline{\mu \epsilon'^2} - \nabla \cdot (-\overline{p' \vec{u}'} + \overline{\mu \epsilon' \vec{u}'}) \quad (2.97)$$

Therefore, from the macroscopic point of view, the apparent work done by the body force takes care of all the contributions from the fluctuating components of velocities and pressure in the corresponding region of the porous medium.

In the limit when the Darcy number is small so that Darcy's law is applicable, the energy equation (2.81) is also simplified to

$$-\nabla p \cdot \vec{q}_s = \frac{\vec{D} \cdot \vec{q}_s}{\eta} \quad (2.98)$$

The integral form of this equation is

$$\int_{\Delta S} -\overline{p} \vec{n} \cdot \vec{q}_s \, dS = \int_{\Delta V} \frac{\vec{D}}{\eta} \cdot \vec{q}_s \, dV \quad (2.99)$$

Equation (2.99) merely expresses the balance between the work done by the pressure and the apparent work done by the body force. There is no dissipative term. In the corresponding porous medium, of course, dissipation is always present, and is in this limiting case provided by the fluctuating components of velocities.

III. INTERFACE BOUNDARY CONDITIONS

From a microscopic point of view, the viscous flow past (as well as through) a porous body is continuous throughout the flow field, which includes the external fluid region and the interior pores of the porous body so long as the fluid within the pores is also in motion. The fluid motion is bounded by solid surfaces; there is no interface of any sort. However, as we already discussed in the last chapter, the complexity of the flow in the pores suggests that it will be more fruitful to describe it macroscopically by regarding the porous region a homogeneous regime in which the original microscopic flow is represented by an apparent mean flow. In this way, we may consider two distinct homogeneous regions--the real fluid region and the imaginary porous one. These two regions are separated by a geometrical interface located at the physical boundary of the porous body.

We are interested in the case when the flow in the fluid region satisfies the Navier-Stokes equations or their limiting forms for small Reynolds number, and the flow in the porous medium satisfies Darcy's law. Although Darcy's law is known to be limited by various physical factors such as the molecular effects, flow turbulence, ion exchanges, and other anomalies, the validity of Darcy's law, according to (2.14) and (2.79), generally requires, among other things, that both the Reynolds number Re and the Darcy number Da must be sufficiently small,

$$\text{Re} = \frac{\rho q d}{\mu} \ll 1, \quad (3.1)$$

$$\text{Da} = \frac{k}{\eta L^2} \ll 1. \quad (3.2)$$

A small Reynolds number means a slow microscopic motion of the fluid inside the pores, while a small Darcy number implies that the macroscopic size of the porous body is much greater than the size of the solid grains composing it. The latter also places a restriction on the porosity of the body. The porosity should never be close to unity, for otherwise k becomes very large and overpowers L^2 .

In order that the solution of the governing differential equations is not to be undeterminate, it is necessary to establish a set of interface boundary conditions to relate the flow variables across the interface. In the formulation of such conditions, there are certain inherent difficulties:

- i. The flow variables, such as velocity and pressure, for the two regions bear the same names but do not have precisely the same meanings.
- ii. Although the interface is considered to be homogeneous in the macroscopic sense, in reality, it is composed partially of solid surfaces and partially of pore surfaces.
- iii. Darcy's law may not be uniformly applicable in the whole porous region even if the Darcy number is small. In fact, there exists a porous layer adjacent to the interface in which the flow needs special consideration.

The first and the second difficulties are removed since we have rigorously defined the macroscopic flow variables in the porous medium with respect to their microscopic counterparts. The third one may be resolved if we either (1) ignore the interface porous layer, which is usually very thin, and establish appropriate interface boundary conditions which relate the viscous flow and the Darcy flow across the layer, or (2) use a more general macroscopic equation valid for the whole porous region, including the interface porous layer, and formulate interface boundary conditions by joining the viscous flow and the macroscopic flow at the interface. Thus, we have two types of interface boundary conditions under consideration. The latter will be taken up first.

3.1. Interface Boundary Conditions of the First Kind--For General Macroscopic Equations of Motion

The general macroscopic equations of motion for flow through porous media, when only the Reynolds number (refer to (3.1)) is small, have been derived in the last chapter.

$$\nabla \cdot \vec{q} = 0 \quad , \quad (2.75)$$

$$-\nabla \bar{p} + \frac{\mu}{\eta} \nabla^2 \vec{q} = \frac{\mu}{k} \vec{q} \quad . \quad (2.76)$$

Only when the Darcy number (see (3.2)) is also small can equation (2.76) reduce to Darcy's law. However, even with a small Darcy number, the full equation (2.76) should still be used for evaluation of the flow wherever the velocity gradient is large.

In the immediate vicinity of an interface, the tangential velocity can vary rapidly under the direct influence of the external

shear. According to what was said above, this is the layer in which Darcy's law ceases to apply, and the full macroscopic equations must be used. In fact, the same macroscopic equations can be applied to the whole porous region without separate consideration of the interface layer. These equations are valid even when the Darcy number is not small.

In the following we shall formulate the interface boundary conditions when the macroscopic equation (2.76) is applied throughout the porous region and a Newtonian viscous fluid exists on the other side. The interface which we will deal with is an ideal one; its surface structure is statistically the same as any other surface cut through the porous medium. It has a surface porosity η , the same in value as the volume porosity of the medium. A schematical representation of such an ideal interface is given in Fig. 5.

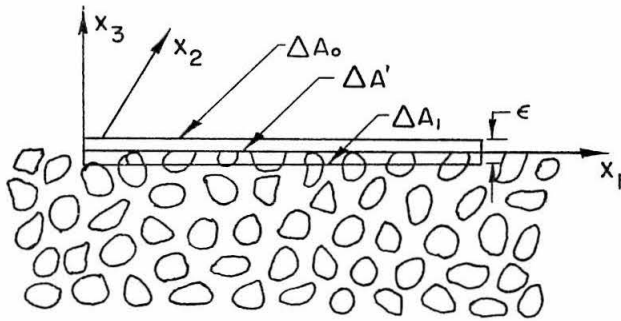


Fig. 5. An ideal interface.

The correct interface boundary conditions may be derived by considering the true mass and momentum conservation across the interface, or by applying the Navier-Stokes equations (2.10) and (2.11) to the fluid portion of a pill box control volume straddling the interface as shown in Fig. 5. The results obtained in terms of the micro-

scopic quantities may then be transformed to the macroscopic ones.

This may be achieved by a simpler, alternative way. All the microscopic variables, \vec{u} , p as well as their derivatives, are continuous through the pores at the interface. We still consider the same pill box and designate the face on the fluid side by ΔA_o , while that on the porous side by ΔA_1 . The box has a small thickness ϵ and a face area A which is small compared with the characteristic macroscopic area but is, however, large enough to include many pores. It always contains the interface $\Delta A'$ even as ϵ tends to zero. We shall also use the subscripts "s" and "f" to indicate the solid and the fluid parts of a surface, respectively.

We first consider the velocity \vec{u} . As $\epsilon \rightarrow 0$ we have

$$\int_{\Delta A_o} \vec{u} dS = \int_{\Delta A'_f} \vec{u} dS + \int_{\Delta A'_s} \vec{u} dS . \quad (3.3)$$

Since \vec{u} vanishes on the solid surfaces $\Delta A'_s$ and its value on $\Delta A'_f$ approaches that on ΔA_{1f} , the above equation reduces to

$$\int_{\Delta A_o} \vec{u} dS = \int_{\Delta A_{1f}} \vec{u} dS . \quad (3.4)$$

Let the local mean velocities be \vec{u}_o for the fluid side and \vec{q}_{s1} for the porous side; these are defined as follows:

$$\vec{u}_o = \frac{1}{A} \int_{\Delta A_o} \vec{u} dS , \quad (3.5)$$

$$\vec{q}_{s1} = \frac{1}{\eta A} \int_{\Delta A_{1f}} \vec{u} dS . \quad (3.6)$$

Equation (3.4) immediately becomes

$$\vec{u}_o = \eta \vec{q}_{s1} , \quad (3.7)$$

or in terms of the superficial velocity \vec{q}_1 , defined as $\eta \vec{q}_{s1}$,

$$\vec{u}_o = \vec{q}_1 . \quad (3.8)$$

The mean velocities \vec{u}_o , \vec{q}_{s1} and \vec{q}_1 are assumed to be continuous along the interface. They are also assumed to be the limits approached uniformly by the corresponding mean velocities \vec{u} , \vec{q}_s and \vec{q} defined in the interior regions. We must also consider the mean flow for the external fluid region because the microscopic external flows near the interface change continuously to those within the porous region and are too complicated to treat. Here we further remark that the mean velocity of the external flow, in the case of slow motion, satisfies the linear Stokes' or Oseen's equations.

Next we consider the derivatives of velocity, i. e., the velocity gradients. Some macroscopic conditions are immediately available from the result of (3.8). Since the velocities \vec{u}_o and \vec{q}_1 are equal on the opposite sides of the interface, so their tangential derivatives must also be equal, that is

$$\left(\frac{\partial u_i}{\partial x_j} \right)_o = \left(\frac{\partial q_i}{\partial x_j} \right)_1 , \quad i = 1, 2, 3 ; j = 1, 2 , \quad (3.9)$$

where (x_1, x_2, x_3) are the local Cartesian coordinates with the x_3 -axis

[†]Note that we use the same notation \vec{u} for both the microscopic velocity and the mean velocity in the fluid region. The same applies to the pressure p .

normal to the interface, as indicated in Fig. 5.

Using the continuity equations (2.10) and (2.75) for the relevant sides of the interface, and utilizing the condition (3.9), the following condition is also immediately obtained:

$$\left(\frac{\partial u_3}{\partial x_3} \right)_0 = \left(\frac{\partial q_3}{\partial x_3} \right)_1 \quad (3.10)$$

It is more difficult to derive the conditions for the remaining two derivatives, that is, for the normal derivatives of the tangential velocities. Starting from the pill box, as ϵ tends to zero, we have again

$$\int_{\Delta A'_0} \frac{\partial u_i}{\partial x_3} dS = \int_{\Delta A'_{1f}} \frac{\partial u_i}{\partial x_3} dS + \int_{\Delta A'_s} \frac{\partial u_i}{\partial x_3} dS, \quad i=1,2. \quad (3.11)$$

But this time we are not so fortunate as in (3.3) to have the integral vanish over $\Delta A'_s$. In fact, this integral remains undetermined and also unrelated to the flow at the face $\Delta A'_1$. Its contribution can only be estimated.

We observe that the velocity gradients, $\frac{\partial u_i}{\partial x_3}$, are continuous along the interface. Their values along the solid faces cannot deviate much from the values over the neighboring pore faces. This is because the length of a pore or solid is only a small fraction of a typical macroscopic length. Therefore, the mean velocity gradient over the solid faces $\Delta A'_s$ should be about the same as the mean value over the entire $\Delta A'$. In other words,

$$\int_{\Delta A'_s} \frac{\partial \dot{u}_i}{\partial x_3} dS \approx (1-\eta) \int_{\Delta A'_o} \frac{\partial u_i}{\partial x_3} dS = (1-\eta) \int_{\Delta A_o} \frac{\partial u_i}{\partial x_3} dS. \quad (3.12)$$

Using this, (3.11) reduces to

$$\eta \int_{\Delta A_o} \frac{\partial u_i}{\partial x_3} dS \approx \int_{\Delta A_{1f}} \frac{\partial u_i}{\partial x_3} dS. \quad (3.13)$$

We may interchange the integration and differentiation, and according to (3.5) and (3.6) we may write the resulting equation in terms of the mean velocities as follows:

$$\eta \left(\frac{\partial u_i}{\partial x_3} \right)_o \approx \left(\frac{\partial q_i}{\partial x_3} \right)_1, \quad i = 1, 2. \quad (3.14)$$

This expression is different from those for the other components of the velocity gradient, the difference being the factor η multiplying the normal derivative of the tangential components of the velocity of the exterior flow.

It is possible to give an order of magnitude estimate of the error involved in the relationship (3.14). Suppose that the characteristic length and velocity associated with the external flow are L and U , respectively. Then the normal velocity gradient at the interface is $O(U/L)$. We further suppose that the characteristic velocity in the pores at the interface is q , then the difference between the velocity gradients on the solid face and those on the neighboring pore face is of the order

$$O\left(\left| \frac{U+q}{L} - \frac{U}{L} \right| \right) = O\left(\frac{q}{L} \right) = O\left(\frac{U}{L} \right) \cdot O\left(\frac{q}{U} \right). \quad (3.15)$$

Accordingly, the corresponding error involved in (3.14) is expected to be of the same order of magnitude as above, i. e. ,

$$\left(\frac{\partial q_i}{\partial x_3} \right)_1 = \eta \left(\frac{\partial u_i}{\partial x_3} \right)_0 \left[1 + O\left(\frac{q}{U} \right) \right]. \quad (3.16)$$

Thus we see that the approximation (3.14) is good when $q/U \ll 1$, as indeed is usually the case.

The conditions on the velocity gradients, equations (3.9), (3.10) and (3.14), may be summarized as follows:

$$\begin{pmatrix} \frac{\partial u_1}{\partial x_1} & \frac{\partial u_1}{\partial x_2} & \eta \frac{\partial u_1}{\partial x_3} \\ \frac{\partial u_2}{\partial x_1} & \frac{\partial u_2}{\partial x_2} & \eta \frac{\partial u_2}{\partial x_3} \\ \frac{\partial u_3}{\partial x_1} & \frac{\partial u_3}{\partial x_2} & \frac{\partial u_3}{\partial x_3} \end{pmatrix}_0 \approx \begin{pmatrix} \frac{\partial q_1}{\partial x_1} & \frac{\partial q_1}{\partial x_2} & \frac{\partial q_1}{\partial x_3} \\ \frac{\partial q_2}{\partial x_1} & \frac{\partial q_2}{\partial x_2} & \frac{\partial q_2}{\partial x_3} \\ \frac{\partial q_3}{\partial x_1} & \frac{\partial q_3}{\partial x_2} & \frac{\partial q_3}{\partial x_3} \end{pmatrix}_1. \quad (3.17)$$

The two relations for $\frac{\partial u_1}{\partial x_3}$ and $\frac{\partial u_2}{\partial x_3}$ are the only exceptions to the condition that the components of the derivatives of the macroscopic velocities \vec{u} and \vec{q} are required to be continuous at the interface. They are also the only two conditions independent of the condition (3.8).

As a result of (3.17), the relationship that exists at the interface between the mean stress tensor τ (see (2.63)) for the fluid side and $\bar{\tau}$ (see (2.77)) for the porous side is now apparent. Note that not every component of these tensors assumes the same type of relationship.

The final interface boundary condition to be obtained is that for the pressure. Similar to the case of the velocity gradient, we

write down

$$\int_{\Delta A_o} p \, dS = \int_{\Delta A_{1f}} p \, dS + \int_{\Delta A'_s} p \, dS . \quad (3.18)$$

By approximating the last integral by

$$\int_{\Delta A'_s} p \, dS \approx (1 - \eta) \int_{\Delta A_o} p \, dS , \quad (3.19)$$

(3.18) reduces to

$$\eta \int_{\Delta A_o} p \, dS \approx \int_{\Delta A_{1f}} p \, dS . \quad (3.20)$$

Again, the mean pressures are defined as follows:

$$p_o = \frac{1}{A} \int_{\Delta A_o} p \, dS , \quad (3.21)$$

$$\bar{p}_1 = \frac{1}{\eta A} \int_{\Delta A_{1f}} p \, dS , \quad (3.22)$$

in terms of which equation (3.20) becomes

$$p_o \approx \bar{p}_1 . \quad (3.23)$$

These mean pressures are also assumed to be the continuous limiting values of the corresponding mean pressures p and \bar{p} within their respective regions.

Equations (3.8), (3.14) and (3.23) give the six interface boundary conditions for the problem of viscous flows past a porous body. These conditions are appropriate when the viscous flow

equations, such as Stokes' equations (2.15) and (2.16), are applied in the fluid region and the full macroscopic equations (2.75) and (2.76) are applied in the porous region. According to the approximation introduced in the derivation, the velocity at the interface should be much smaller than the characteristic mean velocity in the viscous fluid region in order for these conditions to apply.

For later references, the present interface boundary conditions are summarized below in a generalized notation. At the interface,

$$\vec{u} = \vec{q} , \quad (3.24)$$

$$\eta \left(\frac{\partial \vec{u}_t}{\partial n} \right) = \frac{\partial \vec{q}_t}{\partial n} , \quad (3.25)$$

$$p = \bar{p} , \quad (3.26)$$

where it is understood that \vec{u} and p are for the fluid region, whereas \vec{q} and \bar{p} are for the porous region. The subscript "t" indicates the tangential components of the velocity and n is the coordinate normal to the interface.

3.2. An Illustrative Example

We shall now examine a simple problem in which the interface boundary conditions (3.24) - (3.26) are applied. Consider a two-dimensional pure shear flow in a uniform channel bounded by a solid wall on one side and connected to a half-infinite porous medium on the other, as shown in Fig. 6. The flow is in the direction parallel

to the interface. The porous medium has porosity η and permeability k . We are interested in finding whether such a shear flow can really exist, and if so, what is the velocity distribution.

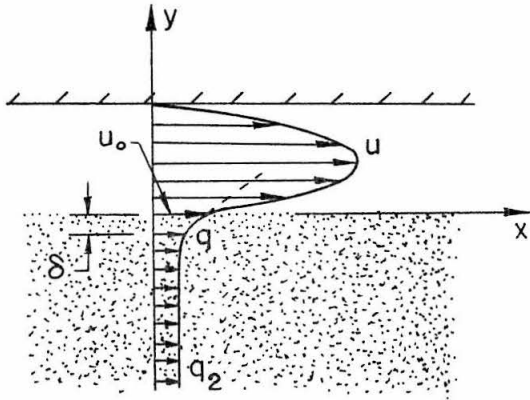


Fig. 6. A schematical representation of a shear flow within and above a half-infinite porous medium.

For a shear flow sketched in Fig. 6, the velocity assumes the following forms:

$$\vec{q} = q(y)\vec{e}_x, \quad \vec{u} = u(y)\vec{e}_x. \quad (3.27)$$

Suppose the general macroscopic equations (2.75) and (2.76) are valid within the porous medium; then for this particular case, (2.75) is automatically satisfied, and (2.76) is simplified to

$$-\frac{\partial \bar{p}}{\partial x} + \frac{\mu}{\eta} \frac{d^2 q}{dy^2} = \frac{\mu}{k} q, \quad (3.28)$$

$$-\frac{\partial \bar{p}}{\partial y} = 0. \quad (3.29)$$

From the above equations, we may already conclude that \bar{p} is independent of y and furthermore

$$\frac{d\bar{p}}{dx} = \text{const.} \quad (3.30)$$

If this pressure gradient is sufficiently large, the Reynolds number (based on the channel width) may become so high that turbulence is produced in the flow. In such a case the Navier-Stokes equations (2.10) and (2.11) are no longer applicable for the mean flow above the porous medium. Instead, equations containing the Reynolds stresses for turbulent flows [15] will be more accurate, especially in the immediate vicinity of the interface where the velocity fluctuation from the mean may be considerable. However, we shall assume that the Reynolds number is so low that the flow is laminar and satisfies the Navier-Stokes equations. Equation (2.10) is again automatically satisfied and (2.11) reduces to

$$-\frac{\partial p}{\partial x} + \mu \frac{d^2 u}{dy^2} = 0, \quad (3.31)$$

$$-\frac{\partial p}{\partial y} = 0. \quad (3.32)$$

Again we conclude that

$$\frac{dp}{dx} = \text{const.} \quad (3.33)$$

Therefore, the pressure gradient is uniform in both regions of the flow.

The general solution of (3.28) is given by

$$q = Ae^{\sqrt{\frac{\eta}{k}} y} + Be^{-\sqrt{\frac{\eta}{k}} y} - \frac{k}{\mu} \frac{d\bar{p}}{dx}. \quad (3.34)$$

By the condition requiring q to be bounded as $y \rightarrow -\infty$, $B = 0$.

We have then

$$q = q_2 = - \frac{k}{\mu} \frac{d\bar{p}}{dx}, \text{ as } y \rightarrow -\infty, \quad (3.35)$$

where q_2 is a constant velocity. This relation is recognized as Darcy's law and implies that the flow satisfies this law in the interior of the porous medium where the surface effects have diminished.

Concurrently, the general solution of (3.31) for the flow velocity within the channel can be written as

$$u = \frac{1}{2\mu} \frac{dp}{dx} y^2 + Cy + D, \quad (3.36)$$

where C and D are two arbitrary constants.

The boundary conditions of this problem are as follows:

$$q = q_2 \quad \text{as } y \rightarrow -\infty, \quad (3.37)$$

$$u = 0, \quad \text{at } y = h. \quad (3.38)$$

The interface boundary conditions (3.24) - (3.26) become for this case

$$q = u = u_o \quad \left. \vphantom{q = u = u_o} \right\} \quad (3.39a)$$

$$\frac{dq}{dy} = \eta \left(\frac{du}{dy} \right) = \eta \left(\frac{du}{dy} \right)_o \quad \left. \vphantom{\frac{dq}{dy} = \eta \left(\frac{du}{dy} \right)} \right\} \quad \text{at } y = 0, \quad (3.39b)$$

$$\bar{p} = p, \quad \left. \vphantom{\bar{p} = p} \right\} \quad (3.39c)$$

where u_o and $\left(\frac{du}{dy} \right)_o$ are the slip velocity and the velocity gradient at the interface. Of course, the quantities u_o and $\left(\frac{du}{dy} \right)_o$ are

unknown at this stage, and will be determined as a part of the problem.

The shear flow requires a constant pressure gradient for both flow regions, as found in (3.30) and (3.33). In order to satisfy the interface boundary condition (3.39c), it is further required that the pressure gradients be equal in the two flow regions,

$$\frac{d\bar{p}}{dx} = \frac{dp}{dx} = -\frac{\mu}{k} q_2, \quad (3.40)$$

where use has been made of (3.35) and (3.37) to relate the pressure gradient with q_2 .

Upon application of the boundary conditions (3.37) and (3.39a) to (3.34), with the aid of (3.40), the following solution for the flow in the porous medium is obtained.

$$q = q_2 + (u_o - q_2) e^{\sqrt{\frac{\eta}{k}} y}. \quad (3.41)$$

The solution for the flow in the fluid region may be found from (3.36) by requiring it to satisfy the boundary conditions (3.38) and (3.39a). The result is

$$u = (u_o - \frac{h}{2\mu} \frac{dp}{dx} y) (1 - \frac{y}{h}). \quad (3.42)$$

In terms of q_2 , the above becomes

$$u = (u_o + \frac{h}{2k} q_2 y) (1 - \frac{y}{h}). \quad (3.43)$$

The above solution still involves the unknown slip velocity u_o ,

which can be determined by applying the remaining interface boundary condition (3.39b). From (3.40) we have

$$\frac{dq}{dy} = \sqrt{\frac{\eta}{k}} (u_o - q_2) , \quad \text{at } y = 0 . \quad (3.44)$$

Hence by (3.39b),

$$u_o - q_2 = \sqrt{\eta k} \left(\frac{du}{dy} \right)_o . \quad (3.45)$$

We also obtain directly from (3.43)

$$\left(\frac{du}{dy} \right)_o = -\frac{u_o}{h} + \frac{h}{2k} q_2 . \quad (3.46)$$

On substituting (3.46) into (3.45), the slip velocity u_o is found to be

$$u_o = \frac{h'(\sqrt{\eta} h' + 2)}{2(h' + \sqrt{\eta})} q_2 , \quad (3.47)$$

where

$$h' = \frac{h}{\sqrt{k}} . \quad (3.48)$$

In terms of $\frac{dp}{dx}$ equation (3.47) may be written as

$$u_o = -\frac{h'(\sqrt{\eta} h' + 2)}{2(h' + \sqrt{\eta})} \frac{k}{\mu} \frac{dp}{dx} = -\frac{\sqrt{\eta} h' + 2}{2(h' + \sqrt{\eta})} \frac{h\sqrt{k}}{\mu} \frac{dp}{dx} . \quad (3.49)$$

With u_o known, the velocity profiles in both flow regions are simply given by (3.41) and (3.42).

Finally, the rate of discharge Q through the channel can be calculated from (3.42) and (3.49). The result is

$$Q = - \frac{h'^2 + 4\sqrt{\eta} h' + 6}{12h'(h' + \sqrt{\eta})} \frac{h^3}{\mu} \frac{dp}{dx} . \quad (3.50)$$

When $h' \rightarrow \infty$, or $k \rightarrow 0$, the above discharge rate tends to that of a channel with solid walls, that is

$$Q_o = - \frac{1}{12} \frac{h^3}{\mu} \frac{dp}{dx} \quad (3.51)$$

Therefore

$$\frac{Q}{Q_o} = 1 + \frac{3(\sqrt{\eta} h' + 2)}{h'(h' + \sqrt{\eta})} . \quad (3.52)$$

The ratio of the slip velocity to the mean velocity Q/h is readily obtained from (3.49) and (3.50) as

$$\frac{u_o}{Q/h} = \frac{6(\sqrt{\eta} h' + 2)}{h'^2 + 4\sqrt{\eta} h' + 6} . \quad (3.53)$$

From the above analysis, we conclude the following:

i. As can be seen from (3.41), the velocity in the porous medium decays exponentially from the interface. Under ordinary circumstances where k is small, the rate of decay is very fast. Hence in such case the velocity variation occurs completely within a thin layer adjacent to the interface. Outside this layer, the velocity is a constant q_2 determined by Darcy's law. This confirms the earlier prediction of the existence of a thin interface layer in which the full macroscopic equations should be applied instead of Darcy's law. A nominal thickness δ of the interface layer may be defined to be the distance through which the velocity difference, $q - q_2$, is

reduced to $1/e = 0.369$ of its initial value, $u_0 = q_2$. Hence

$$\delta = \sqrt{k/\eta} = \sqrt{\frac{\alpha}{\eta}} d . \quad (3.54)$$

ii. As indicated by (3.47), the tangential velocity u_0 immediately above the interface is generally not zero. Thus, the so called non-slip condition on a permeable wall does not hold. In fact, the slip velocity can be many times greater than the velocity q_2 determined by Darcy's law within the porous medium. This is most obvious when $h' \gg 1$, or $h \gg \sqrt{k}$. Under this condition, $u_0 \sim \frac{\sqrt{\eta}}{2} h' q_2$. On the other hand, u_0 is never large compared with the mean velocity Q/h of the channel flow. In particular, when $h' \gg 1$, $u_0 \sim \left(\frac{6\sqrt{\eta}}{h'}\right) \left(\frac{Q}{h}\right)$, namely, u_0 is very small compared with Q/h despite its large magnitude compared with q_2 .

iii. In (3.44), the velocity jump $u_0 - q_2$ across the interface layer is seen to be directly proportional to the normal velocity gradient $\left(\frac{du}{dy}\right)_0$ immediately outside the porous medium. This relationship is derived independent of the particular shear flow prescribed over the porous medium, so its general validity is plausible.

iv. The macroscopic effect of the porous wall is manifested by the increase of the total rate of discharge through the channel in comparison with that corresponding to a channel bounded by two solid walls. It is of significance to note from (3.52) that the increase in the discharge rate is negligibly small when $h' \gg 1$; while under the same circumstances, the slip velocity greatly exceeds the Darcy velocity q_2 in the porous medium. On the other hand, the discharge

rate increases greatly when h is of the same order of magnitude or smaller than \sqrt{k} . Under the latter conditions, however, the depth of channel h would be exceedingly small in the case of an ordinary porous medium with small k .

3.3. Interface Boundary Conditions of the Second Kind--For Darcy's Law

In the preceding discussion we have found that Darcy's law is applicable throughout a porous region except within a thin layer near an interface. It is reasonable to infer that the same is generally true for any porous region, so long as the Darcy number is small. The physical extent of the interface layer is usually so small that we may consider the Darcy equations join with the viscous flow equations right at the interface. To ensure that the solutions are still correct, the interface boundary conditions to be prescribed at the interface should correlate directly the corresponding flow variables across the interface layer. The success of this approach depends on how general these conditions can be established in advance. Although incapable of describing the detailed flow within the interface layer, the present approach will yield the same solution to the shear flow problem discussed previously provided that the interface boundary conditions are given as follows:

$$\left. \begin{aligned} p &= \bar{p} , \\ u - q &= \sqrt{\eta k} \frac{du}{dy} , \end{aligned} \right\} \text{ at } y = 0 , \quad (3.55a)$$

$$(3.55b)$$

where as before, p and u pertain to the fluid region, whereas \bar{p} and q are for the porous region.

The velocity jump condition (3.55b) was examined experimentally by Beavers et al. [8]. Their experiment dealt with the same flow configurations as the example worked out in the preceding section. Relying purely upon dimensional analysis, they assumed

$$u - q = \frac{\sqrt{k}}{\alpha_0} \frac{du}{dy}, \quad \text{at } y = 0, \quad (3.56)$$

where α_0 is an experiment coefficient to be deduced from the discharge rate through the channel above the porous material. They found α_0 to be in the range 0.1 to 4.0 for several porous materials having permeability k ranging from 10^{-6} to 10^{-5} in². Since no porosity data were included in their report, no direct comparison can be made between (3.55b) and (3.56). However, their α_0 apparently takes on values in a wider range than the corresponding theoretical value $1/\sqrt{\eta}$ would allow, because $1/\sqrt{\eta}$ is always greater than unity. This discrepancy may be attributed to the fact that the porous interfaces they used are not the ideal ones as we have assumed.

The validity of (3.55a) and (3.55b) are not so limited to parallel shear flows and flat interfaces only. It is possible to show that they are quite general. For the sake of simplicity, however, we shall consider at present only the case of general two-dimensional flow involving a flat interface. The Darcy number is assumed to be very small.

We assume that an interface layer exists in which the macro-

scopic equations (2.75) and (2.76) hold. In Cartesian coordinates (x, y, z) the flat interface coincides with the x - z plane and the y -axis is perpendicular to it. The thickness of the interface layer δ is assumed to be very small compared with a characteristic macroscopic length L . The flow in the interface layer is joined on the interior side of the layer smoothly to a flow determined by Darcy's law. If we write

$$\vec{q} = \vec{q}_2 = [(q_x)_2, (q_y)_2, 0] \quad (3.57a)$$

$$\bar{p} = \bar{p}_2 \quad \left. \vphantom{\vec{q}} \right\} \text{at } y = -\delta \quad (3.57b)$$

then \vec{q}_2 is given by Darcy's law,

$$\vec{q}_2 = - \frac{k}{\mu} (\nabla \bar{p})_2 \quad (3.58)$$

On the other side of the layer, the flow is related to the mean flow of the viscous fluid region through the interface boundary conditions of the first kind. For plane flow, we have

$$\vec{q} = \vec{u}_o = (u_o, v_o, 0) \quad (3.59a)$$

$$\frac{\partial q_x}{\partial y} = \eta \left(\frac{\partial u}{\partial y} \right)_o \quad \left. \vphantom{\vec{q}} \right\} \text{at } y = 0 \quad (3.59b)$$

$$\bar{p} = p_o \quad (3.59c)$$

All of the above boundary values are functions of x and they are not all independent since there are relationships between them.

We proceed now to simplify the macroscopic equations for this interface layer. In order to achieve this, we shall make estimates of the order of magnitude of each term in the basic equations. First we rewrite the macroscopic equations in dimensionless form by referring all velocities to u_0 , and all linear dimensions to a characteristic length L , which is so selected as to ensure that the dimensionless $\partial q_x / \partial x$ is of order unity. The pressure is made dimensionless with respect to $\mu u_0 L / k$. The result, except for the continuity equation, has been derived before as equation (2.79). For the present plane flow, written with the same symbols as for their dimensional counterparts, we have the following complete set of dimensionless equations:

$$\frac{\partial q_x}{\partial x} + \frac{\partial q_y}{\partial y} = 0 \quad , \quad (3.60)$$

$$O(1) \quad (1)$$

$$- \frac{\partial \bar{p}}{\partial x} + Da \left(\frac{\partial^2 q_x}{\partial x^2} + \frac{\partial^2 q_x}{\partial y^2} \right) = q_x \quad , \quad (3.61a)$$

$$(\delta^2) \left(1 \quad , \quad \frac{1}{\delta^2} \right) \quad O(1)$$

$$- \frac{\partial \bar{p}}{\partial y} + Da \left(\frac{\partial^2 q_y}{\partial x^2} + \frac{\partial^2 q_y}{\partial y^2} \right) = q_y \quad , \quad (3.61b)$$

$$(\delta^2) \left(\delta \quad , \quad \frac{1}{\delta} \right) \quad O(\delta)$$

where $Da = k / \eta L^2$ is the Darcy number.

With the assumption made previously the dimensionless inter-

face layer thickness δ/L , for which we shall retain the symbol δ , is very small compared to unity, namely, $\delta \ll 1$.

Orders of magnitude of the individual terms in the equations above are designated underneath each term.

We see first from the continuity equation (3.60) that since $\partial q_x/\partial x \sim O(1)$, we have $\partial q_y/\partial y \sim O(1)$. However, unlike the ordinary boundary layer theory, we cannot state that q_y is small, because the variation of a large variable can be small as well. Fortunately, since all the equations are linear, we can always superpose another solution to cancel such a large constant term of q_y , if any. In other words, there is no loss of generality if we assume $v_o = 0$ in the present problem. Assuming $v_o = 0$, it is possible to state now $q_y \sim O(\delta)$. Consequently, $\partial q_y/\partial x \sim O(\delta)$, $\partial^2 q_y/\partial x^2 \sim O(\delta)$ and also $\partial^2 q_x/\partial x^2 \sim O(1)$.

Since q_x increases to a value many times that of $(q_x)_2$ within a distance δ , as indicated by the example given in the preceding section, we may assert that $\partial q_x/\partial y \sim 1/\delta$ and $\partial^2 q_x/\partial y^2 \sim 1/\delta^2$. Similarly, $\partial q_y/\partial y \sim O(\delta/\delta) = O(1)$ and $\partial^2 q_y/\partial y^2 \sim O(1/\delta)$.

We see then from (3.61a) that the viscous term, second on the left, is of the same order of magnitude as the drag term on the right only if

$$Da \sim \delta^2 . \quad (3.62)$$

From (3.61b), it may also be inferred that $\partial \bar{p}/\partial y \sim O(\delta)$, or the pressure increase over the interface layer is of order δ^2 , i.e., very small. Thus, the pressure in a direction normal to the interface layer

is practically constant; and it may be assumed equal to that at the porous edge of the layer where its value is determined by Darcy's law, namely

$$\bar{p} = \bar{p}_2 = p_0, \quad (3.63)$$

and

$$\frac{\partial \bar{p}}{\partial x} = -\frac{\mu}{k} (q_x)_2, \quad (3.64)$$

where use has been made of (3.57b), (3.58) and (3.59c).

Finally, with relatively small order terms neglected, equations (3.60) - (3.61a,b) are simplified to the "interface layer equations."

Returning to dimensional quantities, we have

$$\frac{\partial q_x}{\partial x} + \frac{\partial q_y}{\partial y} = 0, \quad (3.65)$$

$$\frac{\partial^2 q_x}{\partial y^2} - \frac{\eta}{k} q_x = -\frac{\eta}{k} (q_x)_2, \quad (3.66)$$

where the macroscopic equation of motion normal to the interface has been dropped, and in (3.66) use has been made of (3.64) in eliminating $\partial \bar{p} / \partial x$. The general solution of (3.66) is given by

$$q_x = (q_x)_2 + A(x)e^{\sqrt{\frac{\eta}{k}}y} + B(x)e^{-\sqrt{\frac{\eta}{k}}y}. \quad (3.67)$$

In order to join the neighboring flows, conditions (3.57a) and (3.59a,b) must be satisfied. Using only the conditions

$$\begin{aligned} q_x &= u_0 \quad , \quad \text{at } y = 0 \quad , \\ q_x &= (q_x)_2 \quad , \quad \text{at } y = -\infty \quad , \end{aligned}$$

the coefficients in (3.67) are fully determined, and we obtain for the tangential velocity distribution in the interface layer

$$q_x = (q_x)_2 + [u_0 - (q_x)_2] e^{\sqrt{\frac{\eta}{k}} y} . \quad (3.68)$$

It is of interest to observe that even though $(q_x)_2$ and u_0 are functions of x , the solution (3.68) is of the same form as (3.41) where the velocities $(q_x)_2$ and u_0 were assumed constant. In other words, the solution is the same as that obtained by assuming locally constant $(q_x)_2$ and u_0 . It is also interesting to note that the velocity varies exponentially in y and hence the interface layer thickness may be defined as

$$\delta = \sqrt{\frac{k}{\eta}} . \quad (3.69)$$

This is independent of x , and so we have a uniformly thin interface layer in spite of any velocity variation along the interface.

To satisfy the other condition

$$\frac{\partial q_x}{\partial y} = \eta \left(\frac{\partial u}{\partial y} \right)_0 \quad , \quad \text{at } y = 0 \quad , \quad (3.59b)$$

we first calculate $\partial q_x / \partial y$ from (3.68) and then substitute the result into the above equation. Once again we obtain the relationship

$$u_0 - (q_x)_2 = \sqrt{\eta k} \left(\frac{\partial u}{\partial y} \right)_0 \quad , \quad (3.70)$$

which is the same as (3.55b); the general validity of this jump condition is thereby confirmed.

We may also calculate the normal velocity q_y from (3.65) by using the result (3.68) and the condition from (3.59a),

$$q_y = 0 \quad , \quad \text{at } y = 0,$$

along with the assumption $v_o = 0$. The solution is then

$$q_y = \left[\frac{d}{dx} (q_x)_z \right] y + \sqrt{\frac{k}{\eta}} \left[\frac{d}{dx} u_o - \frac{d}{dx} (q_x)_z \right] \left[e^{\sqrt{\frac{\eta}{k}} y} - 1 \right], \quad (3.71)$$

and so by (3.57a) and (3.69)

$$(q_y)_z \approx -\sqrt{\frac{k}{\eta}} \left[\frac{d}{dx} u_o \right], \quad (3.72)$$

which is seen to be of the order $(\delta/L)u_o$, the same as was estimated before. Such a small normal velocity may be considered negligible compared to the tangential velocity u_o .

We may superpose a normal flow onto the present solution (3.68) and (3.71):

$$\vec{q} = v_o \vec{e}_y. \quad (3.73)$$

This satisfies all the macroscopic equations of motion provided the corresponding pressure distribution is given by

$$\frac{dp}{dy} = \frac{\mu}{\eta} \frac{d^2 v_o}{dx^2} - \frac{\mu}{k} v_o. \quad (3.74)$$

Integrating (3.74) across the interface layer and using the relations (3.57b) and (3.59c), we obtain for the pressure jump across the interface layer

$$p_o - \bar{p}_2 = \sqrt{\frac{k}{\eta}} \left[\frac{\mu}{\eta} \frac{d^2 v_o}{dx^2} - \frac{\mu}{k} v_o \right]. \quad (3.75)$$

The magnitude of this is seen to be of order $\mu v_o / \sqrt{k\eta}$. This is a very small fraction of the macroscopic variation of pressure over a length L , which is estimated to be of order $\mu v_o L / k$. Therefore, neglecting this pressure jump across the interface will introduce only very small errors to the solution of this category of problems. Hence, we assert that $p_o \approx \bar{p}_2$ for the normal flow v_o through the interface layer.

In summary, we may now write down all the approximate equations relating flow variables across the interface layer. These are the interface boundary conditions of the second kind for plane flow:

$$v_o \approx (q_y)_2, \quad (3.76)$$

$$u_o - (q_x)_2 = \sqrt{\eta k} \left(\frac{\partial u}{\partial y} \right)_o, \quad (3.77)$$

$$p_o \approx \bar{p}_2. \quad (3.78)$$

The first condition is concluded from (3.72) and (3.73), the second is identical to (3.70), and the last results from the approximations discussed subsequent to equations (3.62) and (3.75).

Owing to the linearities of the macroscopic equations, the above interface boundary conditions for plane flow may be easily extended to the three dimensional case when the interface is flat. We

simply write down the results without further discussion.

$$u_n = q_n \tag{3.79}$$

$$\vec{u}_t - \vec{q}_t = \sqrt{\eta k} \frac{\partial \vec{u}_t}{\partial n} \tag{3.80}$$

$$p = \bar{p} \tag{3.81}$$

} at the interface,

where n is the coordinate normal to the interface and t indicates tangential directions.

Actually, these interface conditions can be equally well applied to a curved surface provided certain minor restrictions are met. This will be demonstrated by an example in the next chapter.

It may be that the interface is not an ideal one, namely, that it has a different geometrical construction than its interior region. In such a case k and η in (3.80) should be determined with respect to the interface layer. However, this would be difficult to achieve in practice. It is more practical to introduce another coefficient β such that

$$\vec{u}_t - \vec{q}_t = \frac{\sqrt{\eta k}}{\beta} \frac{\partial \vec{u}_t}{\partial n} \tag{3.82}$$

and to have β determined by experiments. Outside of this modification, the other two conditions (3.79) and (3.81) remain unchanged.

At this stage, we recall that the pressure P in Darcy's law (2.3) has been assumed to be equal to the mean pressure \bar{p} defined in (2.7). This is now well justified, because P is experimentally a measure of the mean pressure in the fluid side of the interface. This

is the mean pressure p on the left side of equation (3.81), and hence should be equal to \bar{p} in the porous region according to condition (3.81).

IV. VISCOUS FLOWS PAST POROUS BODIES OF FINITE SIZE

4.1. Viscous Flow Between a Rotating Solid Cylinder and a Stationary Porous Cylinder

Consider the viscous flow between two concentric cylinders such that the inner porous cylinder is stationary and the outer solid cylinder is rotating at a constant angular speed ω . We are interested in the fluid motion between the cylinders as well as that induced in the porous region. Such a coupled flow is shown schematically in Fig. 7.

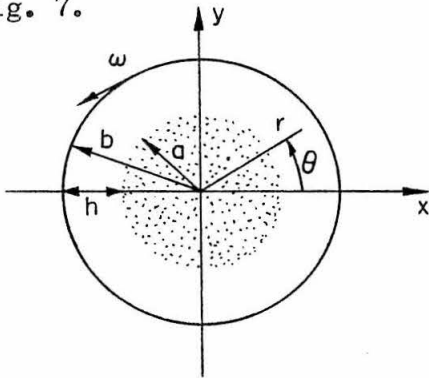


Fig. 7. Viscous flow between a solid and a porous cylinder.

Since the interface boundary conditions of the second kind for a curved interface have not been established, we shall consider the application of the macroscopic equations of motion instead of Darcy's law within the porous region. In fact, it will turn out from the solutions obtained in this example that the same set of interface boundary conditions of the second kind (3.79) - (3.81) is approximately true for a curved interface as well.

We assume that the flow is axisymmetrical and is in the circumferential direction only. For the flow in the porous cylinder, $\vec{q} = q(r)\vec{e}_\theta$. The macroscopic continuity equation (2.75) is auto-

matically satisfied, while the macroscopic equation (2.76) for plane polar coordinates reduces to

$$\frac{d\bar{p}}{dr} = 0 , \quad (4.1)$$

and

$$\frac{d^2q}{dr^2} + \frac{1}{r} \frac{dq}{dr} - \left(\frac{\eta}{k} + \frac{1}{r^2} \right) q = 0 . \quad (4.2)$$

We further assume that the flow between the cylinders is laminar, and satisfies the Navier-Stokes equations. Since $\vec{u} = u(r)\vec{e}_\theta$, the continuity equation (2.10) is automatically satisfied, while the Navier-Stokes equation (2.11) for plane polar coordinates reduces to

$$\frac{dp}{dr} = \frac{\rho u^2}{r} , \quad (4.3)$$

$$\frac{d^2u}{dr^2} + \frac{1}{r} \frac{du}{dr} - \frac{u}{r^2} = 0 . \quad (4.4)$$

The boundary conditions of the problem are as follows:

$$q = \text{finite, at } r = 0 , \quad (4.5a)$$

$$u = b\omega , \text{ at } r = b , \quad (4.5b)$$

and the interface boundary conditions of the first kind (3.24) - (3.26) reduce to

$$u = q \quad (4.6a)$$

$$\eta \frac{du}{dr} = \frac{dq}{dr} \quad (4.6b)$$

$$p = \bar{p} \quad (4.6c)$$

} at $r = a$.

Substitution of $x = \sqrt{\frac{\eta}{k}} r$ into equation (4.2) yields

$$\frac{d^2 q}{dx^2} + \frac{1}{x} \frac{dq}{dx} - \left(1 + \frac{1}{x^2}\right) q = 0 \quad . \quad (4.7)$$

The solutions of this equation are the modified Bessel functions, which are the Bessel functions of purely imaginary arguments.

Usually they are denoted by

$$I_\nu(x) = i^{-\nu} J_\nu(ix) \quad , \quad (4.8a)$$

$$K_\nu(x) = \frac{\pi}{2} i^{\nu+1} H_\nu^{(1)}(ix) \quad , \quad (4.8b)$$

where ν indicates the order. In this case, $\nu = 1$. These functions are real when x is real, and their asymptotic representations are as follows:

For $x \ll 1$:

$$I_\nu(x) \sim \frac{1}{\Gamma(\nu+1)} \left(\frac{x}{2}\right)^\nu \quad , \quad (4.9a)$$

$$\begin{aligned} K_\nu(x) &\sim - \left[\ln\left(\frac{x}{2}\right) + 0.5772 + \dots \right] \quad , \quad \nu = 0 \quad , \\ &\sim \frac{\Gamma(\nu)}{2} \left(\frac{2}{x}\right)^\nu \quad , \quad \nu \neq 0 \quad . \end{aligned} \quad (4.9b)$$

For $x \gg (1, \nu)$

$$I_\nu(x) = \frac{1}{\sqrt{2\pi x}} e^x \left[1 + O\left(\frac{1}{x}\right) \right] \quad , \quad (4.10a)$$

$$K_\nu(x) = \sqrt{\frac{\pi}{2x}} e^{-x} \left[1 + O\left(\frac{1}{x}\right) \right] \quad . \quad (4.10b)$$

They also satisfy the recurrence identity ,

$$I'_{\nu}(x) = I_{\nu-1}(x) - \frac{\nu}{x} I_{\nu}(x) . \quad (4.11)$$

The general solution of (4.2) is therefore given by

$$q = A_1 I_1 \left(\sqrt{\frac{\eta}{k}} r \right) + A_2 K_1 \left(\sqrt{\frac{\eta}{k}} r \right) , \quad (4.12)$$

and the solution of (4.4), which is seen to be Euler's equation, is

$$u = B_1 r + \frac{B_2}{r} . \quad (4.13)$$

The four coefficients A_1 , A_2 , B_1 and B_2 in equations (4.12) and (4.13) can be readily determined by a simple application of the four boundary conditions, (4.5a,b) and (4.6a,b).

We shall write the solutions in terms of the slip velocity u_0 , which is the velocity u at $r = a$. According to (4.6a), we have

$$u = q = u_0, \quad \text{at} \quad r = a . \quad (4.14)$$

In order for q to satisfy (4.5a), the coefficient A_2 in (4.12) must vanish. In terms of u_0 , (4.12) reduces to

$$q(r) = u_0 \frac{I_1 \left(\sqrt{\frac{\eta}{k}} r \right)}{I_1 \left(\sqrt{\frac{\eta}{k}} a \right)} . \quad (4.15)$$

The velocity u must satisfy (4.5b), and so in terms of u_0 , (4.13) becomes

$$u(r) = \frac{b^2 \omega - a u_0}{b^2 - a^2} r + \frac{a b^2 (u_0 - a \omega)}{b^2 - a^2} \frac{1}{r} . \quad (4.16)$$

The slip velocity u_0 is still unknown, and is determined from (4.15) and (4.16) by requiring these velocities to satisfy the interface boundary condition (4.6b). First from (4.15), we obtain

$$\left(\frac{dq}{dr}\right)_{r=a} = \sqrt{\frac{\eta}{k}} \left[\frac{I_0\left(\sqrt{\frac{\eta}{k}} a\right)}{I_1\left(\sqrt{\frac{\eta}{k}} a\right)} - \frac{1}{\sqrt{\frac{\eta}{k}} a} \right] u_0, \quad (4.17)$$

where use has been made of the identity (4.11). Condition (4.6b) is then applied to give the following relation

$$\left(\frac{du}{dr}\right)_{r=a} = \frac{1}{\sqrt{\eta k}} \left[\frac{I\left(\sqrt{\frac{\eta}{k}} a\right)}{I_1\left(\sqrt{\frac{\eta}{k}} a\right)} - \frac{1}{\sqrt{\frac{\eta}{k}} a} \right] u_0. \quad (4.18)$$

By requiring (4.16) to satisfy the above relation, the slip velocity u_0 is finally obtained as

$$u_0 = \frac{2ab^2 \omega \frac{\sqrt{\eta k}}{a}}{(b^2 - a^2) \left[\frac{I_0\left(\sqrt{\frac{\eta}{k}} a\right)}{I_1\left(\sqrt{\frac{\eta}{k}} a\right)} - \frac{1}{\sqrt{\frac{\eta}{k}} a} \right] + (b^2 + a^2) \frac{\sqrt{\eta k}}{a}}. \quad (4.19)$$

With u_0 known, the velocity distributions of the flow in both regions are given by equations (4.15) and (4.16).

We shall examine the solution in the limit when the Darcy number is small. The Darcy number in this problem may be defined as

$$Da = \frac{k}{\eta a^2}. \quad (4.20)$$

In the limit of small Da , the velocity distribution q of (4.15) in the

vicinity of the interface may be expanded to give

$$q(r) \approx u_0 \sqrt{\frac{a}{r}} e^{-\sqrt{\frac{\eta}{k}}(a-r)}, \quad r \sim a. \quad (4.21)$$

Thus, we see that the velocity decays rapidly, in this case reducing to zero within a small distance (a few times the interface layer thickness $\delta = \sqrt{k/\eta}$) from the interface located at $r = a$. This is the same situation as occurred in the vicinity of a flat interface. The thickness δ of the interface layer for the cylindrical interface can also be defined to be $\sqrt{k/\eta}$, and is seen to be uniform along the interface.

The relation (4.18) can also be expanded for small Da by using (4.10a), to give

$$u_0 = \sqrt{\eta k} \left(\frac{du}{dr} \right)_{r=a} [1 + O(Da)]. \quad (4.22)$$

The velocity jump, in this case from 0 to u_0 , is again proportional to the normal velocity gradient provided that Da is sufficiently small.

From this example, we may infer that in general a curved porous interface behaves locally very much the same as a flat interface. The important stipulation is that the local Darcy number $D = k/\eta R^2$, defined with respect to the radius of curvature R , is sufficiently small. With this result, the interface boundary conditions of the second kind for a curved porous interface may be approximated by those established for a flat interface, namely, equations (3.79) to (3.81).

For this particular case, the approximate interface boundary

conditions of the second kind may be written as follows

$$\left. \begin{aligned} u_0 &= \sqrt{\eta k} \left(\frac{du}{dr} \right)_{r=a} \\ p &= \bar{p} \end{aligned} \right\} \text{ at } r = a \quad . \quad (4.23a)$$

$$(4.23b)$$

Using these conditions, solutions for the velocities may be obtained, which satisfy Darcy's law on one side of the interface and (4.4) on the other. The results are the same as (4.15) and (4.16) in the limit of small Da . Of course, detailed knowledge of the flow within the interface layer is now lost.

For small Da , the velocity u is found to be

$$u = \frac{b^2 \omega}{(b^2 - a^2) + (b^2 + a^2) \frac{\sqrt{\eta k}}{a}} \left[\left(1 + \frac{\sqrt{\eta k}}{a} \right) r - \left(1 - \frac{\sqrt{\eta k}}{a} \right) \frac{a^2}{r} \right]. \quad (4.24)$$

The slip velocity u_0 at $r = a$ is then

$$\frac{u_0}{b\omega} = \frac{2ab \frac{\sqrt{\eta k}}{a}}{(b^2 - a^2) + (b^2 + a^2) \frac{\sqrt{\eta k}}{a}} \quad . \quad (4.25)$$

In terms of $h = b - a$, this result becomes

$$\frac{u_0}{b\omega} = \frac{1 + \frac{h}{a}}{\left(\frac{a}{\sqrt{\eta k}} + 1 \right) \left[\frac{h}{a} \left(1 + \frac{h}{2a} \right) \right] + 1} \quad . \quad (4.26)$$

Finally, the torque acting on the outer cylinder, which is required to maintain the motion, is

$$M = 2\pi b^2 \tau(b) = 2\pi b^2 \left[r \frac{d}{dr} \left(\frac{u}{r} \right) \right]_{r=b},$$

so that

$$M = \frac{4\pi\mu a^2 b^2 \omega \left(1 - \frac{\sqrt{\eta k}}{a} \right)}{(b^2 - a^2) + (b^2 + a^2) \frac{\sqrt{\eta k}}{a}}, \quad (4.27)$$

which tends to the value M_s for a solid cylinder as $k \rightarrow 0$, where

$$M_s = \frac{4\pi\mu a^2 b^2 \omega}{b^2 - a^2}. \quad (4.28)$$

The ratio of the torque on a porous cylinder to M_s is then

$$C_M = \frac{M}{M_s} = 1 - \frac{2b^2 \frac{\sqrt{\eta k}}{a}}{(b^2 - a^2) + (b^2 + a^2) \frac{\sqrt{\eta k}}{a}} = 1 - \frac{b}{a} \frac{u_0}{b\omega}, \quad (4.29)$$

or, in terms of h , it becomes

$$C_M = 1 - \frac{\left(1 + \frac{h}{a} \right)^2}{\left(\frac{a}{\sqrt{\eta k}} + 1 \right) \left[\frac{h}{a} \left(1 + \frac{h}{2a} \right) \right] + 1}. \quad (4.30)$$

Equations (4.27) through (4.30) are also valid only when $Da \ll 1$.

The torque coefficient C_M is plotted against $a/\sqrt{\eta k}$ and h/a in Fig. 8. The plot includes only a very small range of $a/\sqrt{\eta k}$ in which the effect of the porous cylinder is more apparent. Beyond this range, the coefficient C_M approaches unity, so that the torque M becomes nearly the same as for solid cylinders, especially when the gap h between the cylinders is moderate or large. This graph

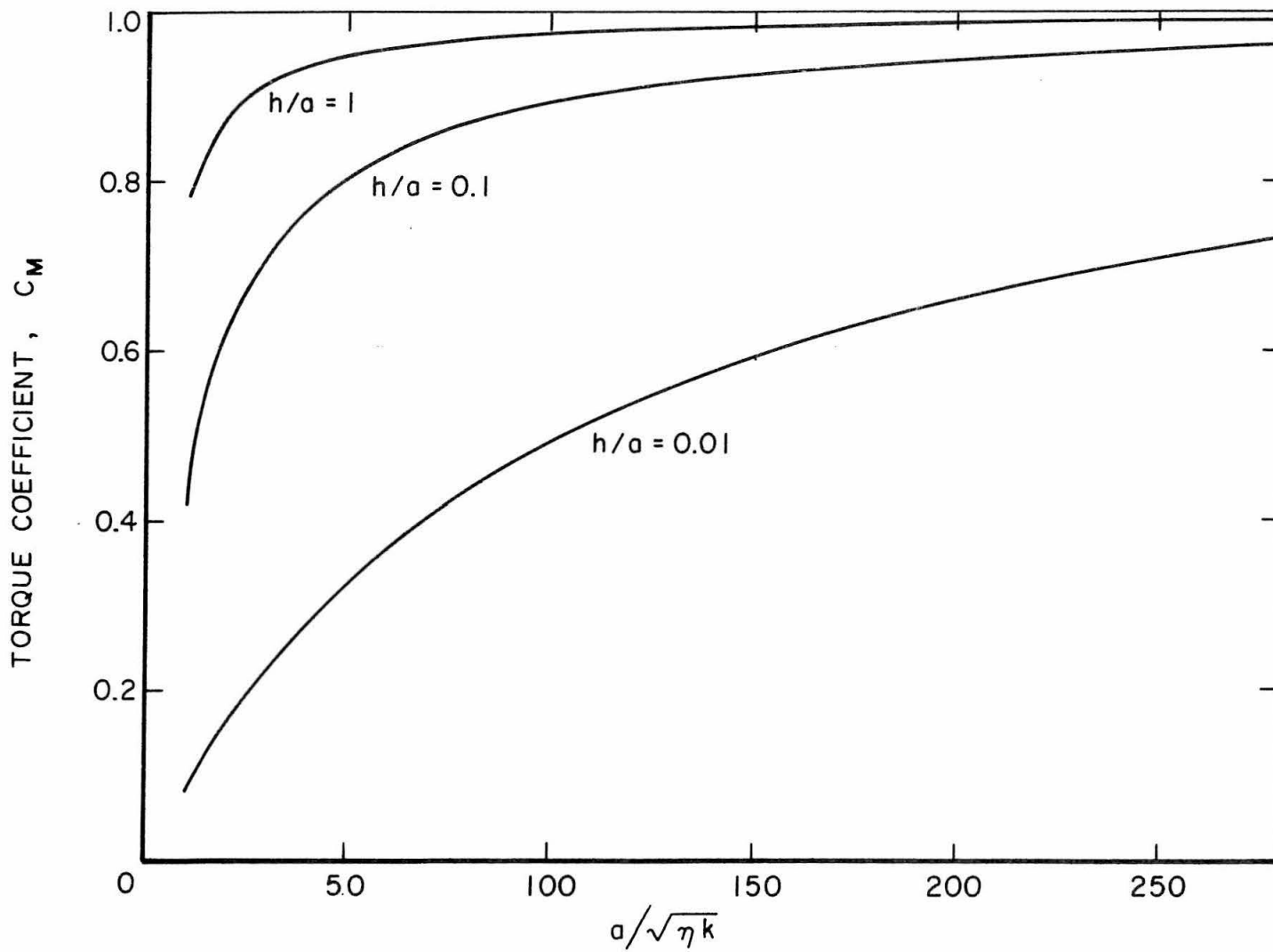


Fig. 8. Torque coefficient for flow between a rotating solid cylinder and a stationary porous cylinder.

also shows that the torque reduction is larger the smaller the gap is. For an ordinary porous cylinder, the value of $a/\sqrt{\eta k}$ is expected to be much larger than the maximum indicated in the plot. Therefore the porous cylinder usually behaves very much like a solid one, unless the gap h is very small.

4.2. Stokes Flow Past a Porous Sphere

Consider the slow uniform flow past a porous sphere, as shown in Fig. 9. The sphere has radius a , porosity η , and permeability k . We assume that the Reynolds number Ud/ν is so small that Stokes' equations can be applied to the fluid region. Consequently, for the flow within the porous sphere, the corresponding Reynolds number qd/ν is even smaller. We further assume that the Darcy number $k/\eta a^2$ is also small, so that Darcy's law can be used within the porous region. This is the same problem treated by Joseph and Tao [3].

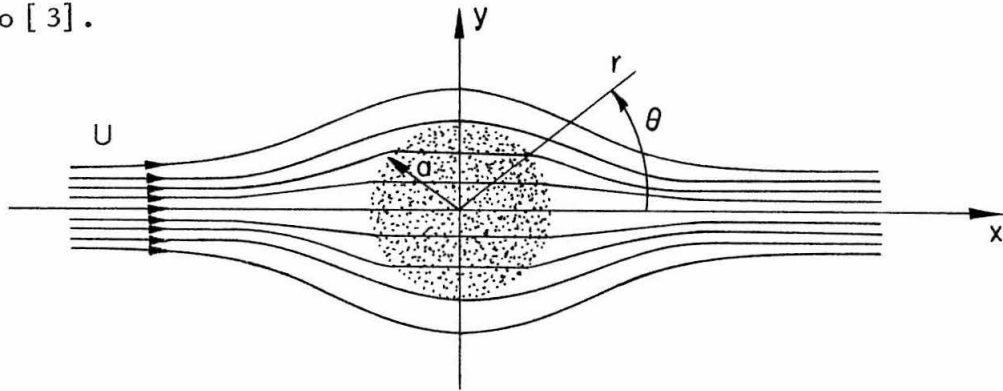


Fig. 9. Stokes flow past a porous sphere.

As Darcy's law will be applied within the porous sphere, we shall use the interface boundary conditions of the second kind. As implied by the preceding example, these conditions for a curved interface may be approximated by equations (3.79) - (3.81), provided the local Darcy number $k/\eta R^2$ is very small. In this case, the radius of curvature R is a constant equal to a , and hence we are assured of a small Darcy number.

Spherical polar coordinates (r, θ, φ) will be used in the analysis. The governing equations are as follows:

$$r > a: \quad \nabla \cdot \vec{u} = 0, \quad (4.31)$$

$$-\nabla p + \mu \nabla^2 \vec{u} = 0, \quad (4.32)$$

$$r < a: \quad \nabla \cdot \vec{q} = 0, \quad (4.33)$$

$$\vec{q} = -\frac{k}{\mu} \nabla \bar{p}. \quad (4.34)$$

The boundary conditions are

$$r \rightarrow \infty: \quad \vec{u} \rightarrow U \vec{e}_1, \quad (4.35a)$$

$$p \rightarrow p_\infty, \quad (4.35b)$$

$$r = a: \quad u_r = q_r, \quad (4.36a)$$

$$u_\theta - q_\theta = \sqrt{\eta k} \frac{\partial u_\theta}{\partial r}, \quad (4.36b)$$

$$p = \bar{p}, \quad (4.36c)$$

$$r = 0: \quad \vec{q} = \text{finite}, \quad (4.37a)$$

$$\bar{p} = \bar{p}_0 \quad . \quad (4.37b)$$

Considering the rotational symmetry of this problem, Stokes' stream functions ψ and Ψ , pertinent to the outside flow and inside flow respectively, are defined by the following equations:

$$\text{For } r > a: \quad u_r = \frac{1}{r^2 \sin \theta} \frac{\partial \psi}{\partial \theta}, \quad u_\theta = -\frac{1}{r \sin \theta} \frac{\partial \psi}{\partial r}; \quad (4.38)$$

$$\text{for } r < a: \quad q_r = \frac{1}{r^2 \sin \theta} \frac{\partial \Psi}{\partial \theta}, \quad q_\theta = -\frac{1}{r \sin \theta} \frac{\partial \Psi}{\partial r} . \quad (4.39)$$

Also, the vorticity outside, $\vec{\omega}$, and inside the sphere, \vec{W} , have the following relationships:

$$\text{For } r > a: \quad \vec{\omega} = \nabla \times \vec{u} = -\frac{D^2 \psi}{r \sin \theta} \vec{e}_\varphi, \quad (4.40)$$

$$\nabla \times \vec{\omega} = -\frac{1}{r \sin \theta} \left(\vec{e}_r \frac{1}{r} \frac{\partial}{\partial \theta} - \vec{e}_\theta \frac{\partial}{\partial r} \right) D^2 \psi, \quad (4.41)$$

$$\nabla^2 \vec{\omega} = -\nabla \times \nabla \times \vec{\omega} = -\frac{\vec{e}_\varphi}{r \sin \theta} D^2 D^2 \psi, \quad (4.42)$$

where

$$D^2 = \frac{\partial^2}{\partial r^2} + \frac{\sin \theta}{r^2} \frac{\partial}{\partial \theta} \left(\frac{1}{\sin \theta} \frac{\partial}{\partial \theta} \right); \quad (4.43)$$

$$\text{for } r < a: \quad \vec{W} = \nabla \times \vec{q} = -\frac{D^2 \Psi}{r \sin \theta} \vec{e}_\varphi. \quad (4.44)$$

Taking the curl of (4.32) and (4.34) gives

$$\nabla^2 \vec{\omega} = 0 \quad (r > a) , \quad (4.45)$$

$$\vec{W} = 0 \quad (r < a) . \quad (4.46)$$

Therefore, upon substitution of (4.42) and (4.44) into the above equations, we obtain

$$D^4 \psi = 0 \quad (r > a) , \quad (4.47)$$

$$D^2 \Psi = 0 \quad (r < a) . \quad (4.48)$$

The boundary condition at infinity becomes

$$\psi \rightarrow \frac{1}{2} U r^2 \sin^2 \theta , \text{ as } r \rightarrow \infty . \quad (4.49)$$

Furthermore, since \vec{q} is required to be regular at $r = 0$, we may stipulate that

$$\Psi = 0, \text{ at } r = 0 . \quad (4.50)$$

Assume a separation of variables for the stream functions

$$\psi = f(r) \sin^2 \theta , \quad (4.51)$$

$$\Psi = F(r) \sin^2 \theta , \quad (4.52)$$

we have

$$D^2 \psi = \mathcal{L}^2 f \cdot \sin^2 \theta , \quad (4.53)$$

$$D^4 \psi = \mathcal{L}^4 f \cdot \sin^2 \theta , \quad (4.54)$$

$$D^2 \Psi = \mathcal{L}^2 F \cdot \sin^2 \theta , \quad (4.55)$$

where

$$\mathfrak{L}^2 = \frac{d^2}{dr^2} - \frac{2}{r^2}, \quad (4.56)$$

and hence

$$\vec{\omega} = -\frac{\mathfrak{L}^2 f}{r} \sin \theta \vec{e}_\varphi, \quad (4.57)$$

$$\nabla \times \vec{\omega} = -\frac{2\mathfrak{L}^2 f}{r^2} \cos \theta \vec{e}_r + \frac{1}{r} \frac{d}{dr} (\mathfrak{L}^2 f) \sin \theta \vec{e}_\theta. \quad (4.58)$$

By using the results (4.54) and (4.55), equations (4.47) and (4.48) reduce to

$$\mathfrak{L}^4 f = f'''' - \frac{4}{r^2} f'' + \frac{8}{r^3} f' - \frac{8}{r} f = 0, \quad (4.59)$$

$$\mathfrak{L}^2 F = F'' - \frac{2}{r^2} F = 0. \quad (4.60)$$

The general solutions for these ordinary differential equations can be written down immediately.

$$\text{For } r > a: \quad f(r) = \frac{A}{r} + Br + Cr^2 + Dr^4; \quad (4.61)$$

$$\text{for } r < a: \quad F(r) = \frac{A_1}{r} + B_1 r^2. \quad (4.62)$$

After taking into consideration the boundary conditions (4.49) and (4.50), the above equations further reduce to

$$f(r) = \frac{1}{2} Ur^2 + Br + \frac{A}{r}, \quad (4.63)$$

$$F(r) = \frac{1}{2} q_0 r^2, \quad (4.64)$$

in which we have written $B_1 = \frac{1}{2} q_0$. Using the above solution $f(r)$,

we find that for $r > a$,

$$\mathfrak{L}^2 f = -\frac{2B}{r}, \quad (4.65)$$

$$\vec{\omega} = \frac{2B}{r^2} \sin \theta \vec{e}_\varphi, \quad (4.66)$$

$$\nabla \times \vec{\omega} = \frac{4B}{r^3} \cos \theta \vec{e}_r + \frac{2B}{r^3} \sin \theta \vec{e}_\theta, \quad (4.67)$$

$$\nabla p = \mu \nabla^2 \vec{u} = -\mu \nabla \times \vec{\omega} = -\frac{4\mu B}{r^3} \cos \theta \vec{e}_r - \frac{2\mu B}{r^3} \sin \theta \vec{e}_\theta. \quad (4.68)$$

The last equation is easily integrated. After applying the boundary condition (4.35b) for p at ∞ the pressure becomes

$$p = p_\infty + \frac{2\mu B}{r^2} \cos \theta \quad (r > a). \quad (4.69)$$

The stream functions, velocities, as well as the pressure distributions in the fluid and the porous regions can easily be found from equations (4.51), (4.52), (4.38), (4.39) and (4.34). The results are summarized as follows:

$r > a$	$r < a$	
$\psi = \left(\frac{1}{2} U r^2 + B r + \frac{A}{r} \right) \sin^2 \theta,$	$\Psi = \frac{1}{2} q_0 r^2 \sin^2 \theta,$	
$u_r = \left(U + \frac{2B}{r} + \frac{2A}{r^3} \right) \cos \theta,$	$q_r = q_0 \cos \theta,$	}
$u_\theta = \left(-U - \frac{B}{r} + \frac{A}{r^3} \right) \sin \theta,$	$q_\theta = -q_0 \sin \theta,$	
$p = p_\infty + \frac{2\mu B}{r^2} \cos \theta,$	$\bar{p} = \bar{p}_0 - \frac{\mu q_0}{k} r \cos \theta.$	

(4.70)

Here we observe that the flow in the porous sphere is uniform and parallel to the x-axis. The same result has been obtained by Joseph and Tao [3], though without specific mention about it. Now we consider the interface boundary conditions (4.36a,b,c) at $r = a$. Simple substitutions of (4.70) in (4.36a,b,c) yield

$$\frac{A}{a^3} + \frac{B}{a} - \frac{q_0}{2} = -\frac{U}{2} , \quad (4.71)$$

$$\left(1 + \frac{3}{\alpha_0 a_0}\right) \frac{A}{a^3} - \left(1 + \frac{1}{\alpha_0 a_0}\right) \frac{B}{a} + q_0 = U , \quad (4.72)$$

$$\frac{B}{a} + \frac{1}{2} a_0^2 q_0 = 0 , \quad (4.73)$$

$$p_0 = p_\infty , \quad (4.74)$$

where a_0, α_0 are defined as

$$a_0 = \frac{a}{\sqrt{k}} , \quad (4.75)$$

$$\alpha_0 = \frac{1}{\sqrt{\eta}} . \quad (4.76)$$

The three unknown coefficients A, B, q_0 can be solved from the three simultaneous equations (4.71) - (4.73). These coefficients are found to be

$$\frac{A}{a^3} = \frac{\ell}{4} U , \quad (4.77a)$$

$$\frac{B}{a} = -m \frac{3}{4} U , \quad (4.77b)$$

$$q_o = m \frac{3}{2} \frac{1}{a_o} U , \quad (4.77c)$$

where ℓ , m are abbreviations for

$$\ell = \frac{1 - \frac{1}{\alpha_o a_o}}{1 + \frac{2}{\alpha_o a_o} + \frac{3}{2} \frac{1}{a_o} \left(1 + \frac{1}{\alpha_o a_o}\right)} , \quad (4.78a)$$

$$m = \frac{1 + \frac{1}{\alpha_o a_o}}{1 + \frac{2}{\alpha_o a_o} + \frac{3}{2} \frac{1}{a_o} \left(1 + \frac{1}{\alpha_o a_o}\right)} . \quad (4.78b)$$

Substituting (4.77a,b,c) into (4.70), we finally obtain the solution:

$$\begin{aligned} \psi &= \frac{1}{2} U a^2 \left[\left(\frac{r}{a}\right)^2 - m \frac{3}{4} \left(\frac{r}{a}\right) + \frac{\ell}{4} \left(\frac{a}{r}\right) \right] \sin^2 \theta , & \Psi &= m \frac{3}{4} k U \left(\frac{r}{a}\right)^2 \sin^2 \theta , \\ u_r &= U \left[1 - m \frac{3}{2} \left(\frac{a}{r}\right) + \frac{\ell}{2} \left(\frac{a}{r}\right)^3 \right] \cos \theta , & q_r &= m \frac{3}{2} \frac{k}{a^2} U \cos \theta , \\ u_\theta &= U \left[-1 + m \frac{3}{4} \left(\frac{a}{r}\right) + \frac{\ell}{4} \left(\frac{a}{r}\right)^3 \right] \sin \theta , & q_\theta &= -m \frac{3}{2} \frac{k'}{a^2} U \sin \theta , \\ p &= p_\infty - m \frac{3}{2} \frac{\mu U a}{r} \cos \theta , & \bar{p} &= p_\infty - m \frac{3}{2} \frac{\mu U r}{a} \cos \theta , \end{aligned} \quad (4.79)$$

This solution is seen to converge to that for a solid sphere as $k \rightarrow 0$

(in which case $\ell \rightarrow 1$, $m \rightarrow 1$), as should be expected.

We now calculate the drag experienced by the porous sphere. To this end, the following components of the viscous stresses in the fluid region are first found from the solution (4.79):

$$\tau_{rr} = 2\mu \frac{\partial u}{\partial r} = \frac{3\mu U}{r} \left(m \frac{a}{r} - \ell \left(\frac{a}{r} \right)^3 \right) \cos \theta , \quad (4.80a)$$

$$\tau_{r\theta} = \mu \left[\frac{1}{r} \frac{\partial u_r}{\partial \theta} + r \frac{\partial}{\partial r} \left(\frac{u_\theta}{r} \right) \right] = -\ell \frac{3}{2} \frac{\mu U}{r} \left(\frac{a}{r} \right)^3 \sin \theta . \quad (4.80b)$$

Thus, at the spherical surface, $r = a$,

$$p = p_\infty - m \frac{3}{2} \frac{\mu U}{a} \cos \theta , \quad (4.81a)$$

$$\tau_{rr} = \frac{3\mu U}{r} (m - \ell) \cos \theta , \quad (4.81b)$$

$$\tau_{r\theta} = -\ell \frac{3}{2} \frac{\mu U}{a} \sin \theta . \quad (4.81c)$$

In Stokes flow, the total force acting on all solid surfaces is equal to the total force on any closed surface surrounding these solids. Therefore, to obtain the total drag D , it is only necessary to integrate the stresses over the spherical surface at $r = a$. We shall do this for each stress component separately in order to see the relative contribution from each.

$$D_p = -\int \int p \cos \theta a^2 d\Omega = m 2\pi\mu Ua , \quad (4.82a)$$

$$D_{\tau_{rr}} = \int \int \tau_{rr} \cos \theta a^2 d\Omega = - (m - \ell) 4\pi\mu Ua , \quad (4.82b)$$

$$D_{\tau_{r\theta}} = - \int \int \tau_{r\theta} \sin \theta a^2 d\Omega = \ell 4\pi\mu Ua . \quad (4.82c)$$

The total drag is simply the summation

$$D = D_p + D_{\tau_{rr}} + D_{\tau_{r\theta}} = (4\ell - m) 2\pi\mu Ua . \quad (4.83)$$

Notice that this reduces to the value of the drag on a solid sphere, $6\pi\mu Ua$, as $k \rightarrow 0$ ($\ell \rightarrow 1, m \rightarrow 1$).

Since the Darcy number $k/\eta a^2$ is assumed to be small, or $a_o \gg 1$, we may expand the drag formula (4.83) with respect to small $1/a_o$. Since

$$\ell = 1 - \frac{3}{\alpha_o a_o} + \left(\frac{6}{\alpha_o^2} - \frac{3}{2} \right) \frac{1}{a_o^2} + O\left(\frac{1}{a_o^3} \right) , \quad (4.84a)$$

$$m = 1 - \frac{1}{\alpha_o a_o} + \left(\frac{2}{\alpha_o^2} - \frac{3}{2} \right) \frac{1}{a_o^2} + O\left(\frac{1}{a_o^3} \right) , \quad (4.84b)$$

equations (4.82a,b,c) become approximately

$$D_p \sim \left[1 - \frac{1}{\alpha_o a_o} + \left(\frac{2}{\alpha_o^2} - \frac{3}{2} \right) \frac{1}{a_o^2} \right] 2\pi\mu Ua , \quad (4.85a)$$

$$D_{\tau_{rr}} \sim - \left[\frac{2}{\alpha_o a_o} - \frac{4}{\alpha_o^2 a_o^2} \right] 4\pi\mu Ua , \quad (4.85b)$$

$$D_{\tau_{r\theta}} \sim \left[1 - \frac{3}{\alpha_o a_o} + \left(\frac{6}{\alpha_o^2} - \frac{3}{2} \right) \frac{1}{a_o^2} \right] 4\pi\mu Ua . \quad (4.85)$$

The formula (4.83) of the total drag, therefore, has the following expansion:

$$D \sim \left[1 - \frac{11}{3} \frac{1}{\alpha_o a_o} + \left(\frac{22}{3\alpha_o^2} - \frac{3}{2} \right) \frac{1}{a_o^2} \right] 6\pi\mu Ua \quad \left(\frac{1}{a_o} \ll 1 \right) . \quad (4.86)$$

A drag coefficient may be formed with respect to the solid sphere drag as follows:

$$C_D = \frac{D}{6\pi\mu Ua} \sim 1 - \frac{11}{3} \frac{\sqrt{\eta k}}{a} + \left(\frac{22}{3} - \frac{3}{2\eta} \right) \frac{\eta k}{a^2} \quad \left(\frac{\sqrt{k}}{a} \ll 1 \right) . \quad (4.87)$$

The drag coefficient C_D plotted against $a/\sqrt{\eta k}$ is presented in Fig. 10. The third order term of (4.87) has been neglected in the plot. It is observed that the drag coefficient is always less than unity. In other words, the porosity effect for a sphere is a reduction in its drag. It is also seen that no appreciable reduction occurs when $a/\sqrt{\eta k} > 200$. A porous sphere which has $a/\sqrt{\eta k} > 200$ may then be considered as equivalent to a solid one insofar as its drag in a Stokes flow is concerned. This is usually the case for a sphere consisting of ordinary porous material which in general has a very small k . Only in the extreme case when the sphere becomes very porous ($\eta \sim 1$), can the porosity effect become great. To see this we assume a small sphere model for the porous medium, as discussed in Section 3 of Chapter II. We further assume that it is a simple cubic array. In order for the value of $a/\sqrt{\eta k}$ to be around 200, the distance between the centers of the spherical particles, according to (2.53) and (2.49), should be twice the particle diameter ($h/d = 2$), when there are assumed to be 100 small particles along a diameter of the porous sphere. The corresponding porosity is 0.93. However, in general practice this cannot be achieved with packed particles. For the same

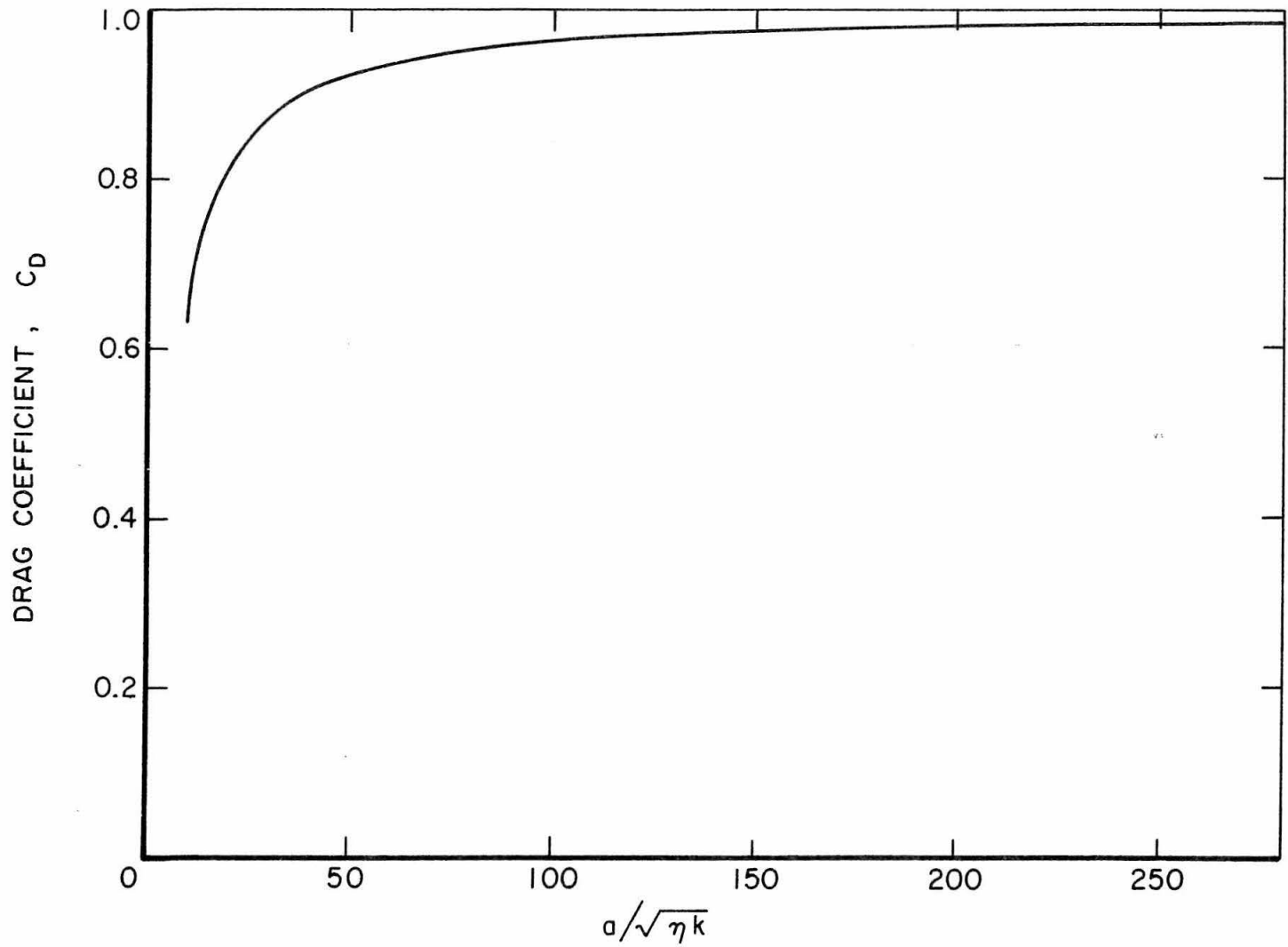


Fig. 10. Drag coefficient for Stokes flow past a porous sphere.

arrangement discussed above a moderate reduction of drag, say 20% occurs only when h/d is as large as 60.

Finally, we shall compare the present formula for the drag coefficient (4.87) with some results obtained by others. The drag derived by Joseph and Tao [3] based on the assumption of no-slip ($u_\theta = 0$ at $r = a$), may be written in coefficient form and expanded in small \sqrt{k}/a to give

$$C_D \sim 1 - \frac{1}{2} \frac{k}{a^2} \quad . \quad (4.88)$$

Assuming that the tangential velocity is continuous across the interface ($u_\theta = q_\theta$), we arrive at a slightly different formula

$$C_D \sim 1 - \frac{3}{2} \frac{k}{a^2} \quad . \quad (4.89)$$

Thus we see that (4.87) increases the accuracy in the representation of the drag coefficient, and it always gives a smaller drag than does either (4.88) or (4.89). Of course, as \sqrt{k}/a becomes very small, the discrepancies diminish.

V. CONCLUSIONS AND DISCUSSION

i. The set of general macroscopic equations of motion (2.75) and (2.76) are derived for flow through a porous medium. They are obtained by averaging Stokes equations over a volume element of the medium. Thus the applicability of the macroscopic equations is limited to small Reynolds numbers based on the pore or the solid grain size of the porous substance ($Re = qd/\nu \ll 1$). Aside from this restriction, the equations are generally valid whether the porosity is small or large. If, in addition, the Darcy number is also small ($Da = k/\eta L^2 \ll 1$), the macroscopic equations reduce to Darcy's law. For a typical porous medium, the Darcy number is usually very small and hence Darcy's law is generally applicable. To see this, we considered k approximated by the Carman-Kozeny equation[†], $k \approx \eta d^2/5$, where d is the hydraulic radius of the medium. This leads to a Darcy number $Da \approx 0.2(d/L)^2$. In a packed bed, d is only a fraction of the particle size. A porous body must include many particles in order to be described macroscopically, hence the macroscopic length L must be many times d , and this assures a very small Darcy number. An equation similar to (2.76) has been suggested by Brinkman [18], [19], for flow through porous media. The present derivation may be considered as a more rigorous justification and a modification of his work.

ii. In order to solve analytically a coupled problem of viscous

[†] See, for example, reference [17].

flow past a porous body, the interface boundary conditions must be established. Two formulations are presented. One involves the macroscopic equations of motion applied throughout the porous region; the second makes direct use of Darcy's law. The purpose of establishing the first type is to build a foundation for the second one, though the former may have its own usage when the Darcy number is not so small.

iii. The interface boundary conditions of the first kind are expressed in (3.24) to (3.26). These equations state that (1) the velocity in the fluid region is joined continuously to the superficial velocity in the porous region. (2) the normal gradient of the tangential velocity on the fluid side is related to that of the superficial tangential velocity on the porous side by a factor η . (3) the mean pressures defined in each region join continuously across the interface. The interface has been assumed as an ideal one, having statistically the same properties as a surface passing arbitrarily through the medium.

iv. We apply the general macroscopic equations of motion, together with the interface boundary conditions of the first kind to a simple problem, namely a Poiseuille channel flow over a permeable bed. The result shows that the velocity field undergoes a transition from that given by Darcy's law to that of the external fluid flow. This transition occurs in a very thin layer in the porous region in the immediate neighborhood of the interface when the Darcy number is small. In the interface layer, the tangential velocity varies

exponentially across the layer, and the nominal thickness δ of this layer is given by (3.54). For an ordinary porous medium, (again according to the Carman-Kozeny equation), δ is about $0.45d$, where the hydraulic radius d is a fraction of the particle size in a packed bed. The macroscopic equations at a small Darcy number are thus only important within a region of depth several times δ , or within a distance comparable to the size of a particle. Beyond that the porous medium flow can be described by Darcy's law. It may be argued that the information obtained about the nature of the transition layer at the interface is not accurate simply because in such a small region there is an insufficient number of particles present to assure the validity of a macroscopic description. This is indeed true. But it may also be reasoned that the average can be taken over planes parallel to the interface. The area of the planes may be chosen so as to include a sufficient number of surface pores, particularly when the interface is flat or possesses a large radius of curvature.

v. Inasmuch as the thickness δ of the interface layer is so very small in the case of small Darcy numbers, it may be argued that the layer is totally negligible and that Darcy's law may be applied in the whole region of the porous medium. However, it is found that the actual tangential velocity varies drastically across the layer. This variation must then be interpreted as a jump condition for the solution of the problem to be physically realistic while at the same time treated as mentioned above. The interface boundary conditions of the second kind are given by (3.76) to (3.78) which state that: (1) the

normal velocity in the fluid region joins continuously with the superficial normal velocity in the porous region. (2) The tangential velocity has a jump, the magnitude of which is linearly proportional to the normal gradient of the tangential velocity on the fluid side. The proportionality factor is $\sqrt{\eta k}$. (3) The relevant mean pressures vary continuously across the interface. These conditions are rigorously demonstrated for a general two dimensional flow with a flat interface and are extended for three dimensional flow with a flat interface. It is also shown that they are approximately valid for a curved interface as well, as long as the local radius of curvature is large; or more precisely, that the local Darcy number $Da = k/\eta R^2$, is small, where R is the radius of curvature.

vi. The derived jump condition (3.77) on the tangential velocity offers a firm theoretical support for the corresponding experimental result (3.56) of Beavers et al. The only discrepancy between the theory and the experiment is in the proportionality coefficient in these relations. The reason for this discrepancy is that equation (3.77) is deduced using the assumption of an ideal interface, while in practice, this is not achievable. Since a realistic interface may be rough and may have a porosity and a permeability near the interface different from those in the interior region, it is suggested that an experimental coefficient β always be incorporated with the jump condition as is shown in equation (3.82). Even when dealing with an ideal interface, it is still worthwhile to use a coefficient β . This is because the accuracy of the macroscopic equation on which the

theoretical jump condition depends has not been really established.

vii. To illustrate the use of the interface boundary conditions established in this work and to calculate the porosity effect of a porous body, two problems have been worked out in detail. One problem is the viscous flow between a rotating solid cylinder and a stationary porous cylinder; and the other is the Stokes flow past a porous sphere. The latter is the same problem treated by Joseph and Tao [3]. In general when the Darcy number is very small, as is usually the case, the viscous flow is insensitive to a naturally porous boundary and the porosity effect is negligible. When the Darcy number is not so small, as for a very porous body, however, the effect may be appreciable as is demonstrated in the reduction of the torque and drag coefficients. The present formulation is considered as an improvement over any others mentioned in the Introduction. The porosity effect is also detectable even with a small Darcy number when the external flow is bounded in a narrow region, as is demonstrated in the first problem with a small gap between the cylinders. From (4.30), it is estimated that a 10% reduction in torque coefficient can result when the gap $h \sim 4\eta d$, based on the assumption that both $a/\sqrt{\eta k}$ and h/a are small and the Carman-Kozeny equation is used to approximate k . This gap is comparable to a particle size, and is thus very small indeed. Unless the interface is smooth, the flow in the gap may be greatly disturbed and invalidate the assumption of circumferential parallel flow made in the problem.

REFERENCES

1. Richardson, J. G., "Flow Through Porous Media," Section 16 of Handbook of Fluid Dynamics, ed. by V. L. Streeter, McGraw-Hill, New York, (1961).
2. Scheidegger, A. E., "Hydrodynamics in Porous Media," of Handbuch der Physik, Vol. VIII/2, pp. 625-653, Springer Verlag, Berlin, (1963).
3. Joseph, D. D. and Tao, L. N., "The Effect of Permeability on the Slow Motion of a Porous Sphere in a Viscous Liquid," ZAMM, Vol. 44 (1964), pp. 361-364.
4. Joseph, D. D., "Note on Steady Flow Induced by Rotation of a Naturally Permeable Disk," Quart. J. Mech. and Appl. Math., Vol. 18, (1965), pp. 325-331.
5. Joseph, D. D. and Tao, L. N., "Ground Flow Induced by a Moving Cylinder," Phys. of Fluid, Vol. 8, (1965), pp. 1438-1499.
6. Joseph, D. D. and Tao, L. N., "Lubrication of a Porous Bearing - Stokes' Solution," J. Appl. Mech., Trans. ASME, (1966), pp. 753-760.
7. Shir, C. C. and Joseph, D. D., "Lubrication of a Porous Bearing - Reynolds' Solution," J. Appl. Mech., Trans. ASME, (1966), pp. 761-767.
8. Beavers, G. S. and Joseph, D. D., "Boundary Conditions at a Naturally Permeable Wall," J. Fluid Mech., Vol. 30, (1967), pp. 197-207.

9. Hunt, J. N., "On the Damping of Gravity Waves Propagated Over a Permeable Surface," J. Geophys. Res., Vol. 64, (1959), pp. 437-442.
10. Murray, J. D., "Viscous Damping of Gravity Waves Over a Permeable Bed," J. Geophys. Res., Vol. 70, (1965), pp. 2325-2331.
11. Illingworth, C. R., "Flow at Small Reynolds Number," Chapt. IV of Laminar Boundary Layers, ed. by L. Rosenhead, Oxford, (1963).
12. Langlois, W. E., Slow Viscous Flow, Macmillan, N.Y., (1964).
13. Keller, J. B., "Viscous Flow Through a Grating or Lattice of Cylinders," J. Fluid Mech., Vol. 18, (1964), pp. 94-96.
14. Hasimoto, H., "On the Periodic Fundamental Solutions of the Stokes' Equations and Their Application to Viscous Flow Past a Cubic Array of Spheres," J. Fluid Mech., Vol. 5, (1959), pp. 317-328.
15. Schlichting, H., Boundary Layer Theory, Chapt. XVIII, pp. 462-464, McGraw-Hill, N.Y., (1960).
16. Carman, P. C., "The Determination of the Specific Surface of Powders, I," J. Soc. Chem. Ind., Trans., Vol., 57 (1938), pp. 225-234.
17. Happel, J. and Brenner, H., Low Reynolds Number Hydrodynamics, Prentice Hall, N. J., (1965).
18. Brinkman, H. C., "A Calculation of the Viscous Force Exerted by a Flowing Fluid on a Dense Swarm of Particles", Appl. Sci. Res.

Vol. A1, (1949),pp. 27-34.

19. Brinkman, H. C., "On the Permeability of Media Consisting of Closely Packed Porous Particles", Appl. Sci. Res., Vol. A1, (1949), pp. 81-86.